UNIVERSITÀ DEGLI STUDI DI PALERMO
INTERNATIONAL PhD IN IMMUNOPHARMACOLOGY
Biomedical Department of Internal and Specialist Medicine (DiBIMIS)
SSD MED/04

THE TUMOR CELL IDENTITY: A GATEWAY TO THE MOLECULAR BASIS OF MALIGNANT TRANSFORMATION

PhD Candidate
Emanuela Scavo

PhD Coordinator
Prof. Francesco Dieli

Supervisor
Prof. Matilde Todaro

Lab Head
Prof. Giorgio Stassi

XXVI CYCLE
ACADEMIC YEAR 2016

Index

Summary

It is now well established that within a tumor mass there is a hierarchical organization, stemming from a cell subpopulation retaining the highest tumorigenic potential, referred as cancer stem cells (CSCs), responsible for tumor initiation and progression.

Although recent advances in stem cell biology led to the acquisition of new view of thyroid carcinoma as a stem cell disease, the cellular origin of thyroid CSCs remains unknown. In **Chapter 1** it is critically discussed the potential role of thyroid stem cells (TSCs) in light of the available information on the oncogenic role of genetic alterations underlying the thyroid carcinogenesis. Understanding the key events that regulate thyroid transformation may be fundamental for clinical intervention in terms of prevention, diagnosis and therapy.

Although stem cells (SCs), with their unique self-renewal potential, are considered the favored candidates for sequential accumulation of genetic alterations in tumor transformation, any cell with proliferative capacity, within the hierarchy in a normal tissues, could be considered a cell of origin able to initiate a tumor. In the second chapter of this thesis (**Chapter 2**), we describe how the *in vitro* differentiation of human embryonic stem cells (hESCs) represents a reliable experimental approach to obtain an unlimited source of derived thyroid cells at different stages of differentiation. Understanding the cellular hierarchy of normal thyroid tissue could allow the identification of cells-of-origin and tumor-related driven mutations underlying the thyroid carcinogenesis.

It is widely assumed that estrogens play an important role in the initiation and progression of different malignancies through their interaction with SC compartment. Based on this scenario, direct effects of estrogens in growth and function of normal and malignant thyroid cells are closely described in **Chapter 3.**

A growing body of evidence suggested that CSCs could be considered a source of primary mediators of chemo-radiation resistance leading to failure in cancer therapy. A better understanding of molecular mechanisms underlying CSCs resistance may

improve the efficacy of current cancer therapies. In the fourth chapter of this thesis (**Chapter 4**), we suggest that targeting CSCs metabolism is a potential alternative strategy to cancer therapy.

Chapter 1

Normal vs cancer thyroid stem cells: the road to transformation

Mariangela Zane*, **Emanuela Scavo***, Veronica Catalano, Marco Bonanno, Matilde Todaro,
Ruggero De Maria and Giorgio Stassi

*These authors contributed equally to this work

Published in *Oncogene*, 2015.

Oncogene (2015), 1–11

www.nature.com/onc

REVIEW

Normal vs cancer thyroid stem cells: the road to transformation

M Zane[1,2,4], E Scavo[1,4], V Catalano[1], M Bonanno[1], M Todaro[1], R De Maria[3] and G Stassi[1]

Recent investigations in thyroid carcinogenesis have led to the isolation and characterisation of a subpopulation of stem-like cells, responsible for tumour initiation, progression and metastasis. Nevertheless, the cellular origin of thyroid cancer stem cells (SCs) remains unknown and it is still necessary to define the process and the target population that sustain malignant transformation of tissue-resident SCs or the reprogramming of a more differentiated cell. Here, we will critically discuss new insights into thyroid SCs as a potential source of cancer formation in light of the available information on the oncogenic role of genetic modifications that occur during thyroid cancer development. Understanding the fine mechanisms that regulate tumour transformation may provide new ground for clinical intervention in terms of prevention, diagnosis and therapy.

Oncogene advance online publication, 11 May 2015; doi:10.1038/onc.2015.138

INTRODUCTION

Thyroid cancer (TC) accounts for 96% of endocrine malignancies with 62 980 new cases expected to be diagnosed in the US in 2014, where it represents the second most common cancer among adolescents ages 15–19 (www.cancer.org). Despite of a global increase in incidence over the past three decades, the mortality rate remains low. This is a consequence of a favourable prognosis for the more frequent well-differentiated forms, subdivided into papillary (PTC) and follicular TC (FTC).[1] By retaining the differentiated features of normal thyrocytes, including the ability to concentrate iodine, in most cases these tumours can be treated successfully by surgical resection, followed by radioactive-iodine administration.[2] In contrast, the rare undifferentiated anaplastic TCs (ATCs), have a very-poor prognosis because of their invasiveness and metastatic behaviour (Figure 1) as well as their insensitivity to radioactive-iodine treatment for lack of an iodine symporter.[3]

Alterations in key signalling pathways are proposed for distinct forms of thyroid transformation. Gain-of-function mutations in the thyrotropin receptor (TSH-R) or Gsα encoding genes, result in increased cAMP accumulation and TSH-independent proliferation, which in turn account for hyperfunctional adenomas, benign lesions without propensity towards malignant progression. Constitutive activation of the MAPK pathway seems to be the hallmark of different forms of TC.[2] Genomic alterations of the proto-oncogene tyrosine-protein kinase receptor Ret, the neurotrophic tyrosine kinase receptor, as well as the intracellular signal transducer Ras and the serine/threonine-protein kinase B-Raf, have clearly been implicated in the pathogenesis of PTCs.[4] Similarly, the chromosomal translocation t(2;3)(q13;p25), which fuses the transcription factor paired box protein Pax-8 (Pax-8) and peroxisome proliferator-activated receptor gamma (PPAR-γ) encoding genes, has been identified in significant proportions in FTCs.[5] In addition to *RAS* mutations, another common event of these tumours is the PI3K pathway aberrant activation through mutation of the catalytic subunit p110 (*PI3KCA*) and loss of PTEN (Figure 2).[6]

The multistep carcinogenesis model suggests that ATCs arise by way of a dedifferentiation process from pre-existing FTC or PTC (Figure 3).[7] The additional genetic events involved in the progression towards tumour dedifferentiation are (i) the inactivating point mutation in the *TP53* gene[8–10] and (ii) the activating mutation in the *β*-catenin encoding gene *CTNNB1*.[11,12] Evidence in favour of this multistep carcinogenesis model includes, the presence of well-differentiated TC within ATC specimens and the coexistence of *BRAF* gene and *TP53* gene mutations in both undifferentiated and differentiated carcinomas.[13,14] However, this model is not in accordance with the rare occurrence of *RET/PTC* and *PAX8/PPARG* rearrangements in ATC[15] and the low turnover rate of thyroid follicular cells (about five renewals per lifetime) that reduces the possibility of accumulating the mutations needed for transformation.[8,16–18]

The existence of several differentiation degrees has led to the assumption that TC cells are derived from remnants of fetal thyroid cells, such as stem cells (SCs) or precursors, rather than mature follicular cells.[9,19,20] According to this fetal cell carcinogenesis model supported by gene expression profiling data, ATC arises from fetal thyroid SCs, marked by the onco-fetal fibronectin expression and lack of differentiation markers. Thyroblasts are hypothesised to be at the origin of PTC and are characterised by the concomitant expression of onco-fetal fibronectin, and the more differentiated marker thyroglobulin (Tg). Remnants of prothyrocytes, which represent a more differentiated cell type not expressing onco-fetal fibronectin, would result in FTC (Figure 3).[7,20] Genomic alterations, including mutations in *TP53* and *BRAF* genes, as well as *RET/PTC* and *PAX8/PPARG* rearrangements, have an oncogenic role by conferring proliferative advantages and preventing fetal thyroid cells from differentiating.

[1]Department of Surgical and Oncological Sciences, University of Palermo, Palermo, Italy; [2]Department of Surgical, Oncological and Gastroenterological Sciences, University of Padua, Padua, Italy and [3]Regina Elena National Cancer Institute, Rome, Italy. Correspondence: R De Maria, Regina Elena National Cancer Institute, Rome, Italy or Professor G Stassi, Department of Surgical and Oncological Sciences, University of Palermo, Via del Vespro, 131, Palermo 90127, Italy.
E-mail: demaria@ifo.it or giorgio.stassi@unipa.it
[4]These authors contributed equally to this work
Received 1 February 2015; revised 24 March 2015; accepted 30 March 2015

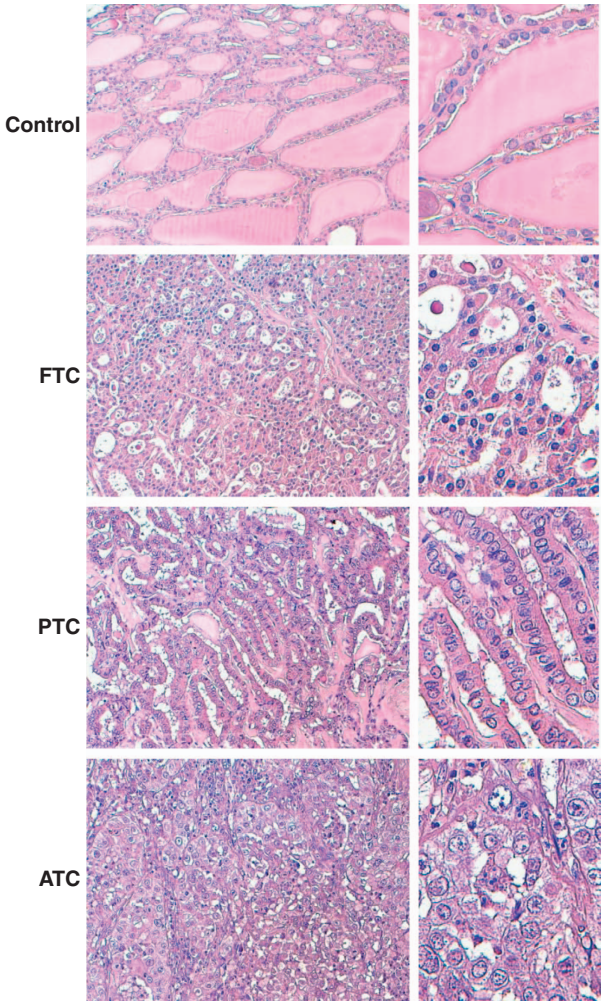

Figure 1. Epithelial thyroid cancer histotypes. Histochemical analysis on paraffin-embedded sections of human thyroid gland control (Control), FTC, PTC and ATC.

This model is sustained by several lines of evidence. Exposure to the radioactive-iodine released after the Chernobyl nuclear accident resulted in a higher incidence of PTCs among infants and young children rather than adults.[21] Furthermore, thyroid-targeted transgenic *RET/PTC1* mice developed PTC and hypothyroidism following the inhibition of thyroid cell differentiation.[7,22]

The third model concerns the so-called cancer SCs (CSCs), a minute population at the apex of a hierarchical pyramid including increasing numbers of progenitors and more differentiated cells. This CSC model is based on the assumption that only a small subset of cells possesses the ability to initiate and spread the tumour. These cells can arise after genetic and epigenetic alterations occurring either in normal SCs or in progenitor/precursor cells that could acquire self-renewal potential in a sort of reprogramming process.[7,23]

Here, we describe the potential role of SCs in thyroid pathogenesis in detail and we address the hypothesis of their possible involvement in metastasis development.

NORMAL THYROID STEM CELLS

SCs are undifferentiated cells characterised by the extraordinary ability to self-renew and give rise to many types of specialised cells.[24] They mostly divide asymmetrically to generate two different daughter cells, one identical to the mother and one more differentiated that will eventually give rise to specialised cells. This mechanism allows to maintain control over the SC pool preserving tissue homeostasis.[25] The protective microenvironment created by the SC niche provides the necessary stimulatory and inhibitory signals for the maintenance of the stemness state.[26] Under particular circumstances requiring the expansion of the SC pool, SCs undergo symmetric division, producing two identical daughter cells able to self-renew and generate a differentiated progeny.[27]

SCs are usually classified into three major groups according to their development potential: embryonic SCs (ESCs), adult SCs (ASCs) and fetal SCs (FSCs).[24] The fate of SCs is influenced by specific signals coming from the microenvironment niche and can be manipulated *in vitro* to form differentiated lineages. ESCs represent a potential source of derived thyroid cells that have a superior predilection to mutate and hence initiate thyroid diseases. During the early stages of embryonic development, visceral endoderm gives rise to extra-embryonic endoderm. Whereas, anterior definitive endoderm migrates to form the primitive gut (foregut, midgut and hindgut). Follicular cells develop from the anterior foregut endoderm and are clearly different from C cells of neuroectodermal origin. Therefore, thyroid cell lineages formed by ESC-derived endoderm could be considered an *in vitro* experimental model adopted for the study of thyroid development.[28–30] Thyroid growth requires a complex network of transcription factors, including Pax-8, thyroid transcription factors 1 (TTF-1, also known as homeobox protein Nkx-2.1) and 2 (TTF-2, also known as forkhead box protein E1, Foxe1), as well as hematopoietically expressed homeobox protein HHEX (Table 1). Each of these factors exhibits distinct roles within different embryonic tissues, but their specific cooperation in progenitor cells is fundamental to uniquely drive thyroid organogenesis.[31] Specifically, TTF-1 and Pax-8 are needed for precursor survival, while TTF-2 promotes their migration. Meanwhile, HHEX works to maintain the expression of these three factors and prevent differentiation.[30] In addition, the surrounding mesenchyme, contributes to expand the pool of thyroid cell progenitors through the release of pro-epidermal growth factor and basic fibroblast growth factor (bFGF, or FGF-2).[31,32] As discussed below, the co-expression of TTF-1 and Pax-8, is an essential event for cell commitment towards follicular cell fate.[33] While, FGF and bone morphogenetic protein (BMP) signalling pathways act in the early stages of thyroid development[34] before TSH/TSH-R and IGF/insulin signalling that promote the full differentiation of follicular cells (Figure 4 and Table 1).[35]

In order to identify early and late markers of thyroid development, several studies are being carried out using mouse ESCs as a source of *in vitro* differentiating thyrocytes. Lin *et al*.[36] demonstrated that mouse ESCs formed embryoid bodies that upon differentiation, express a set of thyroid-specific markers, such as Pax-8, thyroid peroxidase (TPO), Tg, sodium/iodide cotransporter (NIS) and TSH-R. In absence of serum, these differentiated cells did not express Tg. TSH treatment was necessary to maintain Pax-8 and TSH-R expression during embryoid body differentiation, but it was not sufficient to express Tg. This suggests that other factors, besides TSH, are required for long-term maintenance and the maturation of thyrocytes.[36] Later, TSH and activin A, a transforming growth factor β (TGF-β) family member, were proposed as important factors in endoderm specification and thyrocyte differentiation, while insulin and IGF-I promoted the long-term maturation of thyrocytes expressing Tg, NIS and TSH-R.[37] According to these data, TTF-1, TTF-2, and Pax-8 can be considered specific markers of thyroid SC/progenitors, TSH-R a marker of precursor cells, Tg, TPO and NIS markers of fully differentiated thyroid follicles (Figure 4 and Table 1).

Recently, Antonica's research group demonstrated the differentiation of murine ESCs into the thyrocytic lineage, with the

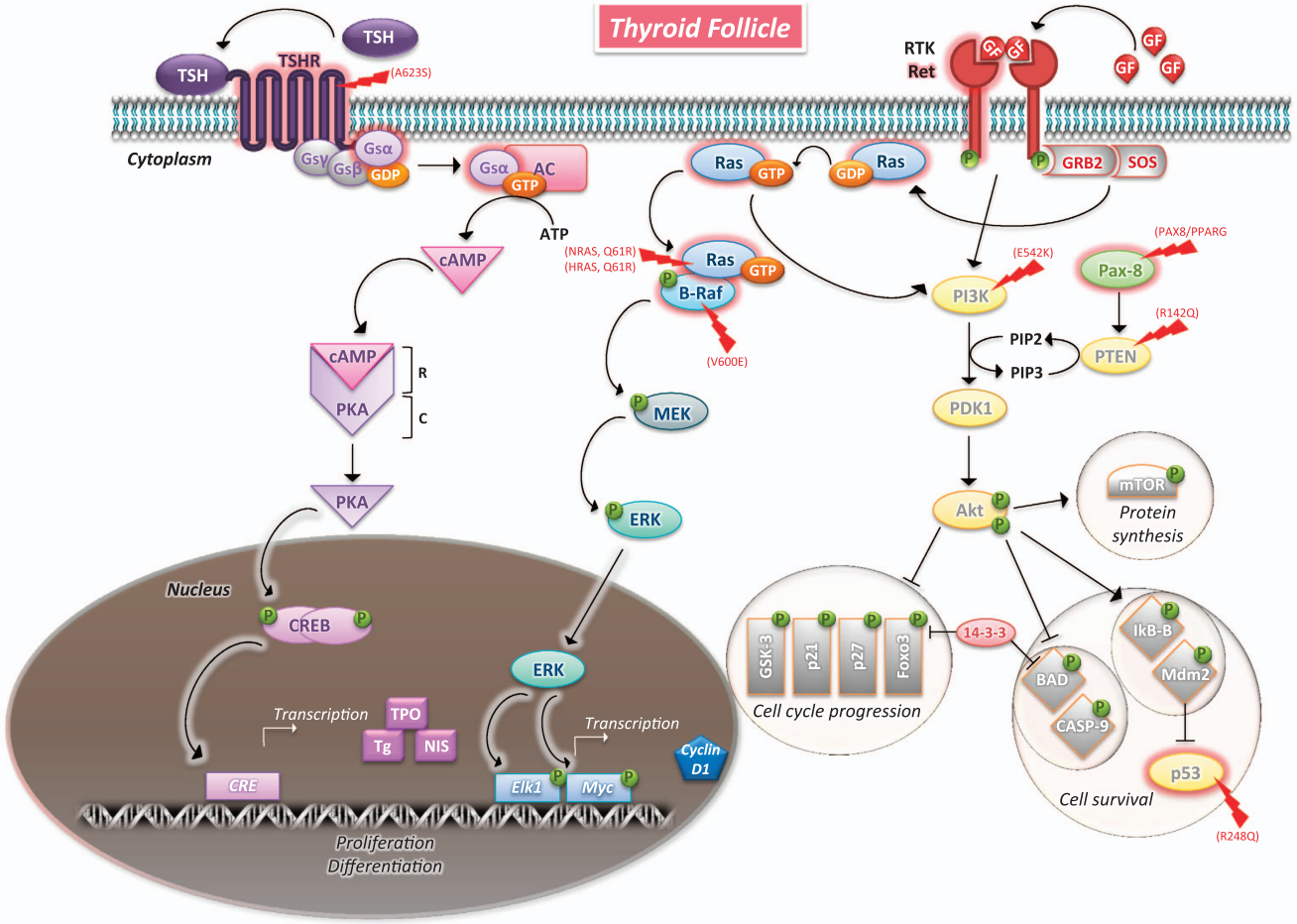

Figure 2. Thyroid follicular cell. The main regulators of thyroid function are TSH signalling through cAMP-dependent pathway, and growth GFs, acting via MAPK and PI3K/Akt signalling pathways. Alterations in key factors of these pathways (indicated in red) could lead to thyroid transformation: gain-of-function, mutations in TSH-R and Gsα encoding genes could result in benign lesions such as hyperfunctional adenomas. *RAS* and *BRAF* mutations in MAPK pathway are frequently observed in PTC. Genetic alterations in genes associated with the PI3K/Akt pathway, i.e., *PAX8* (40%) and *TP53*, are involved in FTC and ATC, respectively. The frequency of BRAFV600E in thyroid carcinomas is 50%. Thyroid tumours have been found to have mutations in *NRAS* (4.6%) and *HRAS* (1.2%) codon 61. Mutations in *TP53* occur in 6% of all thyroid tumours, whereas the frequency of *PTEN* and *PI3K* mutations is 3%. Genetic alterations and mutation frequency reported are referred to http://www.mycancergenome.org and http://cancer.sanger.ac.uk.

formation of thyroid follicles, able to induce iodide organification.[33] In particular, the simultaneous ectopic expression of TTF-1 and Pax-8 induced the *in vitro* differentiation of mouse ESCs into follicular cells. After treatment with TSH, these cells showed molecular, morphological and functional characteristics of thyroid follicles and were able to fulfil thyroid hormone deficits when transplanted orthotopically into an immunodeficient mouse.[33] Pax-8 and TTF-1 co-expression is therefore required for assembling the follicular cells into becoming a follicle-like structure, as recently confirmed.[38]

Longmire *et al.* demonstrated that the presence of activin A led ESCs to differentiate into definitive endoderm, expressing forkhead box protein A2 (Foxa2$^+$). At this stage, if exposed to BMP and activin/TGF-β signalling inhibitors (Noggin and SB431542, respectively) for a specific amount of time, definitive endoderm was shown to be directed towards the lung/thyroid competent definitive endoderm, negative for forkhead box protein A3 (Foxa2$^+$/Foxa3$^-$). Hence, induction of BMP and FGF signalling by exposing cells to high doses of FGF-2 combined with specific factors (that is, BMP-4, Wnt3a, FGF-10, FGF-7, epidermal growth factor and heparin), may promote the initial lineage specification of endodermal TTF-1$^+$ thyroid primordial progenitors. The efficient induction of TTF1 into endodermal progenitors, is restricted by a stage-specific and time-dependent inhibition of BMP and activin/TGF-β signalling, followed by BMP reactivation and combined with FGF signalling.[34,39–41] D'Amour *et al.*[42] reported similar results using human cells, observing that in the presence of FGF-2 high-dose activin A induced a massive differentiation of ESCs into transcription factor SOX-17$^+$/Foxa2$^+$ definitive endodermal cells (Figure 4 and Table 1). Interestingly, Onyshchenko *et al.*[43] used two methods in order to differentiate human ESCs in thyroid follicular cells: (i) an one-step protocol that aims at a direct differentiation through TSH stimulation by avoiding the intermediate endoderm formation and (ii) a two-step protocol with an intermediate passage in endodermal cells, which foresees the TSH stimulation in combination with activin A and FGF-2. In both cases, we were unable to obtain an efficient generation of differentiated cells that express specific thyroid markers. This suggests that, molecular mechanisms involved in mouse and human differentiation are different, and TSH by itself is not sufficient to induce thyrocyte-like cell differentiation *in vitro*.

The thyroid is a low proliferating gland, known for its self-renewal ability.[8,16] It has been suggested that follicle regeneration is maintained by a pool of SCs that reside in the adult gland. ASCs, estimated to be ~0.1% of all thyroid cells, are undifferentiated in a quiescent or slow-cycling state and could replicate themselves to

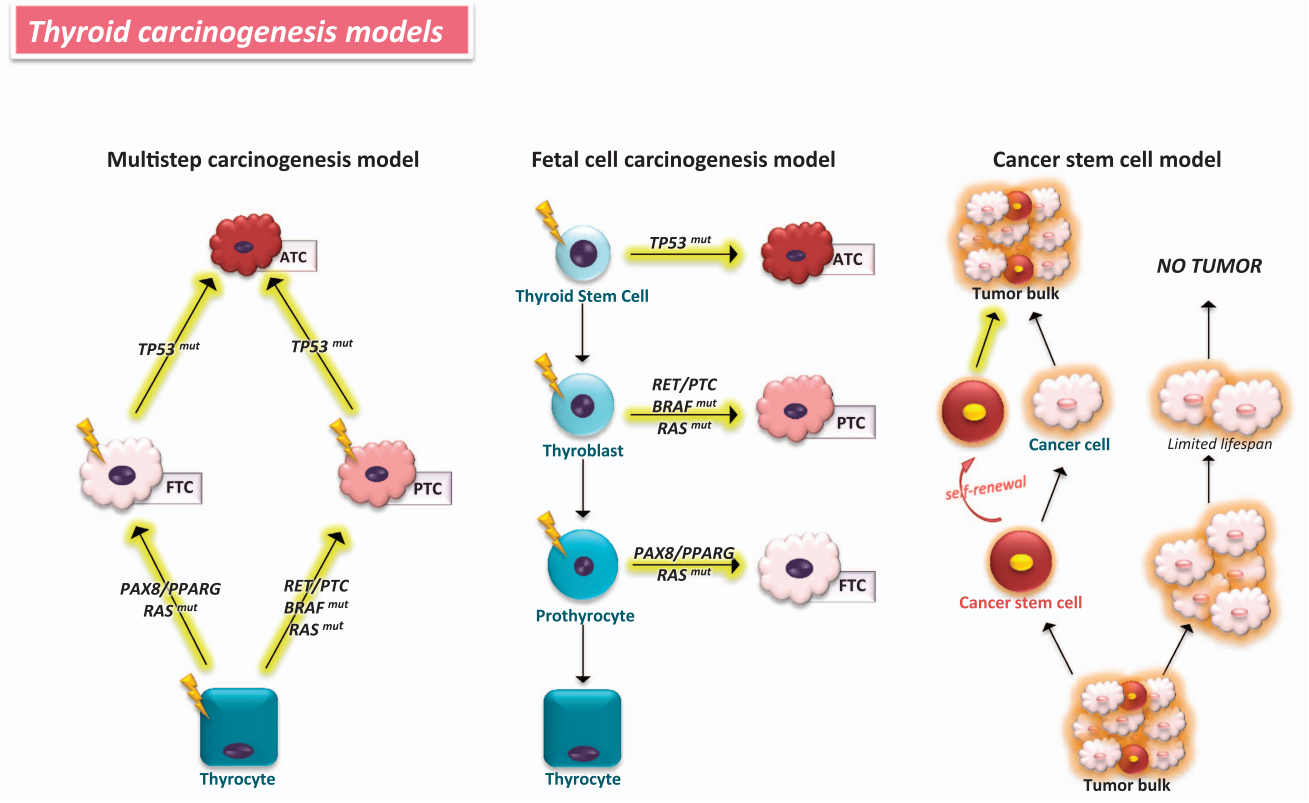

Figure 3. Thyroid carcinogenesis model. The multistep carcinogenesis model suggests that undifferentiated thyroid carcinomas derive from well-differentiated tumours via the sequential accumulation of genetic mutations and dedifferentiation process. According to the fetal cell carcinogenesis model, thyroid cancer cells originate from the transformation of three types of fetal thyroid cells—thyroid stem cells, thyroblasts and pro-thyrocytes, which would result in ATC, PTC and FTC. The CSC model assumes that only a small subset of cells possesses the ability to trigger, reconstitute and sustain tumour growth.

Table 1. Cell markers of thyroid development

Cell specialisation	*Marker*	*Function*	*References*
Thyroid competent definitive endoderm	Transcription factor SOX-17	Transcription factor required for normal development of definitive gut endoderm	32,37,39–43
	Forkhead box protein A2 (Foxa2)	Transcription factor involved in endoderm-derived organ development	32,34,37,39–43,52
Thyroid primordial progenitor	Paired box protein Pax-8 (Pax-8)	Transcription factors that have a role in the regulation of thyroid-specific genes (i.e., *TG*, *TPO*, *TSHR*), needed for the maintenance of thyroid differentiation phenotype. Their co-expression is essential for the survival and the specification towards the thyroid cell type	18,29–34,36,38,41,55
	TTF-1 or Homeobox protein Nkx-2.1		18,29–34,38,40,45,49–51
	TTF-2 or Forkhead box protein E1	Transcription factor involved in thyroid gland organogenesis, promoting cell migration	29–33
	Hematopoietically expressed homeobox protein HHEX	Transcription repressor involved in thyroid development; it maintains gene expression of *PAX8*, *TTF1* and *TTF2* in the thyroid primordium	30–32,34,40,41
Thyroid precursor	TSH-R	Central player in controlling thyroid cell metabolism through the cAMP cascade	18,29,32–34,36–38,43,54,55
Thyrocyte	Tg	Precursor of the iodinated thyroid hormones T3 and T4	29,33,34,36–38,49,50,52–55
	Sodium/iodide cotransporter (NIS)	Symporter that regulates iodide uptake	18,29,33,36–38,43,54,55
	TPO	Enzyme acting in iodination and coupling of the tyrosine residues in Tg to produce T3 and T4	18,29,36–38,43,51,54,55
Solid cell nest	Tumour protein 63 (p63)	Transcription factor implicated in epithelial morphogenesis regulation; the ratio between ΔN/TA-type isoforms may regulate the maintenance of the epithelial stem cell compartment	18,44–50,53

Abbreviations: Tg, thyroglobulin; TPO, thyroid peroxidase; TSH-R, thyrotropin receptor; thyroid transcription factor 1, TTF-1; thyroid transcription factor 2, TTF-2.

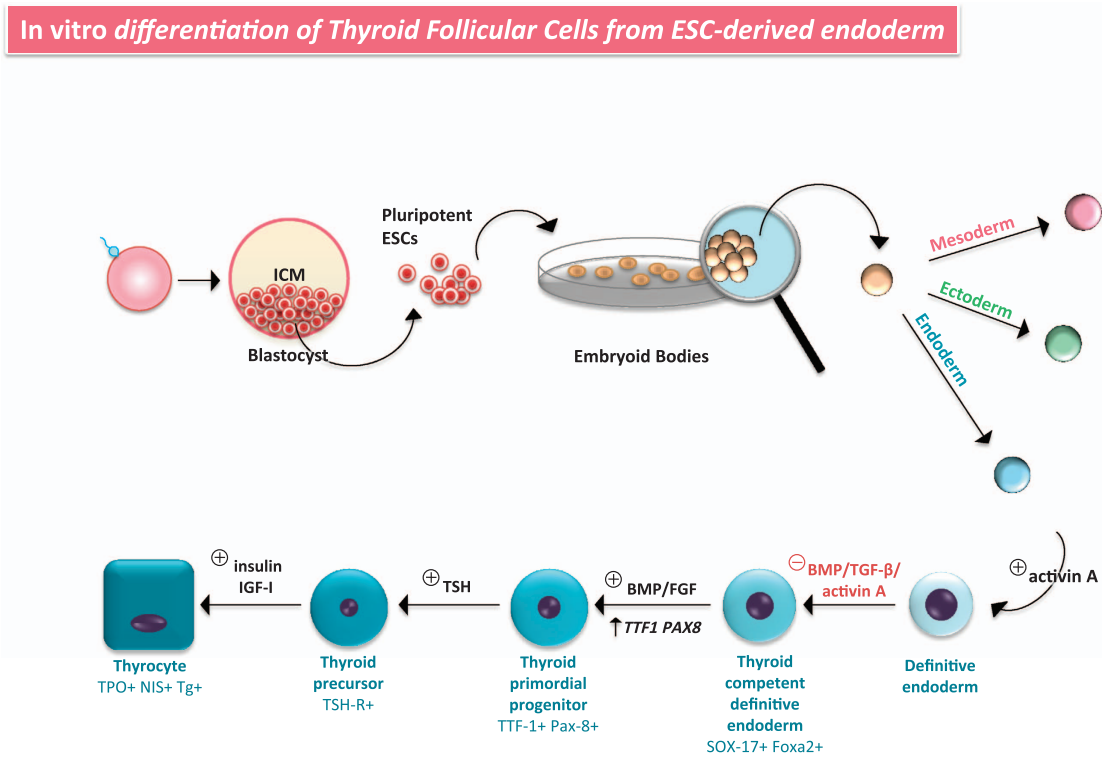

Figure 4. *In vitro* differentiation of thyroid follicular cells from ESC-derived endoderm. Blastocyst-derived ESCs form *in vitro* embryoid bodies able to generate derivatives of the three germ layers. The embryoid bodies differentiate into definitive endoderm in presence of activin A, and into thyroid competent definitive endoderm after exposition to inhibitors of BMP and activin A/TGF-β signalling. At the later stage, the concomitant induction of BMP and FGF signalling, and TTF-1 and Pax-8 co-expression, results in the generation of thyroid primordial progenitors. Thyroid precursors, derived from progenitor cells after TSH treatment, differentiate into Tg-expressing thyrocytes in presence of insulin and IGF-I.

preserve tissue turnover after damage.[17] Embryonic remnants have been identified in adult thyroid tissue as small clusters, the solid cell nests (SCNs), which could represent a potential niche of thyroid SCs defined by the expression of tumour protein 63 (p63, Table 1).[30] SNC is composed of centrally located undifferentiated $p63^-$ cells, and surrounded by $p63^+$ cells with a basal/SC phenotype clustered or structured within a single layer.[44–46] Indeed, some of its stemness features have been demonstrated: the self-renewal capability conferred via telomerase activity and the differentiation potential in more cell types, due to high p63 and Bcl-2 expression.[47,48] Reis-Filho *et al.*[49] identified the SCNs as structures composed of numerous main cells and rare C cells. Main cells are notably characterised with basal/SC marker p63, basal cytokeratins (excluding cytokeratin 20), and the carcinoembryonic antigen. In contrast, C cells lack p63 and are immunoreactive to differentiation markers, such as calcitonin and TTF-1.[49] Hence, it has been proposed that SCN main cells can be considered a pool of multipotent SCs, involved in histogenesis and self-renewal of both follicular and C cells.[47] The potential stem role of SCN main cells was supported by immunohistochemical profile studies.[44,50] Recently, Okamoto *et al.*[51] supported the involvement of SCN in thyroid regeneration, having observed a similar morphology in irregular shaped follicles generated after a partial thyroidectomy in mice. These cells were characterised as SC antigen 1 $(SCA1)^+$/$BrdU^+$/β-gal/$TTF\text{-}1^-$, and temporarily co-expressed cytokeratin 14.[52] They evolve into functional follicles, which express TPO after 120 days, indicating that they consist of newly formed follicular cells, but do not originate from differentiated thyrocytes.[51,52]

Considering the SCN as a source for both follicular and C cells, the presence of three cell types has been hypothesised: (i) progenitors of follicular cells, arisen from the base of the foregut (endodermal origin); (ii) progenitors of C cells, which originate from ultimobranchial bodies (neural crest origin); and (iii) and the follicular and C bipotential progenitor cells.[8]

In 1992, Dumont *et al.*[17] first hypothesised the existence of ASCs within the mature thyroid gland. Thomas *et al.* isolated a population of ASCs from the goitre, characterised by the co-expression of the octamer-binding protein 4 (Oct-4) stem pluripotent marker, the transcription factor GATA-4 and hepatocyte nuclear factor 4-α (HNF-4-α) endodermal markers and Pax-8. These SCs, negative for Tg, were not influenced by TSH treatment.[53] Fierabracci *et al.* obtained a $CD34^+/CD45^-$ subpopulation of cells with self-replicative potential from different human thyroid specimens, characterised by their expression of the pluripotent Oct-4 markers and homeobox transcription factor Nanog (hNanog). Under appropriate culture conditions, these cells were able to generate follicles with thyroid hormonal production.[54]

Hoshi *et al.* identified a side population (SP) able to efflux the vital dye Hoechst 33342 in a thyroid murine. It ranged from 0.3 to 1.4% of the total population and was highly enriched with stem/progenitor cell activity. According to the expression of hematopoietic markers used to define SC populations, SP cells were separated into two cellular subsets, SP1 ($CD45^-$/$c\text{-}kit^-$/$SCA\text{-}1^+$) and SP2 ($CD45^-$/$c\text{-}kit^-$/$SCA\text{-}1^-$). Both SP cells were characterised by high expression levels of ATP-binding cassette sub-family G member 2 and Oct-4, and by a low expression level of thyroid differentiation markers. In particular, SP2 cells seem to have progenitor characteristics because of their low TTF-1 and TSH-R expression that is in line with their involvement in thyroid lineage commitment. Furthermore, the putative SC marker nucleostemin was reported to be downregulated in

undifferentiated thyroid cells.[18] The SP selection method has also been used to isolate ASCs in human thyroid. Lan *et al.* showed that thyroid ASCs isolated from human goitres were able to differentiate into thyroid cells and grow either in a monolayer or embedded in collagen. Under the influence of TSH in a serum-enriched medium, isolated ASCs differentiated into thyrocytes expressing Pax-8, Tg, NIS and TPO. Moreover, when embedded in collagen, they were able to uptake iodine in response to TSH.[55] These results reinforce the reported observations regarding the ability of goitre-derived ASCs, to differentiate into thyroid cells.

THYROID CANCER STEM CELLS

It is becoming increasingly evident that tumours are organised hierarchically similarly to normal tissues, where a small subpopulation named CSCs is responsible for cancer initiation and progression. Assuming the involvement of SCs in thyroid carcinogenesis, it is necessary to clarify the SCs' dual role in the initiation and propagation of a tumour. In cancer initiation, the 'cell-of-origin' concept explains how a normal cell acquires the first mutation able to kick-start the tumour (tumour initiating cells, TICs). TICs constitute a tumour cell subset that sustains tumour growth, but does not necessarily originate from the transformation of normal SCs.[56] However, SCs are able to live for a long time, undergo self-renewal and possess the key features required for the acquisition of genetic or epigenetic changes leading to cancer development.[57] To recognise the cell-of-origin of neoplastic transformation, it is helpful to first enucleate the cellular hierarchy present within the tumour tissue. Putative cells-of-origin are committed progenitor or precursor cells, able to reacquire a SC-like phenotype and functions upon genetic or epigenetic reprogramming.[58] Early progenitors, also known as transit amplifying cells, are facilitated in the acquisition of modifications that drive reprogramming, due to their elevated proliferative capacity and undifferentiated state. Among the TIC population, transit amplifying cells have a predominant role in primary tumour formation, but only a small fraction of them shows detectable self-renewal and metastasis-forming potential. However, initiation and maintenance of the tumour seem to be dynamic processes, characterised by the transition between the self-renewing and transient amplifying phenotypes (Figure 5).[59,60] CSCs are identified due to their ability to self-renew and are represented by: (i) long-term TICs (LT-TICs) able to maintain tumour formation after serial xeno-transplantations and involved in metastasis formation; (ii) delayed contributing TICs (DC-TICs), active only in secondary or tertiary tumour xenografts (Figure 5).[59] The peculiar feature of CSCs concerns the pronounced tendency to undergo symmetric division as compared with normal SCs. This drift is driven by major genetic and epigenetic events conferring unlimited lifespan and to CSCs, which are ultimately responsible for tumour growth and progression.[61] In studying CSCs in the thyroid, several research groups have developed specific methods to isolate TICs from this gland (Table 2). In this overview, we do not take into consideration those studies or single results obtained using ARO, NPA and KAT-4 cell lines, being that they were found not to be of thyroid origin.[62]

Injecting putative CSCs into immunocompromised mouse models[63–65] and following the tumour development constitutes an univocal way of testing their effective tumourigenicity.[66] It has been observed that serial transplantation led to an *in vivo* selection of cells able to generate more aggressive tumours.[67] In particular, transplantations of cells, isolated from secondary and tertiary xenografts, permit to define their long-term tumourigenic potential, as well as their self-renewing ability (Figure 5).

High level of aldehyde dehydrogenase (ALDH) activity is present in stem and progenitor cells, thus it has been used as a functional marker for CSCs isolation in tumours.[30,68] Todaro *et al.* showed that PTC, FTC and ATC contain a small population of tumourigenic cells with high ALDH activity and unlimited replication potential. Expanded indefinitely *in vitro* as tumour spheres, these $ALDH^{high}$ cells contain 25–60% of the clonogenic cells able to generate serial tumour xenografts. Interestingly, the highest percentage (60%) of clonogenic cells present in ATC, defined the cellular subset endowed with a boosted self-renewal activity and a tumourigenic and metastatic potential. This suggests that ATC cells undergo multiple rounds of symmetric division.

In line with this, the injection of $ALDH^{high}$ cells derived from FTC led to a moderately invasive tumour without distant metastasis. Whereas, $ALDH^{high}$ cells derived from ATC, are able to invade adjacent tissues and produce lymph nodes and lung metastasis because of a strong constitutive activation of c-Met/Akt pathways.[63] Elevated ALDH activity was also identified in ATC cell lines: 17–38% of ATC-8505C[30] and 8–13% of SW1736[69] were $ALDH^{high}$.

hNanog, Oct-4 and transcription factor SOX-2 (encoded by *NANOG*, *POU5F1* and *SOX2* genes, respectively) are transcription factors that establish SC features through a pluripotent regulatory network.[70] Detection of high levels of these transcription factors, together with low or absent markers of thyroid differentiation, can help identify putative thyroid CSCs (Figure 6).[30,63,64,71–73] Such identification can be supported by the analysis of biomarker expression belonging to self-renewing control pathways, such as Wnt/ β-catenin, Sonic hedgehog protein and Notch1 (classified also as epithelial–mesenchymal transition (EMT)-inducing signalling pathways).[74] Malaguarnera *et al.*[75] reported that the self-renewal capacity of thyrospheres is also sustained by the over-expression of the insulin receptor and IGF signalling pathway genes (IGF-I receptor, *IGF-I, IGF-II*) promoting their volume, growth and survival.

Recently, Ahn *et al.* identified a small percentage of $CD44^{high}$/$CD24^{low}$ cells with tumourigenic capability in the papillary TPC1 cell line, in six human primary PTCs and in four metastatic lymph node specimens, as well as in two PTC-derived ATC samples. Notably, $CD44^{high}$/$CD24^{low}$ cells showed a higher Oct-4 expression and lower differentiation marker expression than $CD44^{high}$/$CD24^{high}$ cells, together with the ability to form thyrospheroids. However, no tumour was detected after the inoculation of $CD44^{high}$/$CD24^{low}$ human specimens into athymic Ncr-*nu/nu* mice.[65]

Different research groups reported controversial results regarding CD133 (also known as Prominin-1) in TC. In anaplastic KAT18 and FRO cell lines, Zito *et al.*[76] did not find $CD133^+$ cells; Friedman *et al.*[71] identified $CD133^+$ in 6.32% FRO cells, but not in the papillary TPC cell line. Recently, Ke *et al.*[77] described $< 5\%$ $CD133^+$ cells in papillary CG3 and follicular WRO and CGTH cell lines. By using primary tumours, Malaguarnera *et al.*[75] and Tseng *et al.*[73] identified a $CD133^+$ subpopulation in PTC samples, while it was absent in thyroid spheres derived from PTC, FTC and ATC samples analysed by Todaro's research group.[63] Immunohistochemical examinations reported an elevated expression of CD133 in ATC paraffin-embedded tissue sections,[71,78] but only a low variable expression in FTC and PTC adjacent to ATC samples.[78] Besides the inconsistencies in the reported results, another limit of this marker is that its expression is greatly influenced by the cell cycle phase.[79]

SCs are enriched in the SP compartment. However, dye efflux is not a characteristic common to all SCs, and this feature is not limited only to the SC phenotype. This method seems to be associated with a toxic effect on cells.[80] Mitsutake *et al.*[74] found a very small portion of the SP in follicular WRO (0.02%) and anaplastic FRO (0.1%) human cell lines, but not in papillary TPC1. After sorting, these cells showed a higher clonogenic ability than those referred as main population (MP), and were tumourigenic after being injected into nude mice. The two subpopulations showed a different gene expression profile. Microarray experiments revealed an upregulation of ABCG2, Wnt (*MYC*, *JUN*, *FZD5*) and Notch1 pathway genes (*HES1* and *JAG1*) in SP cells. Following

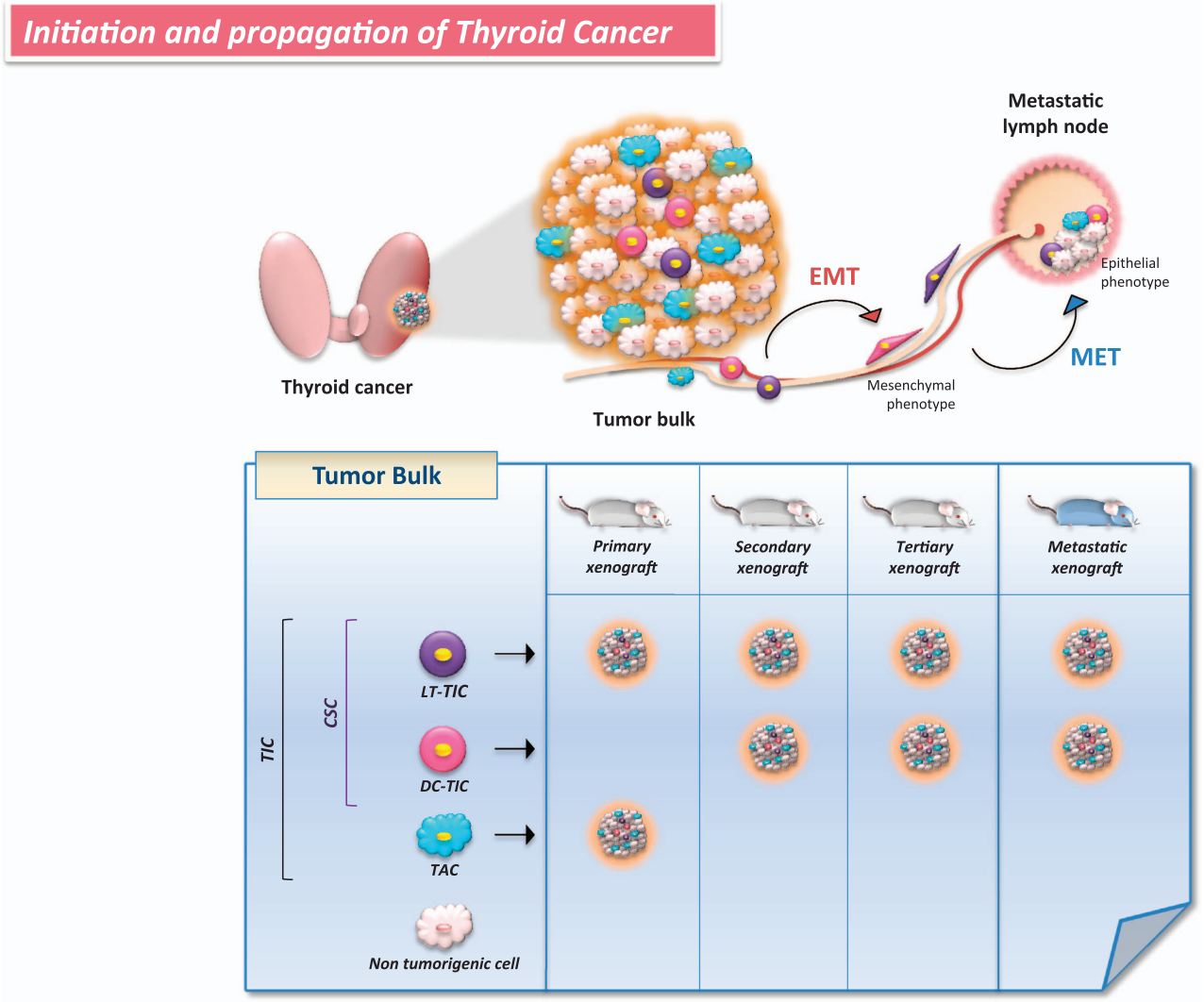

Figure 5. Initiation and propagation of thyroid cancer. Tumour bulk consists of tumourigenic and non-tumourigenic cells. Tumourigenic cells include TICs able to start the tumour; among these, long-term (LT-TIC) and DC-TIC maintain tumour formation after xenograft-transplantation and have characteristics of cancer stem-like cells. Although transit amplifying cells massively contribute to tumour formation, they lack in self-renewal and metastasis-forming features. Some TICs, such as LT-TICs and DC-TICs, are also responsible for tumour dissemination, a mechanism regulated by EMT, whereas the inverse MET drives metastatic colonisation.

10 days *in vitro* expansion, the SP cells reconstituted the full cell population (both SP and MP). MP also generated a small SP, and was tumourigenic in nude mice. This suggests that the SP subset constitutes only a part of the entire CSC component. CSCs are more numerous in the SP, but the two subsets are not identical.[74] Zheng *et al.* identified 0.41–0.83% of the SP in ATC cell lines (SW1736, 0.41%; C643, 0.52%; HTh74, 0.83%) expressing ATP-binding cassette sub-family G member 2 and multidrug resistance protein 1 transporters, which survived a doxorubicin treatment. These cells showed a 10-fold higher clonality and higher invasive features in comparison to the MP. In a 6 months treatment, doxorubicin gradually killed the MP, yet the SP, enriched with Oct-4$^+$ CSCs, constituted 70% of resistant cells. The authors found a composition of thyrospheres in 5% of the SP and $>95\%$ of the MP by FACS analysis.[72] The SP identified in TCs is then characterised by an over-expression of stemness markers and higher clonogenic ability, supported by thyrospheres formation and reconstitution of the MP. Moreover, it displayed chemo-resistance and tumourigenic potential when injected into immunocompromised mice.

THYROID CSCs AND METASTASIS

As observed in the experimental xenograft assay described above, CSCs possess the capacity to seed new tumours when implanted in appropriate animal hosts. This is theoretically analogous to tumour initiation by disseminating tumour cells (DTCs), whose success depends on their ability to spawn an unlimited number of daughter cells (Figure 4). In light of their motility, invasiveness and resistance to apoptosis, CSCs are central players in tumour recurrence and metastasis formation.[81–83] This model is supported by the expression of EMT markers in CSCs and by the activation of SC markers in EMT-induced cells.[84,85]

DTCs are considered the major cause of metastatic disease, chemo-resistance and recurrence, and are characterised by the capacity to migrate from primary tumours to secondary sites. Therefore, DTCs can exist for long time in a quiescent state called dormancy, corresponding to the latent period between primary tumour detection, treatment, recurrence and metastatic spread.[86] The molecular mechanism, responsible for the transition of DTCs from a dormant to a proliferative state, involves a cross-talk between DTCs and the extracellular matrix. Matrix

Table 2. Biological methods for thyroid CSCs isolation and characterisation

Isolation method	*Description*	*Integrative assay*	*References*
Sphere-forming assay	In serum-free non-adherent condition, it allows the purification of CSC population from differentiated thyrocytes and fibroblast, through a negative selection	Clonogenic assay; limiting-diluting assay; colony-forming assay; proliferation and division assay	55,63–65,69,72,73,75
Xenografts assay	The injection of CSCs in immunodeficient mice (NOD/SCID, NSG, nude) led to a tumour formation. Serial transplantations permit the selection of CSCs able to generate more aggressive tumours	Lineage tracing; limiting-dilution injections	63–65
ALDH activity (ALDEFLUOR)	Isolate CSCs based on their elevated ALDH activity: $ALDH^{high}$ cells metabolise their substrate in a fluorescent dye that permits a positive FACS selection		30,63,69
Stemness biomarkers	FACS positive selection based on: ✔*SC transcription factors*: hNanog, Oct-4, transcriptor factor SOX-2 protein ✔*EMT-inducing pathways*: Wnt, Notch1, Sonic hedgehog protein ✔$CD44^{+}/CD24^{-}$ *phenotype* ✔*CD133*	FACS negative selection for differentiation markers: TPO, Tg, NIS, TSH-R	30,63–65,69,71–75,77,78
Side population	Positive selection for drug-resistance based on ABCG2 and ABCB1 activity; these transporters pump out the drug rendering the dye efflux sensitive to verapamil (a Hoechst 33342 inhibitor)		18,72,74

Abbreviations: ALDH, aldehyde dehydrogenase; CSCs, cancer SCs; EMT, epithelial–mesenchymal transition; FACS, fluorescence activated cell sorting; NOD/SCID, non-obese diabetic/severe combined immunodeficiency; NSG, NOD scid gamma; SC, stem cells; Tg, thyroglobulin; TPO, thyroid peroxidase; TSH-R, thyrotropin receptor.

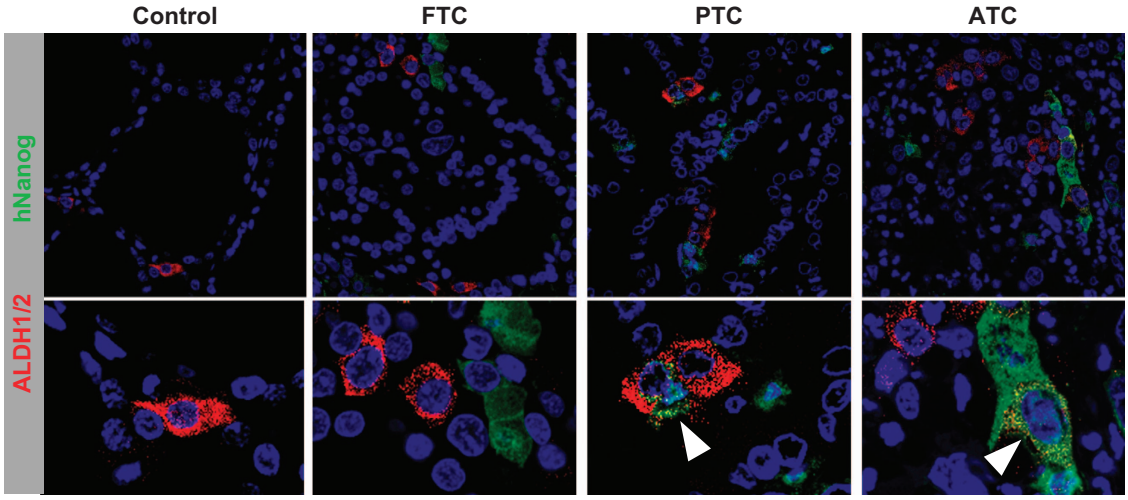

Figure 6. Thyroid CSCs markers. Immunofluorescence analysis of ALDH1/2 and hNanog in control, FTC, PTC and ATC. Arrow heads indicate cells co-expressing ALDH1/2 and hNanog.

metalloproteinases, secreted by stromal cells, induce the switch from tumour dormancy to metastatic growth and vice versa, in some cases through a permissive niche generation. Moreover, integrin signalling regulation directs this mechanism through the extracellular signal-regulated kinase ½ (ERK-1/2) and p38α/β pathways; in particular, high ERK-1/2:p38 signalling ratio promotes primary tumour proliferation and metastatic disease, whereas the opposite determines cellular dormancy.[86,87]

It has become evident that aberrant activation of β-catenin and c-Met is involved in TC progression.[88] Data reported by Todaro *et al.* indicated that Akt, c-Met and β-catenin activation correlates with invasive behaviour of ATC SCs, together with the complete loss of E-cadherin expression. Interestingly, targeted silencing of Akt and c-Met expression, reduced Twist and Snail expression, and abrogated thyroid CSC invasiveness and metastatic capacity.[63]

Other studies identified EMT regulators in TC, with different expression among histotypes. Hardy *et al.* showed decreased E-cadherin expression in differentiated TCs when compared to normal tissues. While *SNAI1* and *SNAI2* were aberrantly transcribed and expressed in follicular (FTC-133), papillary (BCPAP, K1), and anaplastic (CAL-62, 8305C) cell lines, as well as in human cancer samples, in line with the lack of close cellular contact.[89] Vasko *et al.*[90] observed an over-expression of the mesenchymal marker vimentin in PTC human samples, associated with invasion and lymph node metastasis. Moreover, Riesco-Eizaguirre *et al.*[91] reported an over-expression of TGF-β at the invasive front of PTC, suggesting that PTC cells need to undergo EMT and subsequently mesenchymal–epithelial transition (MET), to produce metastasis. In another study, Liu *et al.* found an intense expression of nestin, CD133 and CD44 and an absence of E-cadherin expression in ATC.

Contrarily, PTC and FTC samples showed variability in CD133 and CD44 detection, and were negative for nestin, but positive for E-cadherin.[78]

By tissue microarray analysis, Buehler *et al.* observed that only ATC samples showed a high expression of Snail and Twist associated to a lack of E-cadherin. Otherwise, PTC, FTC and normal specimens were negative for Snail and Twist and, with strong diffused immune reactivity to E-cadherin.[92] Lan *et al.* observed that HIF-1α induced invasive and metastatic properties in follicular cells (FTC-133) through EMT, as confirmed by the downregulation of E-cadherin and upregulation of vimentin. Moreover, it was observed that cells with an over-expression of HIF1α shared stem-like cell features highlighting that EMT induction was directly associated with increased CSC populations.[84]

Several lines of evidence also supported the cross-talk between Twist and ID proteins. Kebebew *et al.*[93] observed over-expression of the DNA-binding protein inhibitor ID-1 in ATC tissues, reporting that the inhibition of ID1 mRNA expression results in decreased growth and reduction of Tg and NIS expression. Moreover, Ciarrocchi *et al.*[94] disclosed that *in vivo* ID-1 expression is associated with aggressiveness and metastatic potential in non-anaplastic tumours, whereas another member of the ID proteins, ID-3 is downregulated in PTC and may be related to the TSH-induced differentiating process.[95]

CONCLUSIONS AND FUTURE PERSPECTIVES

Evidence shows that many pathways underlying the properties of SCs are involved in cancer initiation and progression. A defect in DNA stability is the early event that occurs in tumour transformation followed by a loss of tumour suppressor gene or oncogene activation. Herewith, long-lived SCs rather than short-lived differentiated cells could be the cell compartment in which genetic alterations promote an advantage in clonal propagation. Due to genetic alterations in thyroid cells bearing embryogenesis-associated pathways, transformed SCs represent the undisputed protagonists in the development of TC. In this scenario, further insights into thyroid SC biology could bring to light the molecular mechanisms driving transformation of normal vs cancer SCs and may help design effective anti-cancer strategies.

CONFLICT OF INTEREST

The authors declare no conflict of interest.

ACKNOWLEDGEMENTS

This work was supported by the Italian Association for Cancer Research (AIRC) to GS (AIRC IG 12819). We thank Tatiana Terranova for her editorial assistance and all the colleagues who actively contributed to the completion of this review.

REFERENCES

1 Jemal A, Bray F, Center MM, Ferlay J, Ward E, Forman D. Global cancer statistics. *CA Cancer J Clin* 2011; **61**: 69–90.
2 Kondo T, Ezzat S, Asa SL. Pathogenetic mechanisms in thyroid follicular-cell neoplasia. *Nat Rev Cancer* 2006; **6**: 292–306.
3 Rivera M, Ghossein RA, Schoder H, Gomez D, Larson SM, Tuttle RM. Histopathologic characterization of radioactive iodine-refractory fluorodeoxyglucose-positron emission tomography-positive thyroid carcinoma. *Cancer* 2008; **113**: 48–56.
4 Nikiforov YE, Nikiforova MN. Molecular genetics and diagnosis of thyroid cancer. *Nat Rev Endocrinol* 2011; **7**: 569–580.
5 Kroll TG, Sarraf P, Pecciarini L, Chen CJ, Mueller E, Spiegelman BM *et al.* PAX8-PPARgamma1 fusion oncogene in human thyroid carcinoma [corrected]. *Science* 2000; **289**: 1357–1360.
6 Hou P, Liu D, Shan Y, Hu S, Studeman K, Condouris S *et al.* Genetic alterations and their relationship in the phosphatidylinositol 3-kinase/Akt pathway in thyroid cancer. *Clin Cancer Res* 2007; **13**: 1161–1170.
7 Lin RY. Thyroid cancer stem cells. *Nat Rev Endocrinol* 2011; **7**: 609–616.
8 Gibelli B, El-Fattah A, Giugliano G, Proh M, Grosso E. Thyroid stem cells—danger or resource? *Acta Otorhinolaryngol Ital* 2009; **29**: 290–295.
9 Takano T, Amino N. Fetal cell carcinogenesis: a new hypothesis for better understanding of thyroid carcinoma. *Thyroid* 2005; **15**: 432–438.
10 Nikiforova MN, Nikiforov YE. Molecular diagnostics and predictors in thyroid cancer. *Thyroid* 2009; **19**: 1351–1361.
11 Sastre-Perona A, Santisteban P. Role of the wnt pathway in thyroid cancer. *Front Endocrinol (Lausanne)* 2012; **3**: 31.
12 Garcia-Rostan G, Tallini G, Herrero A, D'Aquila TG, Carcangiu ML, Rimm DL. Frequent mutation and nuclear localization of beta-catenin in anaplastic thyroid carcinoma. *Cancer Res* 1999; **59**: 1811–1815.
13 Quiros RM, Ding HG, Gattuso P, Prinz RA, Xu X. Evidence that one subset of anaplastic thyroid carcinomas are derived from papillary carcinomas due to BRAF and p53 mutations. *Cancer* 2005; **103**: 2261–2268.
14 Hardin H, Montemayor-Garcia C, Lloyd RV. Thyroid cancer stem-like cells and epithelial-mesenchymal transition in thyroid cancers. *Hum Pathol* 2013; **44**: 1707–1713.
15 Nikiforova MN, Ciampi R, Salvatore G, Santoro M, Gandhi M, Knauf JA *et al.* Low prevalence of BRAF mutations in radiation-induced thyroid tumors in contrast to sporadic papillary carcinomas. *Cancer Lett* 2004; **209**: 1–6.
16 Coclet J, Foureau F, Ketelbant P, Galand P, Dumont JE. Cell population kinetics in dog and human adult thyroid. *Clin Endocrinol* 1989; **31**: 655–665.
17 Dumont JE, Lamy F, Roger P, Maenhaut C. Physiological and pathological regulation of thyroid cell proliferation and differentiation by thyrotropin and other factors. *Physiol Rev* 1992; **72**: 667–697.
18 Hoshi N, Kusakabe T, Taylor BJ, Kimura S. Side population cells in the mouse thyroid exhibit stem/progenitor cell-like characteristics. *Endocrinology* 2007; **148**: 4251–4258.
19 Zhang P, Zuo H, Nakamura Y, Nakamura M, Wakasa T, Kakudo K. Immunohistochemical analysis of thyroid-specific transcription factors in thyroid tumors. *Pathol Int* 2006; **56**: 240–245.
20 Takano T. Fetal cell carcinogenesis of the thyroid: theory and practice. *Semin Cancer Biol* 2007; **17**: 233–240.
21 Nikiforov Y, Gnepp DR. Pediatric thyroid cancer after the Chernobyl disaster. Pathomorphologic study of 84 cases (1991-1992) from the Republic of Belarus. *Cancer* 1994; **74**: 748–766.
22 Jhiang SM, Sagartz JE, Tong Q, Parker-Thornburg J, Capen CC, Cho JY *et al.* Targeted expression of the ret/PTC1 oncogene induces papillary thyroid carcinomas. *Endocrinology* 1996; **137**: 375–378.
23 Vermeulen L, Sprick MR, Kemper K, Stassi G, Medema JP. Cancer stem cells—old concepts, new insights. *Cell Death Differ* 2008; **15**: 947–958.
24 Thomas D, Friedman S, Lin RY. Thyroid stem cells: lessons from normal development and thyroid cancer. *Endocr Relat Cancer* 2008; **15**: 51–58.
25 Inaba M, Yamashita YM. Asymmetric stem cell division: precision for robustness. *Cell Stem Cell* 2012; **11**: 461–469.
26 Yamashita YM, Yuan H, Cheng J, Hunt AJ. Polarity in stem cell division: asymmetric stem cell division in tissue homeostasis. *Cold Spring Harb Perspect Biol* 2010; **2**: a001313.
27 Morrison SJ, Kimble J. Asymmetric and symmetric stem-cell divisions in development and cancer. *Nature* 2006; **441**: 1068–1074.
28 Le Douarin N, Fontaine J, Le Lievre C. New studies on the neural crest origin of the avian ultimobranchial glandular cells–interspecific combinations and cytochemical characterization of C cells based on the uptake of biogenic amine precursors. *Histochemistry* 1974; **38**: 297–305.
29 Van Vliet G. Development of the thyroid gland: lessons from congenitally hypothyroid mice and men. *Clin Genet* 2003; **63**: 445–455.
30 Klonisch T, Hoang-Vu C, Hombach-Klonisch S. Thyroid stem cells and cancer. *Thyroid* 2009; **19**: 1303–1315.
31 De Felice M, Di Lauro R. Thyroid development and its disorders: genetics and molecular mechanisms. *Endocr Rev* 2004; **25**: 722–746.
32 Fagman H, Nilsson M. Morphogenetics of early thyroid development. *J Mol Endocrinol* 2011; **46**: R33–R42.
33 Antonica F, Kasprzyk DF, Opitz R, Iacovino M, Liao XH, Dumitrescu AM *et al.* Generation of functional thyroid from embryonic stem cells. *Nature* 2012; **491**: 66–71.
34 Longmire TA, Ikonomou L, Hawkins F, Christodoulou C, Cao Y, Jean JC *et al.* Efficient derivation of purified lung and thyroid progenitors from embryonic stem cells. *Cell Stem Cell* 2012; **10**: 398–411.
35 Davies TF, Latif R, Minsky NC, Ma R. Clinical review: the emerging cell biology of thyroid stem cells. *J Clin Endocrinol Metab* 2011; **96**: 2692–2702.
36 Lin RY, Kubo A, Keller GM, Davies TF. Committing embryonic stem cells to differentiate into thyrocyte-like cells *in vitro*. *Endocrinology* 2003; **144**: 2644–2649.
37 Arufe MC, Lu M, Lin RY. Differentiation of murine embryonic stem cells to thyrocytes requires insulin and insulin-like growth factor-1. *Biochem Biophys Res Commun* 2009; **381**: 264–270.

38 Ma R, Latif R, Davies TF. Thyroid follicle formation and thyroglobulin expression in multipotent endodermal stem cells. *Thyroid* 2013; **23**: 385–391.
39 Green MD, Chen A, Nostro MC, d'Souza SL, Schaniel C, Lemischka IR *et al.* Generation of anterior foregut endoderm from human embryonic and induced pluripotent stem cells. *Nat Biotechnol* 2011; **29**: 267–272.
40 Hannan NR, Fordham RP, Syed YA, Moignard V, Berry A, Bautista R *et al.* Generation of multipotent foregut stem cells from human pluripotent stem cells. *Stem Cell Reports* 2013; **1**: 293–306.
41 Brafman DA, Moya N, Allen-Soltero S, Fellner T, Robinson M, McMillen ZL *et al.* Analysis of SOX2-expressing cell populations derived from human pluripotent stem cells. *Stem Cell Reports* 2013; **1**: 464–478.
42 D'Amour KA, Agulnick AD, Eliazer S, Kelly OG, Kroon E, Baetge EE. Efficient differentiation of human embryonic stem cells to definitive endoderm. *Nat Biotechnol* 2005; **23**: 1534–1541.
43 Onyshchenko MI, Panyutin IG, Panyutin IV, Neumann RD. Stimulation of cultured h9 human embryonic stem cells with thyroid stimulating hormone does not lead to formation of thyroid-like cells. *Stem Cells Int* 2012; **2012**: 634914.
44 Burstein DE, Nagi C, Wang BY, Unger P. Immunohistochemical detection of p53 homolog p63 in solid cell nests, papillary thyroid carcinoma, and hashimoto's thyroiditis: A stem cell hypothesis of papillary carcinoma oncogenesis. *Hum Pathol* 2004; **35**: 465–473.
45 Kusakabe T, Hoshi N, Kimura S. Origin of the ultimobranchial body cyst: T/ebp/Nkx2.1 expression is required for development and fusion of the ultimobranchial body to the thyroid. *Dev Dyn* 2006; **235**: 1300–1309.
46 Ozaki T, Nagashima K, Kusakabe T, Kakudo K, Kimura S. Development of thyroid gland and ultimobranchial body cyst is independent of p63. *Lab Invest* 2011; **91**: 138–146.
47 Cameselle-Teijeiro J, Preto A, Soares P, Sobrinho-Simoes M. A stem cell role for thyroid solid cell nests. *Hum Pathol* 2005; **36**: 590–591.
48 Preto A, Cameselle-Teijeiro J, Moldes-Boullosa J, Soares P, Cameselle-Teijeiro JF, Silva P *et al.* Telomerase expression and proliferative activity suggest a stem cell role for thyroid solid cell nests. *Mod Pathol* 2004; **17**: 819–826.
49 Reis-Filho JS, Preto A, Soares P, Ricardo S, Cameselle-Teijeiro J, Sobrinho-Simoes M. p63 expression in solid cell nests of the thyroid: further evidence for a stem cell origin. *Mod Pathol* 2003; **16**: 43–48.
50 Rios Moreno MJ, Galera-Ruiz H, De Miguel M, Lopez MI, Illanes M, Galera-Davidson H. Inmunohistochemical profile of solid cell nest of thyroid gland. *Endocrine Pathol* 2011; **22**: 35–39.
51 Okamoto M, Hayase S, Miyakoshi M, Murata T, Kimura S. Stem cell antigen 1-positive mesenchymal cells are the origin of follicular cells during thyroid regeneration. *Plos One* 2013; **8**: e80801.
52 Ozaki T, Matsubara T, Seo D, Okamoto M, Nagashima K, Sasaki Y *et al.* Thyroid regeneration: characterization of clear cells after partial thyroidectomy. *Endocrinology* 2012; **153**: 2514–2525.
53 Thomas T, Nowka K, Lan L, Derwahl M. Expression of endoderm stem cell markers: evidence for the presence of adult stem cells in human thyroid glands. *Thyroid* 2006; **16**: 537–544.
54 Fierabracci A, Puglisi MA, Giuliani L, Mattarocci S, Gallinella-Muzi M. Identification of an adult stem/progenitor cell-like population in the human thyroid. *J Endocrinol* 2008; **198**: 471–487.
55 Lan L, Cui D, Nowka K, Derwahl M. Stem cells derived from goiters in adults form spheres in response to intense growth stimulation and require thyrotropin for differentiation into thyrocytes. *J Clin Endocrinol Metab* 2007; **92**: 3681–3688.
56 Visvader JE. Cells of origin in cancer. *Nature* 2011; **469**: 314–322.
57 Visvader JE, Lindeman GJ. Stem cells and cancer—the promise and puzzles. *Mol Oncol* 2010; **4**: 369–372.
58 Chaffer CL, Brueckmann I, Scheel C, Kaestli AJ, Wiggins PA, Rodrigues LO *et al.* Normal and neoplastic nonstem cells can spontaneously convert to a stem-like state. *Proc Natl Acad Sci USA* 2011; **108**: 7950–7955.
59 Dieter SM, Ball CR, Hoffmann CM, Nowrouzi A, Herbst F, Zavidij O *et al.* Distinct types of tumor-initiating cells form human colon cancer tumors and metastases. *Cell Stem Cell* 2011; **9**: 357–365.
60 Zeuner A, De Maria R. Not so lonely at the top for cancer stem cells. *Cell Stem Cell* 2011; **9**: 289–290.
61 Shahriyari L, Komarova NL. Symmetric vs. asymmetric stem cell divisions: an adaptation against cancer? *Plos One* 2013; **8**: e76195.
62 Schweppe RE, Klopper JP, Korch C, Pugazhenthi U, Benezra M, Knauf JA *et al.* Deoxyribonucleic acid profiling analysis of 40 human thyroid cancer cell lines reveals cross-contamination resulting in cell line redundancy and misidentification. *J Clin Endocrinol Metab* 2008; **93**: 4331–4341.
63 Todaro M, Iovino F, Eterno V, Cammareri P, Gambara G, Espina V *et al.* Tumorigenic and metastatic activity of human thyroid cancer stem cells. *Cancer Res* 2010; **70**: 8874–8885.
64 Li W, Reeb AN, Sewell WA, Elhomsy G, Lin RY. Phenotypic characterization of metastatic anaplastic thyroid cancer stem cells. *Plos One* 2013; **8**: e65095.
65 Ahn SH, Henderson YC, Williams MD, Lai SY, Clayman GL. Detection of thyroid cancer stem cells in papillary thyroid carcinoma. *J Clin Endocrinol Metab* 2014; **99**: 536–544.
66 Ailles LE, Weissman IL. Cancer stem cells in solid tumors. *Curr Opin Biotechnol* 2007; **18**: 460–466.
67 Clarke MF, Dick JE, Dirks PB, Eaves CJ, Jamieson CH, Jones DL *et al.* Cancer stem cells—perspectives on current status and future directions: AACR Workshop on cancer stem cells. *Cancer research* 2006; **66**: 9339–9344.
68 Marcato P, Dean CA, Giacomantonio CA, Lee PW. Aldehyde dehydrogenase: its role as a cancer stem cell marker comes down to the specific isoform. *Cell Cycle* 2011; **10**: 1378–1384.
69 Carina V, Zito G, Pizzolanti G, Richiusa P, Criscimanna A, Rodolico V *et al.* Multiple pluripotent stem cell markers in human anaplastic thyroid cancer: the putative upstream role of SOX2. *Thyroid* 2013; **23**: 829–837.
70 Rodda DJ, Chew JL, Lim LH, Loh YH, Wang B, Ng HH *et al.* Transcriptional regulation of nanog by OCT4 and SOX2. *J Biol Chem* 2005; **280**: 24731–24737.
71 Friedman S, Lu M, Schultz A, Thomas D, Lin RY. CD133+ anaplastic thyroid cancer cells initiate tumors in immunodeficient mice and are regulated by thyrotropin. *Plos One* 2009; **4**: e5395.
72 Zheng X, Cui D, Xu S. Brabant G, Derwahl M. Doxorubicin fails to eradicate cancer stem cells derived from anaplastic thyroid carcinoma cells: characterization of resistant cells. *Int J Oncol* 2010; **37**: 307–315.
73 Tseng LM, Huang PI, Chen YR, Chen YC, Chou YC, Chen YW *et al.* Targeting signal transducer and activator of transcription 3 pathway by cucurbitacin I diminishes self-renewing and radiochemoresistant abilities in thyroid cancer-derived CD133 + cells. *J Pharmacol Exp Ther* 2012; **341**: 410–423.
74 Mitsutake N, Iwao A, Nagai K, Namba H, Ohtsuru A, Saenko V *et al.* Characterization of side population in thyroid cancer cell lines: cancer stem-like cells are enriched partly but not exclusively. *Endocrinology* 2007; **148**: 1797–1803.
75 Malaguarnera R, Frasca F, Garozzo A, Giani F, Pandini G, Vella V *et al.* Insulin receptor isoforms and insulin-like growth factor receptor in human follicular cell precursors from papillary thyroid cancer and normal thyroid. *J Clin Endocrinol Metab* 2011; **96**: 766–774.
76 Zito G, Richiusa P, Bommarito A, Carissimi E, Russo L, Coppola A *et al. In vitro* identification and characterization of CD133(pos) cancer stem-like cells in anaplastic thyroid carcinoma cell lines. *Plos One* 2008; **3**: e3544.
77 Ke CC, Liu RS, Yang AH, Liu CS, Chi CW, Tseng LM *et al.* CD133-expressing thyroid cancer cells are undifferentiated, radioresistant and survive radioiodide therapy. *Eur J Nucl Med Mol Imaging* 2013; **40**: 61–71.
78 Liu J, Brown RE. Immunohistochemical detection of epithelialmesenchymal transition associated with stemness phenotype in anaplastic thyroid carcinoma. *Int J Clin Exp Pathol* 2010; **3**: 755–762.
79 Sun Y, Kong W, Falk A, Hu J, Zhou L, Pollard S *et al.* CD133 (prominin) negative human neural stem cells are clonogenic and tripotent. *Plos One* 2009; **4**: e5498.
80 Golebiewska A, Brons NH, Bjerkvig R, Niclou SP. Critical appraisal of the side population assay in stem cell and cancer stem cell research. *Cell Stem Cell* 2011; **8**: 136–147.
81 Hollier BG, Evans K, Mani SA. The epithelial-to-mesenchymal transition and cancer stem cells: a coalition against cancer therapies. *J Mammary Gland Biol Neoplasia* 2009; **14**: 29–43.
82 Raimondi C, Gianni W, Cortesi E, Gazzaniga P. Cancer stem cells and epithelial-mesenchymal transition: revisiting minimal residual disease. *Curr Cancer Drug Targets* 2010; **10**: 496–508.
83 Chaffer CL, Weinberg RA. A perspective on cancer cell metastasis. *Science* 2011; **331**: 1559–1564.
84 Lan L, Luo Y, Cui D, Shi BY, Deng W, Huo LL *et al.* Epithelial-mesenchymal transition triggers cancer stem cell generation in human thyroid cancer cells. *Int J Oncol* 2013; **43**: 113–120.
85 Mani SA, Guo W, Liao MJ, Eaton EN, Ayyanan A, Zhou AY *et al.* The epithelial-mesenchymal transition generates cells with properties of stem cells. *Cell* 2008; **133**: 704–715.
86 Paez D, Labonte MJ, Bohanes P, Zhang W, Benhanim L, Ning Y *et al.* Cancer dormancy: a model of early dissemination and late cancer recurrence. *Clin Cancer Res* 2012; **18**: 645–653.
87 Sosa MS, Avivar-Valderas A, Bragado P, Wen HC, Aguirre-Ghiso JA. ERK1/2 and p38alpha/beta signaling in tumor cell quiescence: opportunities to control dormant residual disease. *Clin Cancer Res* 2011; **17**: 5850–5857.
88 Cassinelli G, Favini E, Degl'Innocenti D, Salvi A, De Petro G, Pierotti MA *et al.* RET/PTC1-driven neoplastic transformation and proinvasive phenotype of human thyrocytes involve Met induction and beta-catenin nuclear translocation. *Neoplasia* 2009; **11**: 10–21.
89 Hardy RG, Vicente-Duenas C, Gonzalez-Herrero I, Anderson C, Flores T, Hughes S *et al.* Snail family transcription factors are implicated in thyroid carcinogenesis. *Am J Pathol* 2007; **171**: 1037–1046.

90 Vasko V, Espinosa AV, Scouten W, He H, Auer H, Liyanarachchi S *et al.* Gene expression and functional evidence of epithelial-to-mesenchymal transition in papillary thyroid carcinoma invasion. *Proc Natl Acad Sci USA* 2007; **104**: 2803–2808.
91 Riesco-Eizaguirre G, Rodriguez I, De la Vieja A, Costamagna E, Carrasco N, Nistal M *et al.* The BRAFV600E oncogene induces transforming growth factor beta secretion leading to sodium iodide symporter repression and increased malignancy in thyroid cancer. *Cancer Res* 2009; **69**: 8317–8325.
92 Buehler D, Hardin H, Shan W, Montemayor-Garcia C, Rush PS, Asioli S *et al.* Expression of epithelial-mesenchymal transition regulators SNAI2 and TWIST1 in thyroid carcinomas. *Mod Pathol* 2013; **26**: 54–61.
93 Kebebew E, Peng M, Treseler PA, Clark OH, Duh QY, Ginzinger D *et al.* Id1 gene expression is up-regulated in hyperplastic and neoplastic thyroid tissue and regulates growth and differentiation in thyroid cancer cells. *J Clin Endocrinol Metab* 2004; **89**: 6105–6111.
94 Ciarrocchi A, Piana S, Valcavi R, Gardini G, Casali B. Inhibitor of DNA binding-1 induces mesenchymal features and promotes invasiveness in thyroid tumour cells. *Eur J Cancer* 2011; **47**: 934–945.
95 Deleu S, Savonet V, Behrends J, Dumont JE, Maenhaut C. Study of gene expression in thyrotropin-stimulated thyroid cells by cDNA expression array: ID3 transcription modulating factor as an early response protein and tumor marker in thyroid carcinomas. *Exp Cell Res* 2002; **279**: 62–70.

Chapter 2

In vitro Human Embryonic Stem Cells differentiation: a reliable model for thyroid carcinogenesis

Emanuela Scavo, Miriam Gaggianesi, Laura Rosa Mangiapane, Tiziana Apuzzo, Antonina Benfante, Simone Di Franco, Matilde Todaro and Giorgio Stassi

Manuscript in preparation

Abstract

Stem cells are unspecialized cells with the ability to perpetuate themselves for long periods and give rise to specialized cell types. Although it was postulated that tumor may often originate from stem cells transformation, the target cell of transforming mutations is still unknown. It is becoming increasingly clear that distinct cancer cells within an organ may derive from different cells-of-origin able to acquire the first driven mutation giving rise to a broad spectrum of cancer histotypes. Here we present an innovative and reliable experimental approach to study the cellular hierarchy of normal thyroid tissue in order to identify the target cells of transforming mutations underling the thyroid carcinogenesis. Identification of the cells-of-origin and tumor-related driven mutations might be an essential prerequisite to design innovative therapeutic approach.

2.1 Introduction

Thyroid cancer (TC) is the most common endocrine malignancy including different histotypes that range from differentiated carcinomas with good prognosis to the lethal undifferentiated disease. Papillary TC (PTC) and follicular TC (FTC) referred as well-differentiated thyroid cancer, and anaplastic TC (ATC), an undifferentiated subtype of thyroid cancer, arise from follicular cells. PTC and FTC are indolent carcinomas and can be treated *via* surgical resection in combination with radioactive iodine and l-thyroxine therapy. The loss expression of typical thyroid differentiation markers such as thyroid-stimulating hormone receptor (TSH-R), thyroglobulin (Tg), thyroid peroxidase (TPO), and sodium iodide symporter (NIS), defines the characteristics of ATC, which has a poor prognosis with no effective therapy. Alterations of key factors in MAPK and PI3K/Akt signalling pathways have been shown to be involved in the development of thyroid carcinoma. *RET/PTC* rearrangements and *BRAF* or *RAS* point mutations are frequently observed in PTC and are considered mutually exclusive. The most common genetic alterations in FTC and ATC are *PAX8/PPARγ* rearrangements and *TP53* point mutations, respectively (1-7).

Recent advances in the field of stem cell biology led to the acquisition of new insights into the molecular mechanisms underlying disease processes. Stem cells (SCs) have self-renewal capability and possess the key features required for the acquisition of genetic or epigenetic changes involved in cancer development (6-11). Research findings supported the concept that tumors are organized in a hierarchy of different tumor cells and only a sub-population with stem-cell like characteristics, called Cancer stem cells (CSCs), is responsible for tumor initiation and progression. Cancer heterogeneity can be impacted by several determinants influencing tumor progression and therapeutic response. Strong evidence is emerging that tumor of a single patient is a mixture of genetically distinct clones. The driver mutations within each clone can influence the tumor features in each in one's own way contributing to functional heterogeneity. At the same time, non-genetic determinants, including developmental pathways and epigenetic modifications contribute to functional heterogeneity. Non-genetic determinants, normally involved in the maintenance of normal tissue stem cell hierarchies, bring to hierarchically organized tumor tissues where CSCs uniquely sustain the malignant growth (12-19). According to this hypothesis, a new view of TC was proposed describing it as a stem cell disease. The CSCs model suggests that only a subpopulation of thyroid cancer cells, with self-renewal ability, was able to

differentiate into diverse cancer cell types that can reconstitute and sustain tumor growth. These cells also mediate metastasis and are refractory to chemo- or radiation therapy (20-23). In order to understand the molecular mechanisms involved in thyroid tumorigenesis and chemotherapy resistance, considerable research efforts have been addressed to identify and isolate thyroid CSCs.

Todaro et al., showed that thyroid cancer tissues derived from PTC, FTC and ATC, contain a small population of CSCs identifiable through their high ALDH activity and unlimited self-renewal ability. These $ALDH^{high}$ cells can be expanded indefinitely *in vitro* as tumor spheres, and when orthotopically injected into the thyroid gland of immunocompromised mice can be able to generate serial tumor xenografts, reproducing the phenotypic characteristics of the parental tumors (24).

Although it is widely assumed that tumor phenotype is influenced by genetic lesions, it is becoming increasingly clear that distinct cancers within an organ may originate from cells at different differentiation stages giving rise to several cancer histotypes. According to this new idea, the cell-of-origin concept explains how an early precursor cell or a more committed cell could acquire the first driven mutation able to initiate the tumor. The cell-of-origin and CSC models are not mutually exclusive but cooperate to determine tumor phenotype by different cellular and molecular mechanisms (12-13). The existence of several differentiation degrees led to the assumption that a pool of SCs at different differentiation stages, prone to gain mutations, is responsible for thyroid cancer initiation and progression. A novel hypothesis about thyroid carcinogenesis posits that thyroid cancer cells derive from the remnants of fetal cells. Regarding to this theory, thyroid cancer cells would be generated from transformation of three types of fetal thyroid cells, thyroid SCs (TSCs), thyroblasts and prothyrocytes, which would result in ATC, PTC and FTC, respectively (21, 25).

Since the tumor bulk is characterized by cells at diverse differentiation stages and assuming the involvement of SCs in thyroid carcinogenesis, it was necessary to clarify the SCs' dual role in tumor initiation and propagation. With the aim to cross the difficulties in purification of cell compartments at diverse stages of differentiation, in the present study we generated TSCs, thyroblasts and prothyrocytes from human embryonic stem cells (hESCs) (26-34). As already described in detail in Chapter 1, human thyroid development requires a network of transcription factors that acts to drive thyroid organogenesis. The thyroid gland consists of two endocrine cell types,

the thyroid follicular cells (TFCs) that produce the thyroid hormones T3 and T4 and the C-cells that produce calcitonin (35). During thyroid organogenesis, TTF-1 and Pax-8 co-expression in a small group of ventral foregut endodermal cells is an essential event for cell commitment towards a TFC fate. (24, 31). The hESC-derived endoderm transition into thyroid progenitors is finely regulated by the time-dependent BMP and activin/TGF-β signaling pathway inhibition, followed by BMP and FGF signaling reactivation (31). Here we speculate that the *in vitro* differentiation of hESCs into thyroid cells represents an innovative and reliable experimental approach to study the cellular hierarchy of normal thyroid tissue in order to provide new ground for the identification of cells-of-origin and tumor-related driven mutations involved in thyroid carcinogenesis. Our intent is to prove that the different thyroid tumor histotypes are determined by distinct genetic alterations occurring within the same target cells, that are TCSs, or specific mutations taking place in distinct cells-of-origin, at different differentiation stages of the thyroid tissue (Fig. 1A and 1B) (6).

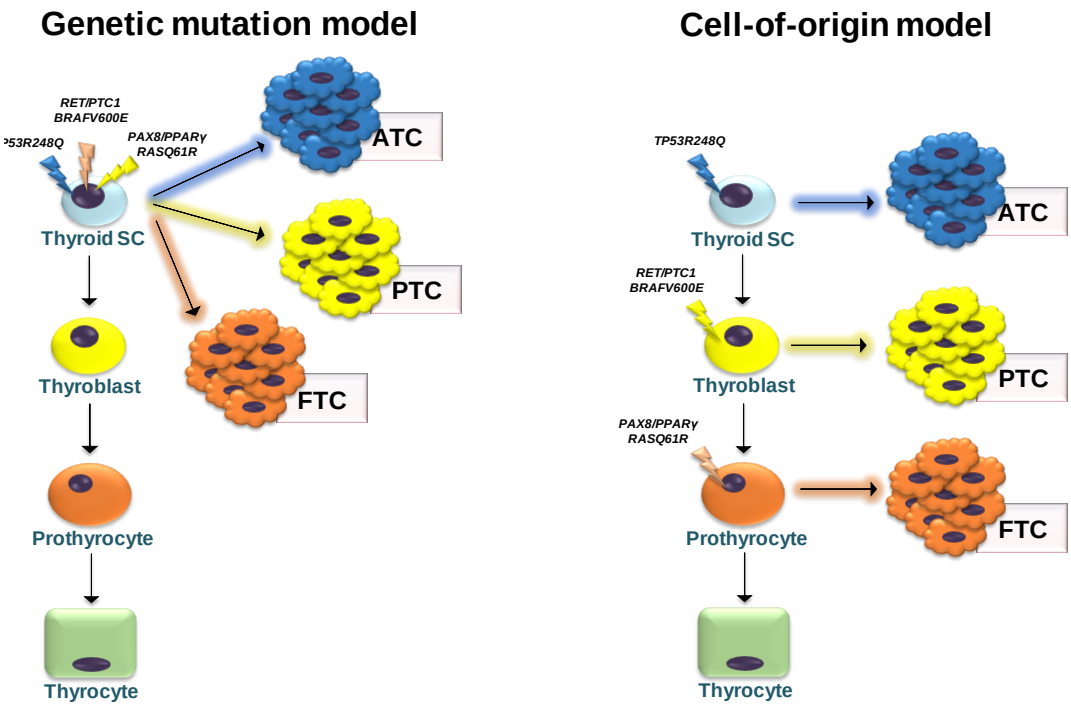

Figure 1. Tumor heterogeneity models. (**A**) In genetic mutation model, different genetic alterations occurring within the same target cells result in various tumor phenotypes. (**B**) In the cell-of-origin model, different tumor phenotypes derive from specific genetic alterations taking place in distinct cell populations that serve as cell-of-origin.

2.2 Materials and Methods

2.2.1 Tissues, cell culture, clonogenic and invasion assays

Thyroid cancer tissues were obtained at the time of thyroidectomy from patients affected by PTC, FTC and ATC in accordance with the ethical standards of the institutional committee responsible for human experimentation. Normal thyroid tissues were obtained from goiters. Diagnosis was based on the histological analysis of thyroid specimens determining size, tumor progression and the involvement of regional lymph nodes. Staging was established according to the UICC TNM classification of malignant tumor (ICD- O C73) (UICC TNM. Classification of Malignant Tumors; 7th Edition. New York: Wiley Liss 2002). Normal and tumor thyroid cells were purified from fresh tissues as described in ref. (24). In these conditions, differentiated cancer cells and normal cells will die by anoikis, while CSCs will grow as sphere aggregates. For clonogenic assay cells were plated on ultra low-adhesion 96-well plates at a concentration of a single cell per well in presence of stem cell medium containing bFGF (20ng/ml, NOVUS Biologicals) and EGF (10ng/ml, NOVUS Biologicals). Wells containing either none or more than one cell were excluded for the analysis. Cell migration was measured using growth factor–depleted Matrigel-coated (BD Biosciences) transwell inserts. Dissociated sphere cells (1.5×10^3) were plated onto Matrigel-coated transwells with 8μm pore size. DMEM supplemented with 5% of human serum was plated in the lower compartment of the transwell. After plating, migrated cells were counted up to 72 hours.

hESCs culture and differentiation

hESCs (line WA26), obtained from National Stem Cell Bank (Madison, WI), were maintained in the undifferentiated state in feeder-free culture conditions using Essential 8^{TM} Medium (Gibco by Thermo Fisher Scientific) on 6-well plates coated with hESCs qualified Matrigel as recommended by manufacturer's instructions (Corning). The culture medium was changed daily, and cells were passaged every four to five days at ratios of 1:2 to 1:4. Cells were cultured at 37°C in a 5% CO^2 humidified incubator. Differentiation of hESCs into definitive endoderm was performed using STEMdiff™ Definitive Endoderm Kit following the manufacturer's instructions (Stemcell technologies). Day 5 hESC-derived endoderm cells, plated onto hESCs qualified matrigel-coated plates, were cultured for 24 hours in Serum free differentiation medium (cSFDM) containing IMDM 375ml, Ham's F12 125ml, B-27

supplement 5ml (Gibco, Thermo Fischer Scientific), N-2 supplement 2.5ml (Gibco, Thermo Fischer Scientific), BSA 7.5% in PBS 3.3ml (USBiological), 200mM L-Glut -1ml (EuroClone) and Ascorbic Acid 1ml of stock 5mg/ml (Sigma), supplemented with 100ng/ml Noggin (R&D System) and 10μM SB431542 (Selleckchem). After 24 hours the media was switched to TTF-1 induction media cSFDM supplemented with 100ng/ml Wnt3a (R&D System), 10ng/ml KGF (Peprotech), 10ng/ml hFGF10 (Peprotech), 10ng/ml BMP4 (R&D System), 20ng/ml hEGF (NOVUS Biologicals), 500ng/ml FGF2 (NOVUS Biologicals) and 100ng/ml Heparin Sodium Salt (Sigma). On day 22, where indicated in the text, the media was switched to thyroid maturation media consisted of Ham's F12 supplemented with 15mM HEPES (pH 7.4), 0.8mM CaCl2, 0.25% BSA, 5μg/ml insulin, 5μg/ml transferrin, 5ng/ml Naselenite (BD Biosciences), 100 U/mL TSH (Sigma), 50ng/mL IGF1 (NOVUS Biologicals), 100 μM NaI.

2.2.2 Flow cytometry

Freshly isolated hESCs (Day 0) and definitive endoderm (Day 5) were stained with conjugated antibodies against SOX-2-ALEXA FLUOR 488 (245610, mouse IgG2a, BD Biosciences), Nanog-ALEXA FLUOR 488 (N31-355, mouse IgG1k, BD Biosciences), SOX-17-ALEXA FLUOR 488 (P7-969, mouse IgG1k, BD Biosciences), Oct-3/4-PE (40/OCT3, mouse IgG1k, BD Biosciences), Foxa2-PE (N17-280, mouse IgG1k, BD Biosciences), CXCR-4-PE (12G5, mouse IgG2a, R&D Systems) or with purified primary TTF-1 (SPT24, mouse IgG_1k; Leica Biosystem), TSH-R (4C1, mouse IgG_2a; Abcam), TPO (EPR5380, rabbit IgG; Abcam), Tg (EPR9730, rabbit IgG; Abcam), NIS (SPM186, mouse IgG1; Abcam), Pax8 (goat polyclonal, IgG; Abcam) and c-Kit (T595, mouse IgG_1k; Leica Biosystem). Then, cells were labeled with goat, rabbit and/or anti-mouse IgG FITC secondary antibody (Invitrogen). Specific corresponding isotype matched antibodies were used as negative controls. Samples were acquired using a FACS ARIA (BD Biosciences) flow cytometer. All data were analyzed using FlowJo software (Tree Star).

2.2.3 Istochemistry and Immunofluorescence

Histochemical is performed on 5-μm-thick paraffin-embedded sections of thyroid specimens. For H&E staining slides were stained for 1 min in hematoxilin, washed in water and then exposed for 30 sec to eosin. Stained sections were dehydrated and mounted in synthetic resin. For immunofluorescence, cytospins of hESCs (Day 0),

definitive endoderm (Day 5), thyroid competent definitive endoderm (Day 6), thyreoblasts (Day 22), prothyrocytes (Day 25) and follicle (day 32) were fixed with 2% paraformaldehyde, permeabilized with 0.1% Triton X-100 and exposed overnight at 4°C to antibodies against to SOX-2 (245610, rabbit polyclonal, IgG polyclonal; Stemgent), Nanog (N17, goat IgG; Santa Cruz Biotechnology), Oct-3/4 (C-10, mouse IgG_2b; Santa Cruz Biotechnology), Foxa2 (N17-280, mouse IgG_1k; BD Biosciences), SOX-17 (P7-969, mouse IgG_1k; BD BD Biosciences), TTF-1 (SPT24, mouse IgG_1k; Leica Biosystem), TSH-R (4C1, mouse IgG_2a; Abcam), TPO (EPR5380, rabbit IgG; Abcam), Tg (EPR9730, rabbit IgG; Abcam), NIS (SPM186, mouse IgG1; Abcam), Pax8 (goat polyclonal, IgG; Abcam), cytocheratin 19 (B170, NCL-CK19, Novocastra) and c-Kit (T595, mouse IgG_1k; Leica Biosystem). Cells were then labeled with FITC or rhodamine red–conjugated secondary antibodies (Invitrogen) plus RNase (200μg/mL; Sigma). Counterstaining was performed using Toto3 iodide (642/660; Invitrogen).

2.2.4 microRNA expression analysis

Total RNA was extracted using a TRIzol® Reagent solution (Ambion) following manufacturer's instructions and microRNA expression analysis was performed by Megaplex pools protocol specific for a set of 384 microRNAs (pool A) as recommended by manufacturer's instructions (Applied Biosystems). The relative quantification of microRNA expression was calculated using the equivalent Ct values where the original Ct values are projected to 100% target efficiency. All the experiments were normalized using global normalization method (39). microRNA arrays were performed for hESCs (Day 0), definitive endoderm (Day 5), thyroid competent definitive endoderm (Day 6), thyreoblasts (Day 22) and prothyrocytes (Day 25). At least 2 replicates were run for each sample. microRNAs with 2 fold changes were considered for analysis.

2.2.5 Production of lentiviral particles and infection

BRAFV600E cDNA with 5'- and 3' cohesive ends was subcloned at XhoI and EcoRV sites, while RET/PTC1 cDNA at XbaI and EcoRV. TP53R248Q cDNA was subcloned at XhoI site. Gene transfer was performed using a TWEEN lentiviral vector containing green fluorescent protein (GFP) and red fluorescent protein (RFP) as reporter gene. Transfection of packaging human embryonic kidney cell line HEK-293T was assessed using FuGENE 6 Reagent (Roche) and following the

manufacturer's instructions. Lentiviral supernatants were collected following 48 hours transfection and filtered with a 45μm mesh. Then, normal thyroid stem cells were exposed to 1mL of viral supernatant of BRAFV600E, RET/PTC1 or TP53R248Q for 40 min by centrifugation at 800 rpm, in the presence of 8μg/μL of polybrene to improve infection efficiency. Infection was repeated twice and efficiency of gene delivery was verified monitoring GFP and/or RFP expression.

2.2.6 Animal model

To evaluate the tumorigenicity and metastatic potential dissociated normal thyrospheres as well as those transduced with lentiviral vectors coding for RET/PTC1, BRAV600E, p53R248Q ($5x10^5$) were injected subcutaneously with Matrigel GF reduced (BD Biosciences) at a 1:1 ratio in a total volume of 100 μL. Tumor size was calculated once a week up for to 10 weeks according to the following formula: ($\pi/6$) x larger diameter x (smaller diameter)^2.

2.3 Results and Discussion

2.3.1 Oncogenes orchestrating the thyroid stem cells transformation

A better knowledge of the genetic alterations which occur in SCs leading to CSCs transformation may provide unique signatures for the development of more effective therapeutic strategies. In our previous study, we investigated whether self-renewal capacity is directly correlated with the most common genetic alterations in thyroid cancer. For this purpose, we generated a single cell cloning assay for TSCs isolated from goiters and transduced with lentiviral vectors coding for R ET/PTC1, BRAFV600E, and/or mutant TP53 (6) in order to determine whether these genetic hits might directly influence the self-renewal capacity (Fig. 2A and 2B). In accordance with the clonogenic potential detected in thyroid CSCs (24), we have interestingly noticed that the exogenous expression of BRAFV600E is associated with a lower clonogenicity than RET/PTC1 rearrangement and mutant p53, while combination of BRAFV600E and mutant TP53, which characterize the aggressive ATC histotype, is associated to the highest clonogenic activity (Fig. 2A and 2B). Furthermore, TSCs, after exogenous expression of RET/PTC1, BRAFV600E, and/or mutant TP53 showed a higher migration capacity than the control TSCs in the invasion assay analysis (Fig. 2C and 2D). In particular, the most invasive cells were those bearing BRAFV600E plus mutant TP53 (Fig. 2C and 2D) . These results resembling the behavior observed on CSCs freshly isolated from ATC, PTC and FTC patients bearing the above mentioned mutations (Fig. 2A, 2B, 2C and 2D) (24).

In order to evaluate the ability to initiate tumor development in recipient animals, a prerequisite of putative CSCs, it has been investigated the *in vivo* tumorigenic capacity of TSCs transduced with the indicated oncogenes by subcutaneous injection in NOD/SCID mice (Fig. 2E). Interestingly, macroscopic examination of xenografts removed after 10 weeks showed that TSCs overexpressing RET/PTC1 rearrangement or mutant TP53 alone were tumorigenic and TSCs bearing BRAFV600E plus mutant TP53 retain the highest tumorigenic capacity (Fig. 2E). Thus, our preliminary data suggest that combined genetic alterations sustain the growth of a tumor cell subset with CSC peculiarities. This population, characterized by unlimited lifespan, not necessarily originate from the transformation of normal SCs but could likely derive from well-differentiated tumor cells *via* the sequential accumulation of genetic mutations and de-differentiation process (6-7).

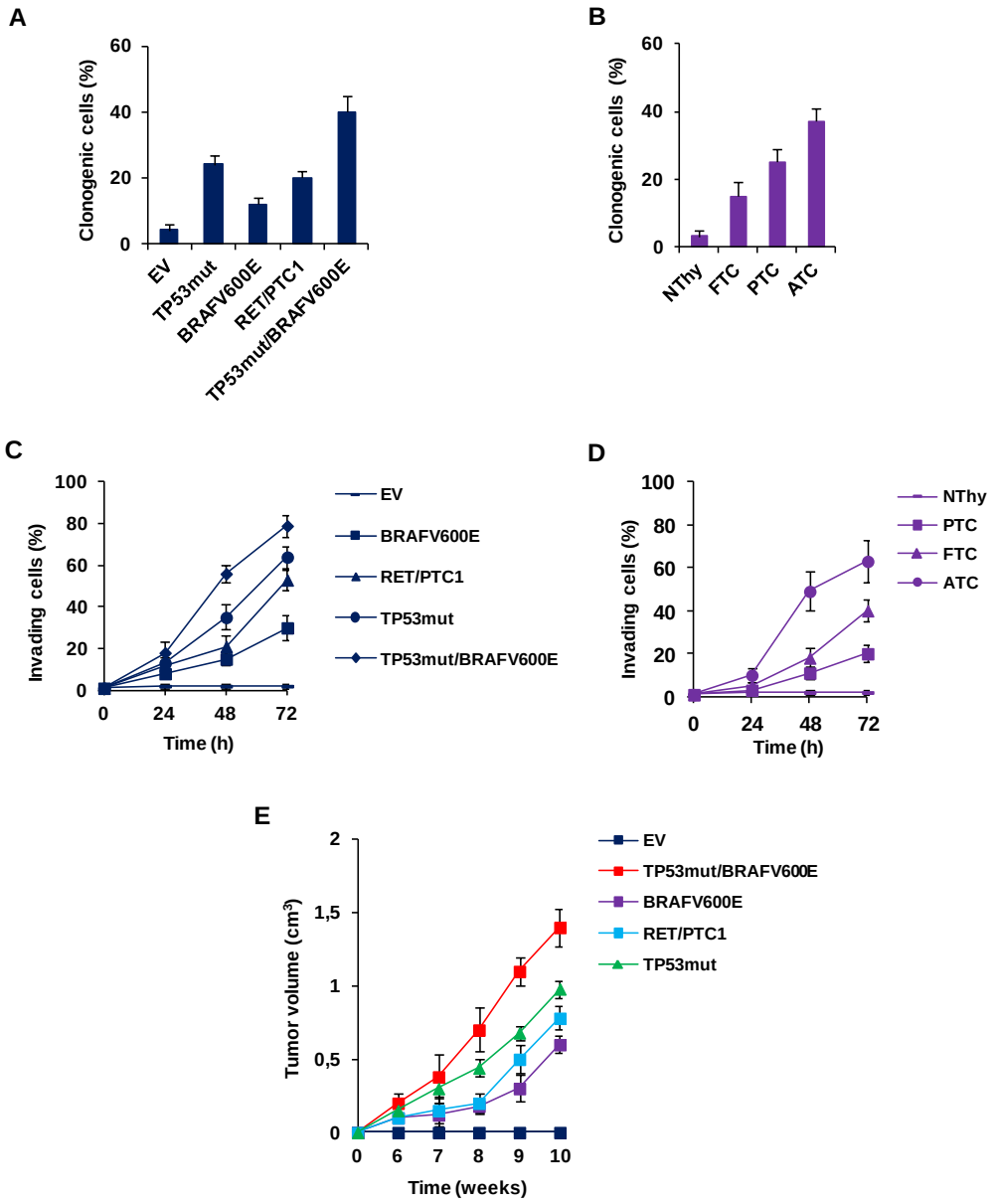

Figure 2. Oncogenes drive transformation of TSCs in tumorigenic cells. (**A**) Clonogenic assay of TSCs isolated from goiters and trasduced with control empty lentiviral vector (EV), and lentiviral vector coding for TP53mut, BRAFV600E, RET/PTC1 and TP53mut/BRAFV600E. (**B**) Clonogenic assay of TSCs isolated from goiters (Nthy, control) and CSCs isolated from ATC, PTC and FTC specimes. (**C**) Invasion assay of TSCs isolated from goiters and trasduced with EV and oncogens above mentioned. (**D**) Invasion assay of TSCs isolated from goiters (Nthy, control) and CSCs isolated from ATC, PTC and FTC specimes. (**E**) Size of tumors developed following subcutane injection of TSCs isolated from goiters and trasduced with EV and oncogens above mentioned.

2.3.2 The time-dependent BMP and activin/TGF-β signaling inhibition renders hESC-derived endodermal cells competent to differentiate into thyroid-like cells

Although SCs, with their unique self-renewal potential, are considered the favored candidates for sequential accumulation of genetic alterations required for tumor transformation, any cell with proliferative capacity, within the hierarchy in a normal tissues, could be considered a cell-of-origin able to initiate a tumor. The growing body of experimental evidence has revealed that an accumulation of genetic alterations in tissue-resident stem cells or in their more committed progenies may result in their malignant transformation. According to this theory, thyroid cancer cells would be generated from transformation of cell compartment at different stages of differentiation, TSCs, thyroblasts and prothyrocytes, which would result in ATC, PTC and FTC, respectively. This observation mostly reflects the need to identify the cells-of-origin and tumor-related driven mutations in order to explain the transition from non-malignant hyper-proliferative lesion to well established thyroid cancers and translate the identified alterations into new therapies. Thus, the aim of this work was to demonstrate that the thyroid tumor histotypes derive from distinct genetic alterations occurring within the same target cells, that are TCSs, or from distinct cells-of-origin, at diverse differentiation stages, able to acquire the first driven-mutation having the ability to initiate the tumor (Fig. 1A and 1B). With a view to differentiate *in vitro* hESCs into thyroid-like cells at different stages of differentiation, we tested various experimental approaches, among which we decided to use the most reliable protocol to recapitulate the key signaling pathways occurring during *in vivo* human thyroid development (Fig 3A, 3B and 3C). The implication of Nodal and Wnt signaling pathways in vertebrate definitive endoderm (DE) differentiation is well described. Activin A and Wnt activators in combination with Noggin, a BMP antagonist, are commonly used to direct the mesendoderm towards anterior foregut endoderm derivatives such as thyroid gland (32, 36-38). Monolayer of hESCs seeded in matrigel and treated with Activin A and low serum produced cultures consisting of up to 80% definitive endoderm cells in 5 days as shown by Foxa2, SOX-17, c-Kit and CXCR-4 endodermal markers expression (Fig. 3A, 3D, 3E, 3F and 3G). In order to direct DE towards the thyroid competent DE positive for SOX-2 and Foxa2 anterior foregut endodermal markers, day 5 hESC-derived endoderm cells were exposed for 24 hours to BMP and activin/TGF-β signalling inhibitors (Noggin and SB431542, respectively) (Fig. 3A, 3F and 3G). Stage-specific inhibition of BMP and TGF-β

signaling renders these endodermal progenitors competent to specify efficiently into endodermal thyroid progenitors expressing TTF-1 (Fig. 3A, 3F and 3G). Induction of BMP and FGF signaling by exposing these cells, until day 22, to specific factors including BMP-4, Wnt3a, FGF-10, FGF-7, EGF, FGF2, FGF10 and heparin (WFKBEF2-F10), resulted in the specification of thyroid competent DE into thyroid progenitor cells expressing specific thyroid markers such as TTF-1, Pax-8, Tg, TPO, TSH-R and NIS (Fig. 3A, 3F and 3G). At this stage, TTF-1 and Pax-8 co-expression is an essential prerequisite to verify that endoderm cells of thyroid lineage has been derived. In order to obtain the full maturation into Day 25 thyroid-like cells, day 22 thyroid progenitors were exposed for 3 days to a maturation media supplemented with TSH, IGF-1 and NaI resulting in up-regulation of specific thyroid differentiation markers (Fig. 3A, 3F and 3G). Day 25 thyroid-like cells in response to a prolonged TSH treatment have the capacity to organize into thyroid-specific three-dimensional structures, the follicles expressing thyroid differentiation markers such as TP0, NIS and Tg (Day 32) (Fig. 3C).

These data argue that the choice to use hESCs could represent a reliable and innovative strategy to reproduce the cellular hierarchy of normal thyroid tissue in *a vitro* experimental setting, breaching toward the cell-of-origin identification.

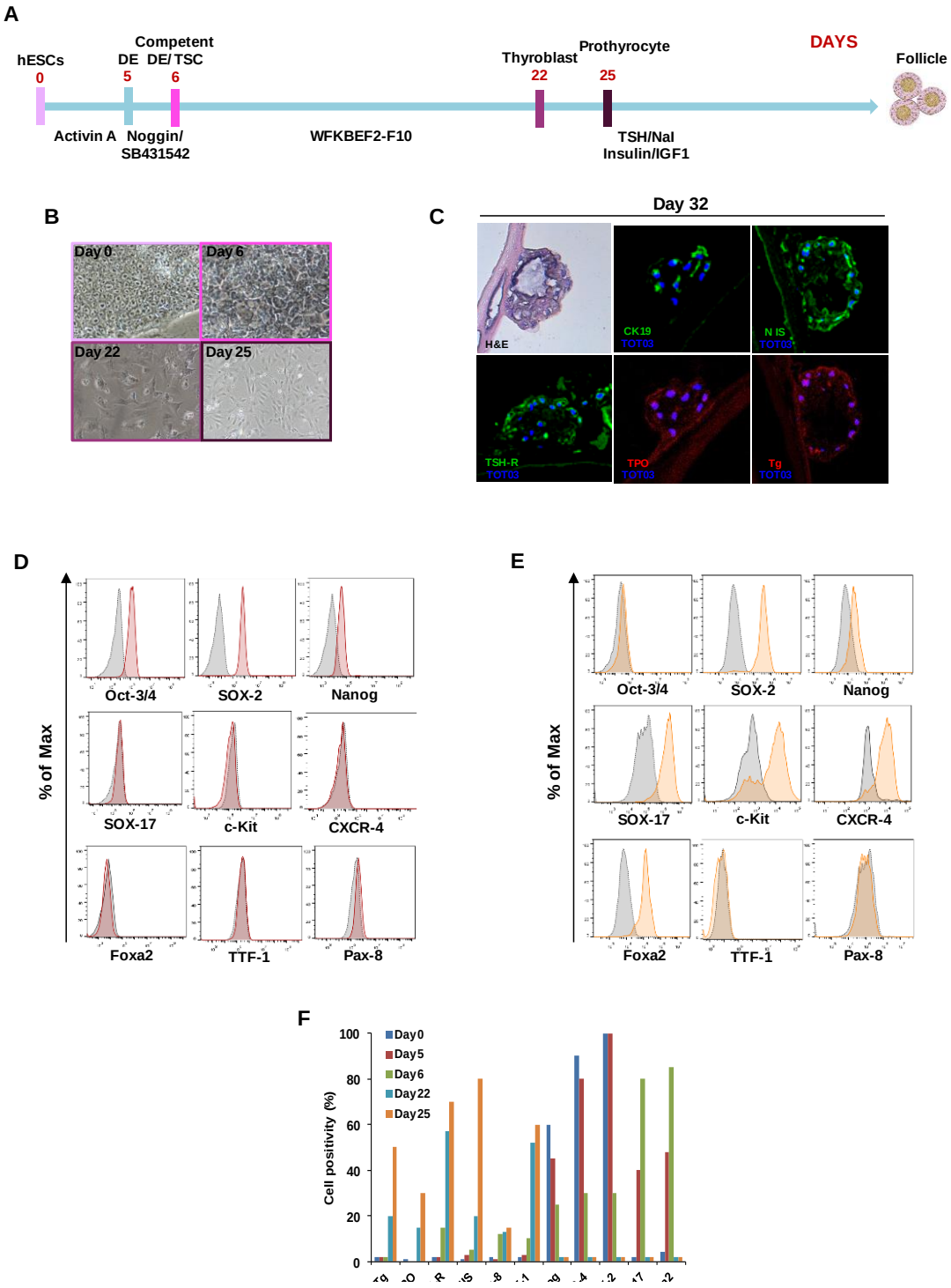
A
hESCs
0
Competent
DE
5
DE/ TSC
6
Activin A
Noggin/
SB431542
WFKBEF2-F10
Thyroblast
22
Prothyrocyte
25
TSH/Nal
Insulin/IGF1
DAYS
Follicle
B
Day 0
Day 6
Day 22
Day 25
C
Day 32
H&E
CK19
TOT03
N IS
TOT03
TSH-R
TOT03
TPO
TOT03
Tg
TOT03
D
% of Max
Oct-3/4
SOX-2
Nanog
SOX-17
c-Kit
CXCR-4
Foxa2
TTF-1
Pax-8
E
% of Max
Oct-3/4
SOX-2
Nanog
SOX-17
c-Kit
CXCR-4
Foxa2
TTF-1
Pax-8
F
Cell positivity (%)
100
80
60
40
20
0
Day 0
Day 5
Day 6
Day 22
Day 25

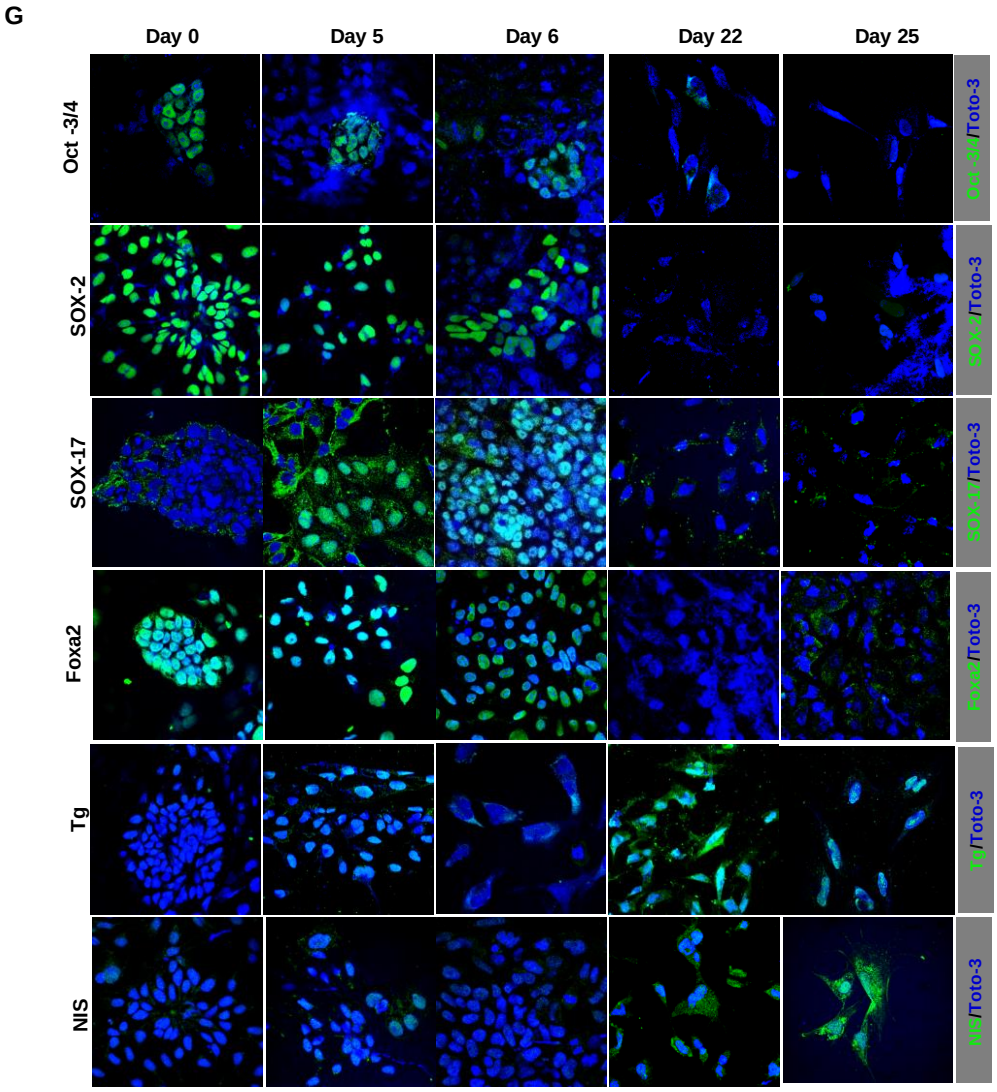

Figure 3. Inhibition of BMP and TGFβ signaling pathways promotes hESC-derived endoderm differentiation into thyroid-like cells. (**A**) Schematic representation of culture protocol for *in vitro* hESCs differentiation into endodermal TTF-1+ cells with thyroid lineage fate. (**B**) Representative phase contrast analysis of hESCs cultures at different differentiation stages (Day 0, hESCs; Day 6, Competent DE; Day 22, thyreoblasts; Day 25 prothyrocytes); (**C**) Immunofluorescence analysis of cytocheratin 19 (CK19), NIS, TSH-R, TPO and Tg in follicle (Day 32) with relative H&E staining on paraffin embedded sections. (**D and E**) Representative flow cytometry profiles of Oct-3/4, SOX-2 and Nanog pluripotent markers, c-Kit, CXCR-4, SOX-17 and Foxa2 definitive endodermal markers, TTF-1 and Pax-8 thyroid markers on hESCs (Day 0) and DE (Day 5), respectively. The grey histograms represent the isotype-matched controls. (**F**) Percentage of Oct-3/4, SOX-2, Nanog, SOX-17, Foxa2, TTF-1, Pax-8, Tg, TPO, TSH-R and NIS positive cells on Day 0 (control), Day 5, Day 6, Day 22 and Day 25 evaluated by immunofluorescent. (**G**) hESCs-derived cultures on Day 0 (control), Day 5, Day 6, Day 22 and Day 25, immunostained for Oct-3/4, SOX-2, SOX-17, Foxa2, Tg and NIS proteins..

2.3.3 microRNAs as regulators of thyroid cell specification

The growing body of experimental evidence has shown that microRNAs play an important role in maintenance and differentiation of stem cells fate (39-44). miRNA expression profiles are highly variable during embryonic development and in adulthood (45). Increasly evidences demonstrated that an intact microRNAs processing machinery is an essential prerequisite for proper function of several organs including thyroid gland (46-48). Although it is well established that microRNAs finely modulate the expression of thyroid specific genes involved in maintenance of tissue homeostasis, the role of these short-non-coding RNAs in normal thyroid development is still poorly clarified. In order to enrich the knowledge regarding the *in vitro* differentiation of hESCs into thyroid cells, it would be helpful thoroughly clarify the regulatory mechanisms that contribute to thyroid cell specification. Therefore, we investigated the differentially expressed microRNAs during *in vitro* hESCs differentiation into thyroid cell lineage to elucidate their potential role in normal thyroid tissue development.

We compared microRNA expression profiles among hESCs at diverse differentiation stages and we found that miR-375, known to be highly expressed in hESCs-derived definitive endoderm (49), is up-regulated in definitive endoderm and especially in competent definitive endoderm than in hESCs, and its expression level declined later during the differentiation process (Fig. 4A). miR-375 acts regulating target genes, including the endodermal marker SOX-17, involved in development of endodermally derived organs such as thyroid gland (49). Likewise, some of the miR-302 family members, essential for maintenance and renewal of the hESCs (40-41), is up-regulated in hESCs and its expression levels resulted down-regulated during cell lineage specification (Fig. 4A). Furthermore, we showed that the expression of miR-143, miR-145 and some of the let-7 family members was low in hESCs but highly up-regulated during *in vitro* differentiation of DE into thyroid cells (Fig. 4A). Our data are strongly supported by recent finding claiming that let-7 family plays an important role in regulating cell proliferation and differentiation during development and furthermore, that the expression levels of miR-143 and miR-145 are highly up-regulated during cell specification (50-52). It is well known that pluripotency genes Oct-3/4 and SOX-2 are direct targets of miR-145 and that over-expression of the same microRNA results in inhibition of its pluripotency targets inducing lineage differentiation (50-51). Several investigators reported altered miR-145 expression

levels in ATC cell lines (50). According to these evidences, we observed that the expression levels of miR-145 are significantly down-regulated in CSCs from ATC specimens as compared with CSCs from well differentiated thyroid carcinoma FTC, hESCs-derived TSCs and hESCs-derived thyroid-like cells (Fig. 4B). Given the low expression levels of miR-145 in CSCs from ATC specimens, characterized by a down-regulation of thyroid differentiation markers such as NIS, Pax-8 and Tg (2-3, 7, 51), it could be hypothesized that miR-145 may modulate differentiation of thyroid follicular cells. Indeed, research findings demonstrated that inhibition of miR-145 in primary cultures of normal thyroid tissue samples results in down-regulation of specific thyroid differentiation markers (51).

According to our preliminary data we could speculate that an undamaged microRNAs processing machinery is an essential prerequisite for maintenance and differentiation *in vitro* of hESCs towards a TFC fate. These results suggest that microRNAs play an important role in proper development and function of thyroid gland supporting the well known concept that deregulation of specific microRNAs are involved in human thyroid diseases.

A

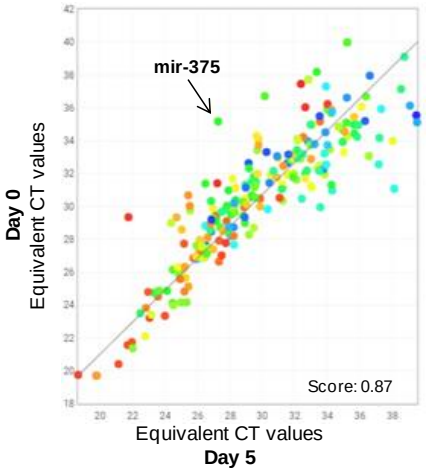
mir-375
Score: 0.87
Day 0
Equivalent CT values
Equivalent CT values
Day 5

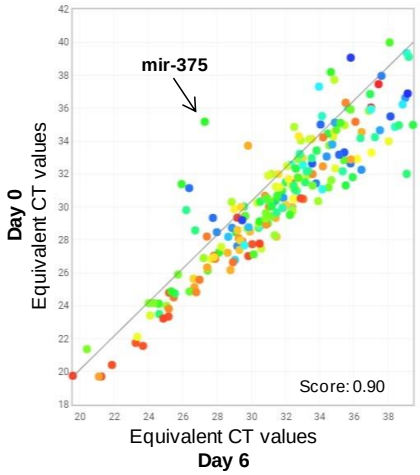
mir-375
Score: 0.90
Day 0
Equivalent CT values
Equivalent CT values
Day 6

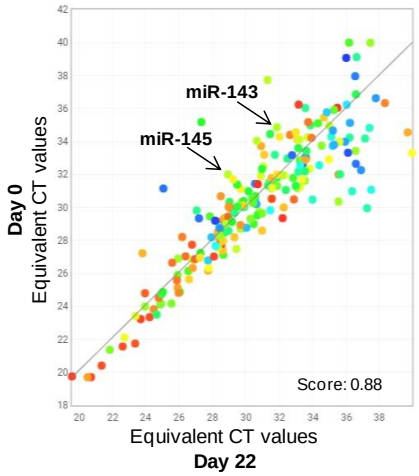
miR-143
miR-145
Score: 0.88
Day 0
Equivalent CT values
Equivalent CT values
Day 22

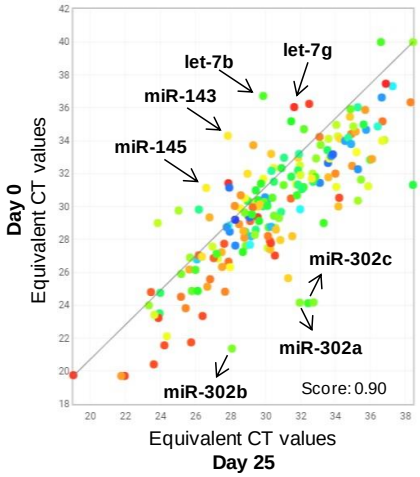
let-7b
let-7g
miR-143
miR-145
miR-302c
miR-302a
miR-302b
Score: 0.90
Day 0
Equivalent CT values
Equivalent CT values
Day 25

B

Sample	Ct (miR-145)
Day 6	32,598
Day 25	26,625
FTC	35,215
PTC	over 40
ATC	over 40

Figure 4. microRNAs regulate normal development and function of thyroid gland. (A) Correlation plot of up- and down-regulated microRNAs in Day 0 hESCs, Day 5 DE, Day 6 Competent DE; Day 22 thyreoblasts and Day 25 prothyrocytes using equivalent C_T values where the original C_T values are projected to 100% target efficiency. (**B**) Basal expression levels of miR-145 in hESC-derived TSCs (day 6), hESC-derived thyroid-like cells (Day 25) and CSCs isolated from ATC, PTC and FTC specimens.

2.4 Future perspectives and conclusions

Since the miR-145 role in pluripotency maintenance and cellular differentiation, it has been proposed to be a tumor suppressor in several tumors. Research findings showed that undifferentiated thyroid carcinomas are characterized by loss of specific thyroid follicular cell markers expression resulting in a decrease of adjuvant therapies efficacy. Given our preliminary data regarding the loss of miR-145 expression in CSCs from ATC specimens, it could be hyphotized that miR-145 may modulate differentiation of thyroid follicular cells. In our previously published work we demonstrated that in accordance with its undifferentiated phenotype, CSCs isolated from ATC specimens did not express Tg, whereas CSCs isolated from PTC and FTC specimens showed a diffuse expression (24). In order to clarify the potential role of miR-145 in thyroid carcinogenesis, we will investigate the association between miR-145 expression levels and specific thyroid differentiation markers in CSCs isolated from ATC, PTC and FTC specimens.

Recent advantages in genome editing have enabled to efficiently modify endogenous genes in a wide variety of cells. CRISPR (clustered regularly interspaced short palindromic repeats)/Cas9 technology represents a significant improvement over other next-generation genome editing tools, reaching a new level of targeting, efficiency, and ease of use. The CRISPR/Cas9 system allows for site-specific genomic targeting in virtually any organism. Our intent was to prove that the different thyroid tumor histotypes were determined by different genetic alterations occurring within the same target cell or inside distinct cells-of-origin constituting the thyroid tissue. To address this point, we will transfect TSC compartment with CRISPR Cas9 bearing TP53R248Q alone and in combination with BRAFV600E, RET/PTC1 or NRASQ61R, thyroblasts with CRISPR Cas9 bearing BRAFV600E or RET/PTC1, and prothyrocytes with CRISPR Cas9 bearing NRASQ61R (6).

We will investigate whether self-renewal capacity is directly correlated with the above mentioned genetic alterations common in thyroid tumor histotypes. Moreover, cells bearing these genetic alterations will be orthotopically injected into the thyroid mice gland. Furthermore, target cells over-expressing the above mentioned oncogenes and their matched xenografts will be analyzed for post-translational modifications analysis of the proteins commonly related to the metastatic and tumorigenic signaling pathways. Moreover, such knowledge could potentially lead to the creation of animal models useful to understand the strengths and limitations of new individualized

treatment regiments. According to the well known concept that SCs and CSCs share the ability to self-renew, it is reasonable to propose that cancer cells use the self-renewal machinery normally exploited in stem cells. It has been already established that many pathways classically associated to cancer progression may also regulate the SCs maintenance, and also that the events underlining the tumor transformation followed by tumor suppressor gene loss or oncogene activation can occur both in long-lived somatic stem cells and in short-lived differentiated cells. These findings together with our preliminary observations could define a good model to identify the cells-of-origin and tumor-related driven mutations designing a gateway to clarify the molecular basis of malignant thyroid transformation.

References

1. Jemal A, Bray F, Center MM, Ferlay J, Ward E, Forman D. Global cancer statistics. CA Cancer J Clin 2011; 61: 69-90.
2. Kondo T, Ezzat S, Asa SL. Pathogenetic mechanisms in thyroid follicular-cell neoplasia. Nat Rev Cancer 2006; 6: 292-306.
3. Rivera M, Ghossein RA, Schoder H, Gomez D, Larson SM, Tuttle RM. Histopathologic characterization of radioactive iodine-refractory fluorodeoxyglucose-positron emission tomography-positive thyroid carcinoma. Cancer 2008; 113: 48-56.
4. Nikiforov YE, Nikiforova MN. Molecular genetics and diagnosis of thyroid cancer. Nat Rev Endocrinol 2011; 7: 569-580.
5. Kroll TG, Sarraf P, Pecciarini L, Chen CJ, Mueller E, Spiegelman BM et al. PAX8-PPARgamma1 fusion oncogene in human thyroid carcinoma. Science 2000; 289: 1357-1360.
6. Zane M, Scavo E, Catalano V, Bonanno M, Todaro M, De Maria R et al. Normal vs cancer thyroid stem cells: the road to transformation. Oncogene 2015; 1–11.
7. Zane M, Catalano V, Scavo E, Bonanno M, Pelizzo MR, Todaro M et al. Estrogens and stem cells in thyroid cancer. Frontiers in Endocrinology 2014; 5:124.
8. Thomas D, Friedman S, Lin RY. Thyroid stem cells: lessons from normal development and thyroid cancer. Endocr Relat Cancer 2008; 15: 51-58.
9. Inaba M, Yamashita YM. Asymmetric stem cell division: precision for robustness. Cell Stem Cell 2012; 11: 461 -469.
10. Yamashita YM, Yuan H, Cheng J, Hunt AJ. Polarity in stem cell division: asymmetric stem cell division in tissue homeostasis. Cold Spring Harb Perspect Biol 2010; 2: a001313.
11. Morrison SJ, Kimble J. Asymmetric and symmetric stem-cell divisions in development and cancer. Nature 2006; 441: 1068-1074.
12. Kreso A, Dick JE. Evolution of the cancer stem cell model. Cell Stem Cell. 2014; 6;14(3):275-91.
13. Visvader JE. Cells of origin in cancer. Nature. 2011; 469(7330):314-22.
14. Visvader JE, Lindeman GJ. Cancer stem cells in solid tumours: accumulating evidence and unresolved questions. Nat Rev Cancer. 2008; 8(10):755-68.
15. Burrell RA, McGranahan N, Bartek J, Swanton C. The causes and consequences of genetic heterogeneity in cancer evolution. Nature. 2013; 501(7467):338-45.
16. Greaves M1, Maley CC. Clonal evolution in cancer. Nature. 2012; 481(7381):306-13.
17. Dick JE. Stem cell concepts renew cancer research. Blood. 2008; 112(13):4793-807.
18. Meacham CE1, Morrison SJ. Tumour heterogeneity and cancer cell plasticity. Nature. 2013; 501(7467):328-37.

19. Shackleton M, Quintana E, Fearon ER, Morrison SJ. Heterogeneity in cancer: cancer stem cells versus clonal evolution. Cell. 2009; 138:822–829.
20. Davies TF, Latif R, Minsky NC, Ma R. Clinical review: the emerging cell biology of
thyroid stem cells. J Clin Endocrinol Metab 2011; 96: 2692–2702
21. Lin RY. Thyroid cancer stem cells. Nat Rev Endocrinol. 2011; 7(10):609-16.
22. Klonisch T, Hoang-Vu C, Hombach-Klonisch S. Thyroid stem cells and cancer.
Thyroid 2009; 19: 1303–1315.
23. De Felice M, Di Lauro R. Thyroid development and its disorders: genetics and molecular mechanisms. Endocr Rev 2004; 25: 722–746
24. Todaro M, Iovino F, Eterno V, Cammareri P, Gambara G, Espina V et al. Tumorigenic and Metastatic Activity of Human Thyroid Cancer Stem Cells. Cancer Res. 2010; 70(21):8874-85.
25. Takano T. Fetal cell carcinogenesis of the thyroid: theory and practice. SeminCancer Biol 2007; 17: 233–240.
26. Lin RY and. Davies TF. Differentiating thyroid cells Thyroid. 2010 Jan;20(1):1-2.
27. Lin, "Directed differentiation of mouse embryonic stem cells into thyroid follicular cells," *Endocrinology*, vol. 147, no. 6, pp. 3007–3015, 2006.
28. Van Vliet G. Development of the thyroid gland: lessons from congenitally hypothyroid mice and men. Clin Genet 2003; 63: 445–455.
29. Fagman H, Nilsson M. Morphogenetics of early thyroid development. J Mol Endocrinol 2011; 46: R33–R42.
30. Antonica F, Kasprzyk DF, Opitz R, Iacovino M, Liao XH, Dumitrescu AM et al. Generation of functional thyroid from embryonic stem cells. Nature 2012; 491: 66–71.
31. Longmire TA, Ikonomou L, Hawkins F, Christodoulou C, Cao Y, Jean JC et al. Efficient derivation of purified lung and thyroid progenitors from embryonic stem cells. Cell Stem Cell 2012; 10: 398–411.
32. Green MD, Chen A, Nostro MC, d'Souza SL, Schaniel C, Lemischka IR et al. Generation of anterior foregut endoderm from human embryonic and induced pluripotent stem cells. Nat Biotechnol 2011; 29: 267–272.
33. Hannan NR, Fordham RP, Syed YA, Moignard V, Berry A, Bautista R et al. Generation of multipotent foregut stem cells from human pluripotent stem cells. Stem Cell Reports 2013; 1: 293–306.
34. Brafman DA, Moya N, Allen-Soltero S, Fellner T, Robinson M, McMillen ZL et al. Analysis of SOX2-expressing cell populations derived from human pluripotent stem cells. Stem Cell Reports 2013; 1: 464–478.
35. De Felice, M. & Di Lauro, R. Minireview: intrinsic and extrinsic factors in thyroid
gland development: an update. Endocrinology 2011; 52, 2948–2956.

36. Kevin A D'Amour, Alan D Agulnick, Susan Eliazer, Olivia G Kelly, Evert Kroon & Emmanuel E Baetge. Efficient differentiation of human embryonic stem cells to definitive endoderm. Nat Biotechnol. 2005; 23(12):1534-41.
37. Hannan NRF, Fordham RP, Syed Y, Moignard V, Berry A, Jensen KBet al. Generation of Multipotent Foregut Stem Cells from Human Pluripotent Stem Cells. Stem Cell Reports 2013; Vol. 1 293–306.
38. Atsushi Kubo, Katsunori Shinozaki, John M. Shannon, Valerie Kouskoff, Marion Kennedy, Savio Woo, Hans Joerg Fehling, Gordon Keller. Development of definitive endoderm from embryonic stem cells in culture. Development and disease 2004; 1651-1662.
39. Mestdagh P, Van Vlierberghe P, De Weer A, Muth D, Westermann F, Speleman F et al. A novel and universal method for microRNA RT-qPCR data normalization. J. Genome Biol. 2009; 10(6):R64.
40. Yu Z1, Li Y, Fan H, Liu Z, Pestell RG. miRNAs regulate stem cell self-renewal and differentiation. Front Genet. 2012; 3:191.
41. Card DA, Hebbar PB, Li L, Trotter KW, Komatsu Y, Mishina Y, Archer TK. Oct4/Sox2-regulated miR-302 targets cyclin D1 in human embryonic stem cells. Mol Cell Biol. 2008; 28(20):6426-38
42. Li MA, He L. microRNAs as novel regulators of stem cell pluripotency and somatic cell reprogramming. Bioessays 2012; 34: 670-680.
43. Guan D, Zhang W, Zhang W, Liu GH, Belmonte JC. Switching cell fate, ncRNAs coming to play. Cell Death Dis 2013; 4: e464.
44. Frezzetti D, Reale C, Calı G, Nitsch L, Fagman H, Nilsson O et al. The microRNA-Processing Enzyme Dicer Is Essential for Thyroid Function. PLoS ONE 2011; LoS ONE 6(11): e27648.
45. Francis N, Moore M, Asan SG, Rutter GA, Burns C. Changes in microRNA expression during differentiation of embryonic and induced pluripotent stem cells to definitive endoderm. Gene Expression Patterns 2015; 70-82
46. Murchison EP, Partridge JF, Tam OH, Cheloufi S, Hannon GJ. Characterization of Dicer-deficient murine embryonic stem cells. Proc Natl Acad Sci USA 2005; 102: 12135-12140
47. Wang Y, Medvid R, Melton C, Jaenisch R, Blelloch R. DGCR8 is essential for microRNA biogenesis and silencing of embryonic stem cell self-renewal. Nat Genet 2007; 39: 380-385
48. Berardi E, Pues M, Thorrez L, Sampaolesi M. miRNAs in ESC differentiation. Am J Physiol Heart Circ Physiol 2012; 303: H931-H939
49. Xueling Li. miR-375, a microRNA related to diabetes. Gene 2014; 1–4
50. Na Xu, Thales Papagiannakopoulos, Guangjin Pan, James A. Thomson, and Kenneth S. Kosik. MicroRNA-145 Regulates OCT4, SOX2, and KLF4 and Represses Pluripotency in Human Embryonic Stem Cells. Cell 2009; 137, 647–658.
51. Boufraqech M, Zhang L, Jain M, Patel D, Ellis R, Xiong Y et al. miR-145 suppresses thyroid cancer growth and metastasis and targets AKT3. Endocrine-Related Cancer 2014; 21, 517–531.

52. Boyerinas B, Park SM, Hau A, Murmann AE, Peter ME. The role of let-7 in cell differentiation and cancer. Endocrine-Related Cancer 2010; 17 F19–F36.

Chapter 3

Estrogens and stem cells in thyroid cancer

Mariangela Zane*, Veronica Catalano*, **Emanuela Scavo**, Marco Bonanno, Maria Rosa Pelizzo, Matilde Todaro and Giorgio Stassi

*These authors contributed equally to this work

Published in *frontiers in Endocrinology*, 2014.

frontiers in
ENDOCRINOLOGY

MINI REVIEW ARTICLE
published: 25 July 2014
doi: 10.3389/fendo.2014.00124

Estrogens and stem cells in thyroid cancer

Mariangela Zane[1,2†], Veronica Catalano[1†], Emanuela Scavo[1], Marco Bonanno[1], Maria Rosa Pelizzo[2], Matilde Todaro[1] and Giorgio Stassi[1]*

[1] *Department of Surgical and Oncological Sciences, University of Palermo, Palermo, Italy*
[2] *Department of Surgical, Oncological and Gastroenterological Sciences, University of Padua, Padua, Italy*

Edited by:
Terry Francis Davies, Icahn School of Medicine at Mount Sinai, USA

Reviewed by:
Carmelo Nucera, Harvard Medical School, USA
Antonio Di Cristofano, Albert Einstein College of Medicine, USA

***Correspondence:**
Giorgio Stassi, Laboratory of Cellular and Molecular Pathophysiology, Department of Surgical and Oncological Sciences, University of Palermo, Via Liborio Giuffrè 5, Palermo 90127, Italy
e-mail: giorgio.stassi@unipa.it

[†] *Mariangela Zane and Veronica Catalano have contributed equally to this work.*

Recent discoveries highlight the emerging role of estrogens in the initiation and progression of different malignancies through their interaction with stem cell (SC) compartment. Estrogens play a relevant role especially for those tumors bearing a gender disparity in incidence and aggressiveness, as occurs for most thyroid diseases. Although several experimental lines suggest that estrogens promote thyroid cell proliferation and invasion, their precise contribution in SC compartment still remains unclear. This review underlines the interplay between hormones and thyroid function, which could help to complete the puzzle of gender discrepancy in thyroid malignancies. Defining the association between estrogen receptors' status and signaling pathways by which estrogens exert their effects on thyroid cells is a potential tool that provides important insights in pathogenetic mechanisms of thyroid tumors.

Keywords: thyroid cancer, stem cells, cancer stem cells, estrogens, thyroid hormones, growth factors

INTRODUCTION

The endocrine system consists of a network of glands secreting hormones, which are chemical messengers that cooperate in growth, development, metabolism, and reproductive functions. The largest endocrine organ in the human body is the thyroid gland, whose function is the systemic metabolic regulation through thyroid hormones (THs) produced by follicular cells, and calcitonin produced by parafollicular cells. Different malignancy histotypes can arise from these cells: papillary (PTC), follicular (FTC), and anaplastic thyroid carcinomas (ATC) originate from follicular cells, while medullary thyroid carcinomas (MTC) derive from parafollicular cells (1). Notably, more than 95% of thyroid carcinomas (TCs) arise from follicular cells. These malignancies are indolent tumors treated by surgical resection with or without radioactive-iodine ablation since they maintain their distinct potential to concentrate Iodine. The loss of typical thyroid cell characteristics and functions, including expression of the thyroid-stimulating hormone (TSH) receptor (TSH-R), thyroglobulin (Tg), thyroid peroxidase (TPO), and sodium iodide symporter (NIS), defines the hallmark of ATCs, which are lethal malignancies with no effective therapy (1–3).

Besides genetic alterations in mitogen-activated protein kinase (MAPK), PI-3 kinase (PI3K), and TSH signaling pathways, thyroid carcinogenesis is fostered by the microenvironment, growth factors (GFs), and various hormones, including estrogens (4). Hormones can set off a cascade of signaling pathways, enhancing or contrasting specific effects triggered by other factors. Based on this *scenario*, the role of estrogens has been proposed in the pathogenesis of thyroid proliferative and neoplastic disorders. This hypothesis is supported by data regarding gender incidence, which reported a frequency of thyroid nodules about three to four times higher in women than in men with a peak rate occurring earlier in women (5, 6). Furthermore, the clarification of the estrogen-driven pathogenesis could be crucial in explaining why PTC constitutes the seventh most common cancer in the female gender (7, 8). An *in vivo* study reported that circulating estrogens are directly responsible for the increased female susceptibility to thyroid disease, through PI3K pathway activation and repressing p27 expression. The authors also observed a significant estrogen role in the transcriptional regulation of TPO, DUOX1, and NIS genes (9). Although several studies have demonstrated a direct action by estrogens on thyroid growth and function (7, 10–12), the precise mechanism underlying the proliferative and neoplastic disorders still remains undefined. In particular, it would be interesting to explore the role of hormones in TC initiation.

The cellular origin of TCs has been explained by different models (**Figure 1**). The multistep carcinogenesis model predicts that TC originates from follicular cells as a consequence of multiple mutations accumulated throughout their life-span. These events are characterized by a dedifferentiation process with a marked epithelial-to-mesenchymal transition (EMT), in which well-differentiated TC cells transform into a more undifferentiated phenotype (1). The fetal cell carcinogenesis model hypothesizes that TC cells would be generated by transforming three types of fetal thyroid cells, stem cells (SCs), thyroblasts, and prothyrocytes, which result in ATC, PTC, and FTC, respectively (13, 14). The heterogeneity of tumor bulk had led to a cancer stem cells (CSCs) model to propose TC as an SC disease. The growing body of experimental evidence has revealed that an accumulation of genetic abnormalities in tissue-resident SCs or in their more committed progenies, concomitant with the niche epigenetic alterations, result in their malignant transformation (15, 16).

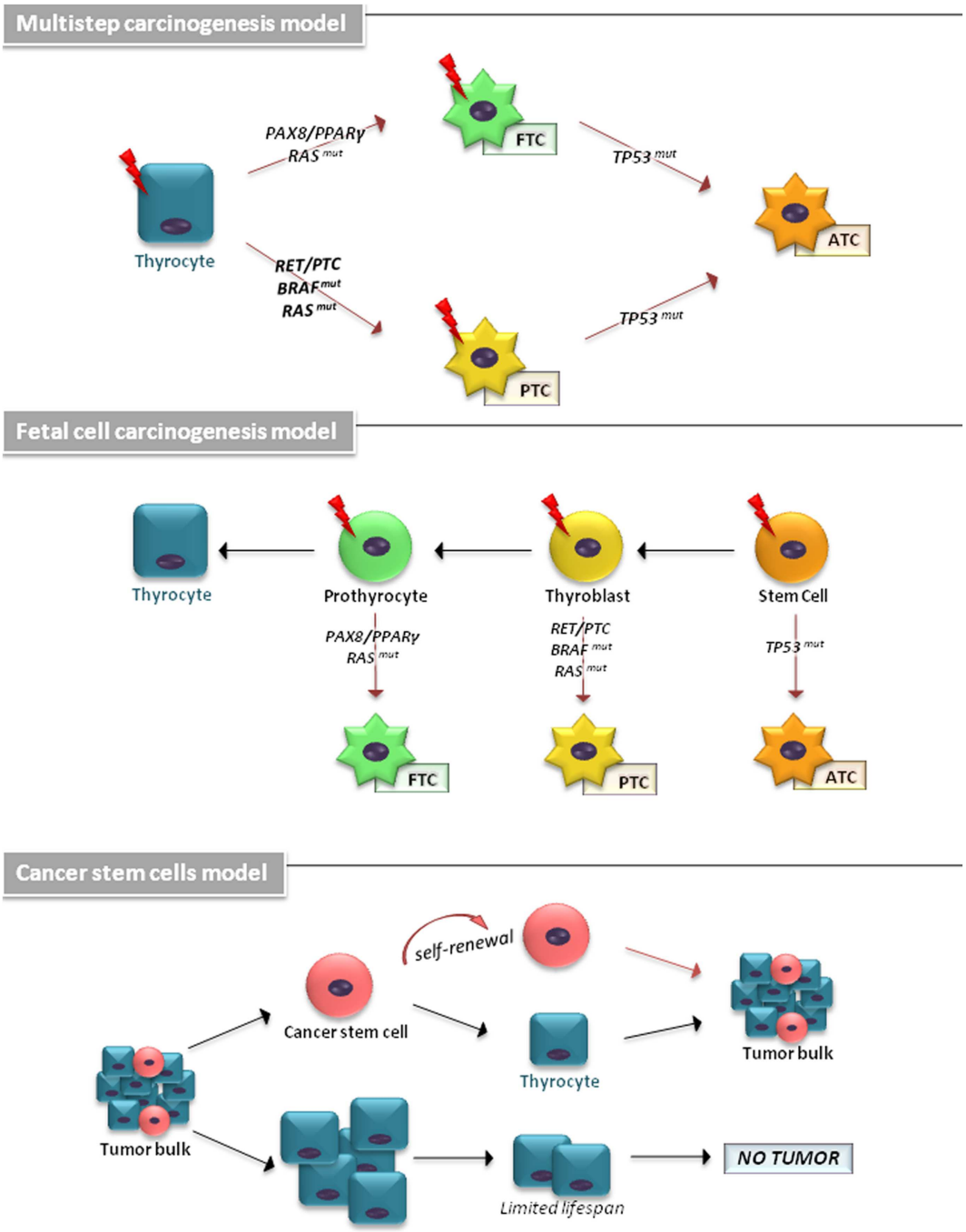

FIGURE 1 | The cellular origin of thyroid carcinomas is shown. According to the multistep carcinogenesis model, TC originates from follicular cells as a consequence of multiple mutations accumulated throughout their life-span. Thyrocytes could give rise to PTC by RAS and BRAF mutations or RET/PTC and NTRK1 rearrangements and to FTC by point mutations of the RAS gene and PAX8/PPARγ rearrangement. ATC derive from PTC and FTC after deregulation of the p53 and the Wnt/β-catenin pathway. In fetal cell carcinogenesis model, three types of fetal thyroid cells were proposed to generate different forms of thyroid cancer. Fetal thyroid stem cells, characterized by expression of the oncofetal fibronectin (OF), generate ATC, thyroblasts, which express OF and the differentiation marker Tg, are proposed to be the cellular origin of PTC. The more differentiated prothyrocytes, expressing Tg, give rise to FTC. The cancer stem cells model proposes TC as an SC disease. The accumulation of mutations in differentiated thyrocytes leads to their transformation. A subset of these cells may (in more aggressive tumor types) dedifferentiate and assume CSC characteristics.

The "cell-of-origin" concept explains how a normal cell acquires the first alteration able to trigger tumor initiation (tumor-initiating cells, TICs) (17). Wnt pathway plays a crucial role in SC/progenitor compartment maintenance, and has been described in several tumors, including TC, resulting in nuclear β-catenin-induced proliferation (18–20).

In this review, the most current findings supporting the carcinogenesis effects of estrogens and THs will be addressed. A special emphasis will be given to the role of exogenous and endogenous GFs affecting thyroid proliferative pathways in SC compartment.

ESTROGENS

As recently published by Morrison's research group, estrogens are involved in increasing hematopoietic SC self-renewal in female subjects and more specifically during pregnancy (21). It is likely that normal and tumor thyroid tissues, which express estrogen receptors (ER), could be subject to the same mechanism of estrogen action (10, 22–24).

Involved in cellular processes such as growth, cell motility, and apoptosis, in reproductive tissues and other organs, including endocrine glands, estrogens are mainly produced by the adrenal cortex and ovary, but also by the thyroid (25, 26). They are present in women and men with a notable increase in women at reproductive age. The three principal estrogens, estrone (E1), estradiol (E2), and estriol (E3), are processed in metabolites with different estrogenic abilities, which create a different risk in developing cancer (27–29).

Estradiol is the most potent estrogen since it has the highest affinity to its receptors. Estrogens perform their function by binding to ER alpha and beta (ER-α, ER-β), and a transmembrane intracellular non-classical ER G-protein-coupled receptor 30 (GPR30) (**Figure 2**). ER-α and ER-β are soluble intracellular nuclear receptors, belonging to a ligand-dependent nuclear receptor superfamily of transcription factors (TFs) (25, 26). ER-α is the key factor of E2-induced proliferation with an anti-apoptosis effect. In females of reproductive age, ER-α levels are higher in PTC compared to nodular goiter patients, showing a positive correlation between ER-α and Ki-67 expression levels. In contrast, ER-β is associated with apoptosis and growth inhibition, providing a negative correlation with mutant P53 (30). PPARγ also interacts with ER-α inhibiting each other, and with ER-β enhancing their inhibitory effect on cell proliferation and migration (31). In light of this, the ER-α/ER-β *ratio* could be helpful to elucidate the TC pathophysiology (25, 32).

The interaction between estrogens and ERs signals through different pathways:

- Genomic (or classical) estrogen-signaling: after accessing the cell through passive diffusion, E2 binds to ER, which changes its conformation and homo- or heterodimerizes (E2–ER). This complex translocates into the nucleus, where it binds to the 15-bp palindromic estrogen response element (ERE) located in the regulatory regions of target genes. This interaction leads to a co-activators recruitment, which in turn allows expression of genes involved in proliferation (33, 34).
- Estrogen response element-independent genomic actions (TFs cross-talk): ERE-lacking genes can be activated by modulating other TFs through protein–protein interactions. This molecular mechanism induces chromatin remodeling, histone unwinding, and interaction with the basal transcription machinery complex (35–37).
- Non-genomic (or membrane-initiated) estrogen-signaling: E2 activation of plasma membrane-associated ER and GPR30 promotes the MAPK and PI3K signaling pathways and/or increases the Ca^{2+} levels (10, 38–40). They can also activate G-proteins resulting in cAMP production, similar to TSH signaling in thyrocytes, and assist the activation of metalloproteinases (MMPs) and the GF pathway (5).
- Ligand-independent signaling: in absence of E2, GFs can stimulate ERs directly or indirectly through MAPK and/or PI3K pathways (41).

The cross-talk between genomic and non-genomic pathways, as well as the integrative signaling by E2 in different cell compartments, leads to a synergy that provides plasticity in cell response. Estrogens dispatch their proliferative role also by increasing T_3 levels and stimulating the iodine-uptake and TPO activity (42).

Furlanetto et al. (43) reported that E2 increases proliferation of thyroid cells down-regulating NIS. These data underline the pivotal role of estrogens in the SC compartment maintenance. In normal and tumor thyroid cell lines, Rajoria et al. documented that E2 is associated with increased proliferation, adhesion, invasion, and migration via β-catenin (7) and MMP-9 modulation (44). Likewise, E-cadherin down-regulation and β-catenin translocation sustain the metastatic activity of TC cells (24). These results confirmed the findings by Kouzmenko et al., which reported the first evidence of cross-talk between estrogens and Wnt pathways through functional interaction of β-catenin with ER-α (45).

Xu et al. (8) analyzed whether differentiated and SC/progenitors could be target of estrogen action in thyroid. SCs isolated from goiter tissue enhanced their sphere-forming ability in presence of E2. Moreover, thyroid-sphere cells showed ER-α mRNA levels eight times higher than those of more differentiated thyrocytes. This suggests the gender discrepancy in TC incidence and a difference in terms of aggressiveness and survival.

THYROID HORMONES

Thyroid hormones control the secretion of thyrotropin-releasing hormone (TRH) from the hypothalamus and TSH from the anterior pituitary through negative feedback loops (1). Thyroid homeostasis and function are regulated by a concert of signals accumulated from TSH and GF pathways. TSH binds to TSH-R and induces the coupling of different G-proteins, stimulating adenylate cyclase (AC) and phospholipase C (PLC) (**Figure 2**). This promotes iodide uptake and TG, TPO, and NIS expression, producing thyroxine (T_4) and triiodothyronine (T_3) (19, 46). On the contrary, intracellular Ca^{2+} and PLC regulate iodine release, H_2O_2 production, and Tg iodination (47, 48). Although cAMP is the main mediator of TSH stimulation in thyroid cell growth, TSH via PI3K increases cyclin E levels leading to cell cycle progression (49, 50). TSH-R is also associated to the MAPK pathway through its desensitization and internalization apparatus (51).

Gain-of-function mutations in TSH-R or Gs genes result in increased cAMP accumulation and TSH-independent proliferation, which account for hyperfunctioning nodules in patients with multinodular goiters (52, 53). These alterations result insufficient

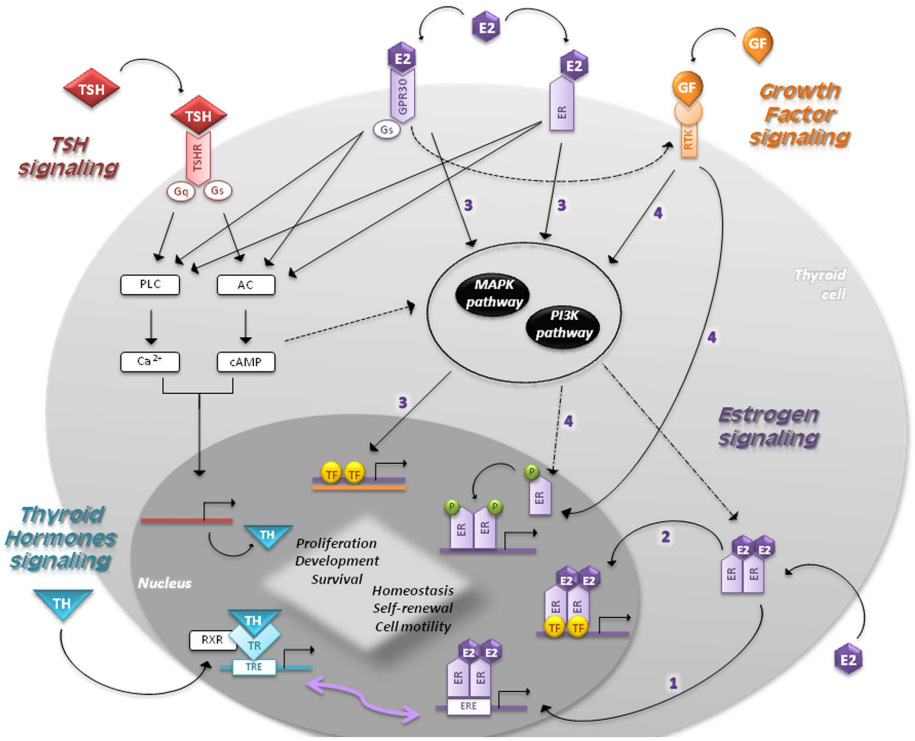

FIGURE 2 | Signaling pathways in follicular cells are shown. The main regulators of thyroid proliferation and function act through TSH signaling and GF pathway. THs control the secretion of TSH, which binds to TSH-R and induces the coupling of G-proteins stimulating AC and PLC. TSH also acts via PI3K pathway. GFs act via MAPK and PI3K pathways regulating the expression of genes involved in survival, cell cycle progression, and proliferation. Estrogens regulate proliferation, cell motility, differentiation, and apoptosis through four different mechanisms: (1) *genomic (or classical) estrogen-signaling*: E2–ER complex translocates into the nucleus, where it binds to ERE-sequences; (2) *ERE-independent genomic actions (TFs cross-talk)*: genes lacking in ERE-sequences are activated by other TFs in the nucleus through protein–protein interactions; (3) *non-genomic (or membrane-initiated) estrogen-signaling*: E2 activation of plasma membrane-associated ER and GPR30 trigger the activation of MAPK and PI3K pathways and/or increases the Ca^{2+} levels; (4) *ligand-independent signaling*: in absence of E2, GFs can stimulate ERs directly or indirectly through MAPK and/or PI3K pathways. THs play a critical role in development and homeostasis. Nuclear TRs activate gene expression by binding to RXR, which in turn bind to TRE-sequences. Given that EREs share a similar nucleotide sequence with TREs, ERs and TRs can interact and regulate several transcriptional responses. The cross-talk between genomic and non-genomic pathways and other integrative signaling lead to a synergic cell response.

for the malignant transformation of thyroid cells (54, 55). Hence, it is likely that other factors intervene in the SC compartment, which is assumed to be the target of neoplastic transformation. Alterations of the Wnt pathway effectors are involved in cancer initiation and progression (56). In particular, TSH-mediated Wnt-1 over-expression and GSK-3β inhibition promote thyroid cell proliferation (57, 58).

Thyroid hormones play a critical role in the tissue development and homeostasis by direct transcriptional regulation or modulation of different pathways (59). Although T_4 is the predominant hormone produced by the thyroid, T_3 is the active form that mediates gene regulation binding with a higher affinity to thyroid receptors (TRs) (60). Nuclear TRs activate gene expression by binding with the retinoid X receptors (RXRs) to TH response elements (TRE), located on the promoters of target genes (**Figure 2**) (61). Given that EREs share a similar nucleotide sequence with TREs, ERs and TRs can interact and regulate several transcriptional responses to environmental *stimuli* (5). Interestingly, ERE can act as a peroxisome proliferator responsive elements (PPRE), binding PPARγ/RXR. It can henceforth inhibit ER transactivation through a competition for ERE binding (62). In line with this cross-interaction, the proliferative effect of estrogens on human NPA-87-1 PTC cell line is TSH-independent (63). Lima et al. demonstrated a more direct proliferative effect since E2 administration to prepubertal and adult rats enhances thyroid weight without significant changes in T_3, T_4, and TSH hematopoietic levels (42).

Recent studies in human cancers and mouse models provide strong evidence that the loss of TRs function contributes to cancer initiation and progression (64). While the TRα1 trigger directly promotes transcription of CTNNB1 (65, 66), the effect generated by the TRα2 stimulation in SC compartment is still unknown. Cross-talk between THs-TRα1 and Wnt pathway has been confirmed by the up-regulation of several SC markers (67). Furthermore, it was reported that aberrant nuclear localization of β-catenin-induced by CTNNB1 mutations contributes to the progression of ATCs (68). Data reported by Todaro et al. showed that E-cadherin down-regulation together with β-catenin activation confers an invasive capacity and higher metastatic rate to thyroid CSCs (18).

GROWTH FACTORS

In thyroid, GFs exert their proliferative effects by inducing the RTK dimerization that activates the downstream PI3K pathway and the MAPK cascade via G-proteins (**Figure 2**). Alterations in genes involved in the MAPK pathway led to its constitutive activation, which represents a typical feature of TC (1). In particular, mutations in RET and NTRK and alterations in RAS and BRAF intracellular signal-transducers are clearly implicated in PTC pathogenesis (69). RAS point mutations and PAX8/PPARγ rearrangement have been frequently implicated in FTC pathogenesis (70, 71). The inactivation of *RASAL1* (encoding a RAS GTPase-activating protein) by hypermethylation and mutations provides a new genetic background for FTCs and ATCs (72). Besides nuclear β-catenin accumulation and p53 inactivation, oncogenic activation of MAPK and PI3K/Akt/Foxo3a are frequently found in ATCs (2, 73, 74). The acquisition of a TERT promoter mutation was recently associated with clinical–pathological aggressiveness in FTCs and BRAF mutation-positive PTCs (72, 75).

The mesenchymal tissue is involved in thyroid development being that it releases Pro-epidermal growth factor (EGF) and basic fibroblast growth factor-2 (FGF-2), promoting cell proliferation and repressing differentiation (76, 77). Estrogens play a pivotal role in this context by inducing the production of EGF and other TFs, such as TGF-α (5).

After EGF binding, RTKs of the ErbB family (EGFR/ErbB1, ErbB2, ErbB3, and ErbB4) achieve activation through the arrangement in homo- and/or heterodimeric complexes (78, 79). In thyroid, TSH increases the expression of EGFRs that in turn promote the EGF mitogenic effect and contribute to gland homeostasis. The combination of specific EGFRs regulates the stimulation intensity, inducing transformation. Indeed, an increased expression of EGFRs in TCs compared to normal tissue has been reported (80). EGFR/ErbB1 over-expression and its constitutive phosphorylation have been observed on ATC samples and cell lines (81). Their expression has been retrieved in 90% of the PTC samples examined by Song (82). In combination with the repression of VEGF, EGF inhibitors could be a promising therapy for ATCs as demonstrated by *in vitro* studies (83, 84). EGF is also supplemented in the serum-free culture medium, which is used to isolate SCs and CSCs *in vitro* (18, 85–90).

Similarly, the cell response to FGF is regulated by FGF RTKs (FGFRs 1–4). FGF-2 exerts autocrine and paracrine stimulatory effects on thyroid growth, since the basement membrane of thyrocytes is able to produce FGF itself. FGF is also used *in vitro* for the maintenance of SC niche (18, 91); in particular, it could have an inhibitory effect on thyroid function through cAMP inhibition and TSH's activity weakening (79). In TC, increased FGF-2 levels and FGFR2 over-expression are critical in tumor progression and neovascularization (92, 93). Therefore, the differential expression in normal and malignant conditions could make this receptor a potential diagnostic marker for TCs (94).

Growth factors also affect development and metabolic processes through insulin-like growth factor (IGF). After binding of their ligands, IGF receptors (IGF-Rs) autophosphorylate their intracellular domain and activate the MAPK and PI3K cascade (95). Consistently, IGF enhances the TSH mitogenic effect on follicular cells (96); on the other hand, it also cooperates with FGF-2 in establishing and maintaining the SC niche *in vitro* (96). Indeed, IGF pathway effectors are over-expressed in CSCs: IGFR2 is involved in an autocrine loop that sustains SC renewal, and IGF increases the expression of Oct-4 and Nanog when added to the culture medium (87, 97, 98).

ESTROGEN-GROWTH FACTORS INTERACTING PROTEINS

Recently, there has been a focus on importance of the ER-GFs interacting proteins on cancer cell proliferation and invasivity. An example is mediator of ERbB2-driven cell motility (MEMO), which enhances ER-α extra-nuclear functions through the interaction with IGFR1 and ERbB2, activating MAPK and PI3K signaling (99).

CONCLUDING REMARKS

Since the theory of fetal carcinogenesis has initially been postulated, thyroid CSCs have been studied for their potential role as TICs. It has been hypothesized that various factors could be involved in the malignant transformation, such as aberrant molecular events converging to RTK, MAPK, and PI3K pathway activation. Besides the oncogenes contribution, it is likely that a network of various hormones and GFs could maintain the SC niche and enhance the proliferation of progenitors sustaining tumor bulk growth. Indeed, recent studies demonstrate that sexual hormones could exert a supportive role in the propagation of SCs and progenitors, as suggested by the cross-talk between estrogen-signaling and Wnt pathway. Furthermore, the latter pathway has also been observed interacting with THs in SC compartment and so accelerating tumorigenic processes. This mechanism could be benefited by the interaction between different cascades, which enhances or contrasts specific cellular response in tumor conditions. In conclusion, an in-depth study on the concert between estrogens, THs, and GFs could be helpful to elucidate hormones-driven thyroid carcinogenesis. Gaining more insight into this interaction could also explain the gender imbalance in tumor incidence for the purpose of identifying a more targeted approach in TC therapy.

ACKNOWLEDGMENTS

This study was supported by grants from AIRC to Giorgio Stassi (IG12819). Mariangela Zane is Ph.D., student in Oncology and Surgical Oncology at University of Padua. Emanuela Scavo and Marco Bonanno are Ph.D., students at University of Palermo, in International Immunopharmacology and in Cellular and Developmental Biology, respectively. We would like to thank Tatiana Terranova for her thoroughness and passion in editing this review.

REFERENCES

1. Kondo T, Ezzat S, Asa SL. Pathogenetic mechanisms in thyroid follicular-cell neoplasia. *Nat Rev Cancer* (2006) **6**:292–306. doi:10.1038/nrc1836
2. Nikiforova MN, Nikiforov YE. Molecular genetics of thyroid cancer: implications for diagnosis, treatment and prognosis. *Expert Rev Mol Diagn* (2008) **8**:83–95. doi:10.1586/14737159.8.1.83
3. Smallridge RC, Marlow LA, Copland JA. Anaplastic thyroid cancer: molecular pathogenesis and emerging therapies. *Endocr Relat Cancer* (2009) **16**:17–44. doi:10.1677/ERC-08-0154
4. Rahbari R, Zhang L, Kebebew E. Thyroid cancer gender disparity. *Future Oncol* (2010) **6**:1771–9. doi:10.2217/fon.10.127
5. Rajoria S, Suriano R, George AL, Shanmugam A, Jussim C, Shin EJ, et al. Estrogen activity as a preventive and therapeutic target in thyroid cancer. *Biomed Pharmacother* (2012) **66**:151–8. doi:10.1016/j.biopha.2011.11.010

6. Siegel R, Naishadham D, Jemal A. Cancer statistics, 2013. *CA Cancer J Clin* (2013) **63**:11–30. doi:10.3322/caac.21166
7. Rajoria S, Suriano R, Shanmugam A, Wilson YL, Schantz SP, Geliebter J, et al. Metastatic phenotype is regulated by estrogen in thyroid cells. *Thyroid* (2010) **20**:33–41. doi:10.1089/thy.2009.0296
8. Xu S, Chen G, Peng W, Renko K, Derwahl M. Oestrogen action on thyroid progenitor cells: relevant for the pathogenesis of thyroid nodules? *J Endocrinol* (2013) **218**:125–33. doi:10.1530/JOE-13-0029
9. Antico-Arciuch VG, Dima M, Liao XH, Refetoff S, Di Cristofano A. Cross-talk between PI3K and estrogen in the mouse thyroid predisposes to the development of follicular carcinomas with a higher incidence in females. *Oncogene* (2010) **29**:5678–86. doi:10.1038/onc.2010.308
10. Zeng Q, Chen GG, Vlantis AC, Van Hasselt CA. Oestrogen mediates the growth of human thyroid carcinoma cells via an oestrogen receptor-ERK pathway. *Cell Prolif* (2007) **40**:921–35. doi:10.1111/j.1365-2184.2007.00471.x
11. Ceresini G, Milli B, Morganti S, Maggio M, Bacchi-Modena A, Sgarabotto MP, et al. Effect of estrogen therapy for 1 year on thyroid volume and thyroid nodules in postmenopausal women. *Menopause* (2008) **15**:326–31. doi:10.1097/gme.0b013e318148b83e
12. Vaiman M, Olevson Y, Sandbank J, Habler L, Zehavi S, Kessler A. Are estrogen receptors alpha detectable in normal and abnormal thyroid tissue? *Eur Arch Otorhinolaryngol* (2010) **267**:1753–7. doi:10.1007/s00405-010-1269-0
13. Takano T, Amino N. Fetal cell carcinogenesis: a new hypothesis for better understanding of thyroid carcinoma. *Thyroid* (2005) **15**:432–8. doi:10.1089/thy.2005.15.432
14. Takano T. Fetal cell carcinogenesis of the thyroid: theory and practice. *Semin Cancer Biol* (2007) **17**:233–40. doi:10.1016/j.semcancer.2006.02.001
15. Vermeulen L, Sprick MR, Kemper K, Stassi G, Medema JP. Cancer stem cells – old concepts, new insights. *Cell Death Differ* (2008) **15**:947–58. doi:10.1038/cdd.2008.20
16. Lin RY. Thyroid cancer stem cells. *Nat Rev Endocrinol* (2011) **7**:609–16. doi:10.1038/nrendo.2011.127
17. Visvader JE. Cells of origin in cancer. *Nature* (2011) **469**:314–22. doi:10.1038/nature09781
18. Todaro M, Iovino F, Eterno V, Cammareri P, Gambara G, Espina V, et al. Tumorigenic and metastatic activity of human thyroid cancer stem cells. *Cancer Res* (2010) **70**:8874–85. doi:10.1158/0008-5472.CAN-10-1994
19. Sastre-Perona A, Santisteban P. Role of the wnt pathway in thyroid cancer. *Front Endocrinol (Lausanne)* (2012) **3**:31. doi:10.3389/fendo.2012.00031
20. Van Camp JK, Beckers S, Zegers D, Van Hul W. Wnt signaling and the control of human stem cell fate. *Stem Cell Rev* (2014) **10**:207–29. doi:10.1007/s12015-013-9486-8
21. Nakada D, Oguro H, Levi BP, Ryan N, Kitano A, Saitoh Y, et al. Oestrogen increases haematopoietic stem-cell self-renewal in females and during pregnancy. *Nature* (2014) **505**:555–8. doi:10.1038/nature12932
22. Manole D, Schildknecht B, Gosnell B, Adams E, Derwahl M. Estrogen promotes growth of human thyroid tumor cells by different molecular mechanisms. *J Clin Endocrinol Metab* (2001) **86**:1072–7. doi:10.1210/jcem.86.3.7283
23. Lee ML, Chen GG, Vlantis AC, Tse GM, Leung BC, Van Hasselt CA. Induction of thyroid papillary carcinoma cell proliferation by estrogen is associated with an altered expression of Bcl-xL. *Cancer J* (2005) **11**:113–21. doi:10.1097/00130404-200503000-00006
24. Dong W, Zhang H, Li J, Guan H, He L, Wang Z, et al. Estrogen induces metastatic potential of papillary thyroid cancer cells through estrogen receptor alpha and beta. *Int J Endocrinol* (2013) **2013**:941568. doi:10.1155/2013/941568
25. Santin AP, Furlanetto TW. Role of estrogen in thyroid function and growth regulation. *J Thyroid Res* (2011) **2011**:875125. doi:10.4061/2011/875125
26. Arciuch Antico VG, Di Cristofano A. Estrogen signaling and thyrocyte proliferation. In: Ward DL, editor. *Thyroid and Parathyroid Diseases – New Insights into Some Old and Some New Issues.* InTech (2012). 318 p. doi:10.5772/35913
27. Thiruvengadam A, Govindarajulu P, Aruldhas MM. Modulatory effect of estradiol and testosterone on the development of N-nitrosodiisopropanolamine induced thyroid tumors in female rats. *Endocr Res* (2003) **29**:43–51. doi:10.1081/ERC-120018675
28. Heldring N, Pike A, Andersson S, Matthews J, Cheng G, Hartman J, et al. Estrogen receptors: how do they signal and what are their targets. *Physiol Rev* (2007) **87**:905–31. doi:10.1152/physrev.00026.2006
29. Zahid M, Goldner W, Beseler CL, Rogan EG, Cavalieri EL. Unbalanced estrogen metabolism in thyroid cancer. *Int J Cancer* (2013) **133**:2642–9. doi:10.1002/ijc.28275
30. Huang Y, Dong W, Li J, Zhang H, Shan Z, Teng W. Differential expression patterns and clinical significance of estrogen receptor-alpha and beta in papillary thyroid carcinoma. *BMC Cancer* (2014) **14**:383. doi:10.1186/1471-2407-14-383
31. Chu R, Van Hasselt A, Vlantis AC, Ng EK, Liu SY, Fan MD, et al. The cross-talk between estrogen receptor and peroxisome proliferator-activated receptor gamma in thyroid cancer. *Cancer* (2014) **120**:142–53. doi:10.1002/cncr.28383
32. Leitman DC, Paruthiyil S, Vivar OI, Saunier EF, Herber CB, Cohen I, et al. Regulation of specific target genes and biological responses by estrogen receptor subtype agonists. *Curr Opin Pharmacol* (2010) **10**:629–36. doi:10.1016/j.coph.2010.09.009
33. Klinge CM. Estrogen receptor interaction with co-activators and co-repressors. *Steroids* (2000) **65**:227–51. doi:10.1016/S0039-128X(99)00107-5
34. Nilsson S, Makela S, Treuter E, Tujague M, Thomsen J, Andersson G, et al. Mechanisms of estrogen action. *Physiol Rev* (2001) **81**:1535–65.
35. Bjornstrom L, Sjoberg M. Mechanisms of estrogen receptor signaling: convergence of genomic and nongenomic actions on target genes. *Mol Endocrinol* (2005) **19**:833–42. doi:10.1210/me.2004-0486
36. Ascenzi P, Bocedi A, Marino M. Structure-function relationship of estrogen receptor alpha and beta: impact on human health. *Mol Aspects Med* (2006) **27**:299–402. doi:10.1016/j.mam.2006.07.001
37. Osmanbeyoglu HU, Lu KN, Oesterreich S, Day RS, Benos PV, Coronnello C, et al. Estrogen represses gene expression through reconfiguring chromatin structures. *Nucleic Acids Res* (2013) **41**:8061–71. doi:10.1093/nar/gkt586
38. Acconcia F, Kumar R. Signaling regulation of genomic and nongenomic functions of estrogen receptors. *Cancer Lett* (2006) **238**:1–14. doi:10.1016/j.canlet.2005.06.018
39. Chen JQ, Brown TR, Yager JD. Mechanisms of hormone carcinogenesis: evolution of views, role of mitochondria. *Adv Exp Med Biol* (2008) **630**:1–18. doi:10.1007/978-0-387-78818-0_1
40. He YY, Cai B, Yang YX, Liu XL, Wan XP. Estrogenic G protein-coupled receptor 30 signaling is involved in regulation of endometrial carcinoma by promoting proliferation, invasion potential, and interleukin-6 secretion via the MEK/ERK mitogen-activated protein kinase pathway. *Cancer Sci* (2009) **100**:1051–61. doi:10.1111/j.1349-7006.2009.01148.x
41. Roman-Blas JA, Castaneda S, Largo R, Herrero-Beaumont G. Osteoarthritis associated with estrogen deficiency. *Arthritis Res Ther* (2009) **11**:241. doi:10.1186/ar2791
42. Lima LP, Barros IA, Lisboa PC, Araujo RL, Silva AC, Rosenthal D, et al. Estrogen effects on thyroid iodide uptake and thyroperoxidase activity in normal and ovariectomized rats. *Steroids* (2006) **71**:653–9. doi:10.1016/j.steroids.2006.03.007
43. Furlanetto TW, Nguyen LQ, Jameson JL. Estradiol increases proliferation and down-regulates the sodium/iodide symporter gene in FRTL-5 cells. *Endocrinology* (1999) **140**:5705–11. doi:10.1210/endo.140.12.7197
44. Rajoria S, Suriano R, Wilson YL, George AL, Geliebter J, Schantz SP, et al. Estradiol-mediated tumor neo-vascularization. *Oncol Lett* (2011) **2**:453–7. doi:10.3892/ol.2011.283
45. Kouzmenko AP, Takeyama K, Ito S, Furutani T, Sawatsubashi S, Maki A, et al. Wnt/beta-catenin and estrogen signaling converge in vivo. *J Biol Chem* (2004) **279**:40255–8. doi:10.1074/jbc.C400331200
46. Postiglione MP, Parlato R, Rodriguez-Mallon A, Rosica A, Mithbaokar P, Maresca M, et al. Role of the thyroid-stimulating hormone receptor signaling in development and differentiation of the thyroid gland. *Proc Natl Acad Sci U S A* (2002) **99**:15462–7. doi:10.1073/pnas.242328999
47. Medina DL, Santisteban P. Thyrotropin-dependent proliferation of in vitro rat thyroid cell systems. *Eur J Endocrinol* (2000) **143**:161–78. doi:10.1530/eje.0.1430161
48. Kimura T, Van Keymeulen A, Golstein J, Fusco A, Dumont JE, Roger PP. Regulation of thyroid cell proliferation by TSH and other factors: a critical evaluation of in vitro models. *Endocr Rev* (2001) **22**:631–56. doi:10.1210/edrv.22.5.0444
49. Cass LA, Summers SA, Prendergast GV, Backer JM, Birnbaum MJ, Meinkoth JL. Protein kinase A-dependent and -independent signaling pathways contribute to cyclic AMP-stimulated proliferation. *Mol Cell Biol* (1999) **19**:5882–91.

50. Roger PP, Van Staveren WC, Coulonval K, Dumont JE, Maenhaut C. Signal transduction in the human thyrocyte and its perversion in thyroid tumors. *Mol Cell Endocrinol* (2010) **321**:3–19. doi:10.1016/j.mce.2009.11.015
51. Kursawe R, Paschke R. Modulation of TSHR signaling by posttranslational modifications. *Trends Endocrinol Metab* (2007) **18**:199–207. doi:10.1016/j.tem.2007.05.002
52. Tallini G. Molecular pathobiology of thyroid neoplasms. *Endocr Pathol* (2002) **13**:271–88. doi:10.1385/EP:13:4:271
53. Krohn K, Fuhrer D, Bayer Y, Eszlinger M, Brauer V, Neumann S, et al. Molecular pathogenesis of euthyroid and toxic multinodular goiter. *Endocr Rev* (2005) **26**:504–24. doi:10.1210/er.2004-0005
54. Matsuo K, Friedman E, Gejman PV, Fagin JA. The thyrotropin receptor (TSH-R) is not an oncogene for thyroid tumors: structural studies of the TSH-R and the alpha-subunit of Gs in human thyroid neoplasms. *J Clin Endocrinol Metab* (1993) **76**:1446–51. doi:10.1210/jcem.76.6.8501149
55. Spambalg D, Sharifi N, Elisei R, Gross JL, Medeiros-Neto G, Fagin JA. Structural studies of the thyrotropin receptor and Gs alpha in human thyroid cancers: low prevalence of mutations predicts infrequent involvement in malignant transformation. *J Clin Endocrinol Metab* (1996) **81**:3898–901. doi:10.1210/jcem.81.11.8923835
56. Reya T, Clevers H. Wnt signalling in stem cells and cancer. *Nature* (2005) **434**:843–50. doi:10.1038/nature03319
57. Kim WB, Lewis CJ, Mccall KD, Malgor R, Kohn AD, Moon RT, et al. Overexpression of Wnt-1 in thyrocytes enhances cellular growth but suppresses transcription of the thyroperoxidase gene via different signaling mechanisms. *J Endocrinol* (2007) **193**:93–106. doi:10.1677/JOE-06-0025
58. Chen G, Jiang Q, You Z, Yao J, Mou L, Lin X, et al. Regulation of GSK-3 beta in the proliferation and apoptosis of human thyrocytes investigated using a GSK-3 beta-targeting RNAi adenovirus expression vector: involvement the Wnt/beta-catenin pathway. *Mol Biol Rep* (2010) **37**:2773–9. doi:10.1007/s11033-009-9819-5
59. Pascual A, Aranda A. Thyroid hormone receptors, cell growth and differentiation. *Biochim Biophys Acta* (2013) **1830**:3908–16. doi:10.1016/j.bbagen.2012.03.012
60. Cheng SY, Leonard JL, Davis PJ. Molecular aspects of thyroid hormone actions. *Endocr Rev* (2010) **31**:139–70. doi:10.1210/er.2009-0007
61. Yen PM, Ando S, Feng X, Liu Y, Maruvada P, Xia X. Thyroid hormone action at the cellular, genomic and target gene levels. *Mol Cell Endocrinol* (2006) **246**:121–7. doi:10.1016/j.mce.2005.11.030
62. Keller H, Givel F, Perroud M, Wahli W. Signaling cross-talk between peroxisome proliferator-activated receptor/retinoid X receptor and estrogen receptor through estrogen response elements. *Mol Endocrinol* (1995) **9**:794–804. doi:10.1210/mend.9.7.7476963
63. Banu SK, Govindarajulu P, Aruldhas MM. Developmental profiles of TSH, sex steroids, and their receptors in the thyroid and their relevance to thyroid growth in immature rats. *Steroids* (2002) **67**:137–44. doi:10.1016/S0039-128X(01)00144-1
64. Kim WG, Cheng SY. Thyroid hormone receptors and cancer. *Biochim Biophys Acta* (2013) **1830**:3928–36. doi:10.1016/j.bbagen.2012.04.002
65. Plateroti M, Kress E, Mori JI, Samarut J. Thyroid hormone receptor alpha1 directly controls transcription of the beta-catenin gene in intestinal epithelial cells. *Mol Cell Biol* (2006) **26**:3204–14. doi:10.1128/MCB.26.8.3204-3214.2006
66. Kress E, Samarut J, Plateroti M. Thyroid hormones and the control of cell proliferation or cell differentiation: paradox or duality? *Mol Cell Endocrinol* (2009) **313**:36–49. doi:10.1016/j.mce.2009.08.028
67. Kress E, Skah S, Sirakov M, Nadjar J, Gadot N, Scoazec JY, et al. Cooperation between the thyroid hormone receptor TRalpha1 and the WNT pathway in the induction of intestinal tumorigenesis. *Gastroenterology* (2010) **138**:1863–74. doi:10.1053/j.gastro.2010.01.041
68. Garcia-Rostan G, Camp RL, Herrero A, Carcangiu ML, Rimm DL, Tallini G. Beta-catenin dysregulation in thyroid neoplasms: down-regulation, aberrant nuclear expression, and CTNNB1 exon 3 mutations are markers for aggressive tumor phenotypes and poor prognosis. *Am J Pathol* (2001) **158**:987–96. doi:10.1016/S0002-9440(10)64045-X
69. Nikiforov YE, Nikiforova MN. Molecular genetics and diagnosis of thyroid cancer. *Nat Rev Endocrinol* (2011) **7**:569–80. doi:10.1038/nrendo.2011.142
70. Kroll TG, Sarraf P, Pecciarini L, Chen CJ, Mueller E, Spiegelman BM, et al. PAX8-PPARgamma1 fusion oncogene in human thyroid carcinoma [corrected]. *Science* (2000) **289**:1357–60. doi:10.1126/science.289.5483.1357
71. Garcia-Rostan G, Zhao H, Camp RL, Pollan M, Herrero A, Pardo J, et al. Ras mutations are associated with aggressive tumor phenotypes and poor prognosis in thyroid cancer. *J Clin Oncol* (2003) **21**:3226–35. doi:10.1200/JCO.2003.10.130
72. Liu D, Yang C, Bojdani E, Murugan AK, Xing M. Identification of RASAL1 as a major tumor suppressor gene in thyroid cancer. *J Natl Cancer Inst* (2013) **105**:1617–27. doi:10.1093/jnci/djt249
73. Bellelli R, Castellone MD, Garcia-Rostan G, Ugolini C, Nucera C, Sadow PM, et al. FOXM1 is a molecular determinant of the mitogenic and invasive phenotype of anaplastic thyroid carcinoma. *Endocr Relat Cancer* (2012) **19**:695–710. doi:10.1530/ERC-12-0031
74. Nehs MA, Nucera C, Nagarkatti SS, Sadow PM, Morales-Garcia D, Hodin RA, et al. Late intervention with anti-BRAF(V600E) therapy induces tumor regression in an orthotopic mouse model of human anaplastic thyroid cancer. *Endocrinology* (2012) **153**:985–94. doi:10.1210/en.2011-1519
75. Landa I, Ganly I, Chan TA, Mitsutake N, Matsuse M, Ibrahimpasic T, et al. Frequent somatic TERT promoter mutations in thyroid cancer: higher prevalence in advanced forms of the disease. *J Clin Endocrinol Metab* (2013) **98**:E1562–6. doi:10.1210/jc.2013-2383
76. De Felice M, Di Lauro R. Thyroid development and its disorders: genetics and molecular mechanisms. *Endocr Rev* (2004) **25**:722–46. doi:10.1210/er.2003-0028
77. Fagman H, Nilsson M. Morphogenetics of early thyroid development. *J Mol Endocrinol* (2011) **46**:R33–42. doi:10.1677/JME-10-0084
78. Yarden Y, Sliwkowski MX. Untangling the ErbB signalling network. *Nat Rev Mol Cell Biol* (2001) **2**:127–37. doi:10.1038/35052073
79. Konturek A. Thyroid growth factors. In: Ward DL, editor. *Thyroid and Parathyroid Diseases – New Insight into Some Old and Some New Issues*. InTech (2012). 318 p. doi:10.5772/37570
80. Kato S, Kobayashi T, Yamada K, Nishii K, Sawada H, Ishiguro H, et al. Expression of erbB receptors mRNA in thyroid tissues. *Biochim Biophys Acta* (2004) **1673**:194–200. doi:10.1016/j.bbagen.2004.04.016
81. Bergstrom JD, Westermark B, Heldin NE. Epidermal growth factor receptor signaling activates met in human anaplastic thyroid carcinoma cells. *Exp Cell Res* (2000) **259**:293–9. doi:10.1006/excr.2000.4967
82. Song B. Immunohistochemical demonstration of epidermal growth factor receptor and ceruloplasmin in thyroid diseases. *Acta Pathol Jpn* (1991) **41**:336–43.
83. Schiff BA, Mcmurphy AB, Jasser SA, Younes MN, Doan D, Yigitbasi OG, et al. Epidermal growth factor receptor (EGFR) is overexpressed in anaplastic thyroid cancer, and the EGFR inhibitor gefitinib inhibits the growth of anaplastic thyroid cancer. *Clin Cancer Res* (2004) **10**:8594–602. doi:10.1158/1078-0432.CCR-04-0690
84. Hoffmann S, Glaser S, Wunderlich A, Lingelbach S, Dietrich C, Burchert A, et al. Targeting the EGF/VEGF-R system by tyrosine-kinase inhibitors – a novel antiproliferative/antiangiogenic strategy in thyroid cancer. *Langenbecks Arch Surg* (2006) **391**:589–96. doi:10.1007/s00423-006-0104-y
85. Lan L, Cui D, Nowka K, Derwahl M. Stem cells derived from goiters in adults form spheres in response to intense growth stimulation and require thyrotropin for differentiation into thyrocytes. *J Clin Endocrinol Metab* (2007) **92**:3681–8. doi:10.1210/jc.2007-0281
86. Zheng X, Cui D, Xu S, Brabant G, Derwahl M. Doxorubicin fails to eradicate cancer stem cells derived from anaplastic thyroid carcinoma cells: characterization of resistant cells. *Int J Oncol* (2010) **37**:307–15. doi:10.3892/ijo_00000679
87. Malaguarnera R, Frasca F, Garozzo A, Giani F, Pandini G, Vella V, et al. Insulin receptor isoforms and insulin-like growth factor receptor in human follicular cell precursors from papillary thyroid cancer and normal thyroid. *J Clin Endocrinol Metab* (2011) **96**:766–74. doi:10.1210/jc.2010-1255
88. Tseng LM, Huang PI, Chen YR, Chen YC, Chou YC, Chen YW, et al. Targeting signal transducer and activator of transcription 3 pathway by cucurbitacin I diminishes self-renewing and radiochemoresistant abilities in thyroid cancer-derived CD133+ cells. *J Pharmacol Exp Ther* (2012) **341**:410–23. doi:10.1124/jpet.111.188730
89. Li W, Reeb AN, Sewell WA, Elhomsy G, Lin RY. Phenotypic characterization of metastatic anaplastic thyroid cancer stem cells. *PLoS One* (2013) **8**:e65095. doi:10.1371/journal.pone.0065095
90. Ahn SH, Henderson YC, Williams MD, Lai SY, Clayman GL. Detection of thyroid cancer stem cells in papillary thyroid carcinoma. *J Clin Endocrinol Metab* (2014) **99**:536–44. doi:10.1210/jc.2013-2558

91. Longmire TA, Ikonomou L, Hawkins F, Christodoulou C, Cao Y, Jean JC, et al. Efficient derivation of purified lung and thyroid progenitors from embryonic stem cells. *Cell Stem Cell* (2012) **10**:398–411. doi:10.1016/j.stem.2012.01.019
92. Eggo MC, Hopkins JM, Franklyn JA, Johnson GD, Sanders DS, Sheppard MC. Expression of fibroblast growth factors in thyroid cancer. *J Clin Endocrinol Metab* (1995) **80**:1006–11. doi:10.1210/jcem.80.3.7533768
93. Guo M, Liu W, Serra S, Asa SL, Ezzat S. FGFR2 isoforms support epithelial-stromal interactions in thyroid cancer progression. *Cancer Res* (2012) **72**:2017–27. doi:10.1158/0008-5472.CAN-11-3985
94. Redler A, Di Rocco G, Giannotti D, Frezzotti F, Bernieri MG, Ceccarelli S, et al. Fibroblast growth factor receptor-2 expression in thyroid tumor progression: potential diagnostic application. *PLoS One* (2013) **8**:e72224. doi:10.1371/journal.pone.0072224
95. Laron Z. Insulin-like growth factor 1 (IGF-1): a growth hormone. *Mol Pathol* (2001) **54**:311–6. doi:10.1136/mp.54.5.311
96. Bendall SC, Stewart MH, Menendez P, George D, Vijayaragavan K, Werbowetski-Ogilvie T, et al. IGF and FGF cooperatively establish the regulatory stem cell niche of pluripotent human cells in vitro. *Nature* (2007) **448**:1015–21. doi:10.1038/nature06027
97. Vella V, Pandini G, Sciacca L, Mineo R, Vigneri R, Pezzino V, et al. A novel autocrine loop involving IGF-II and the insulin receptor isoform-A stimulates growth of thyroid cancer. *J Clin Endocrinol Metab* (2002) **87**:245–54. doi:10.1210/jcem.87.1.8142
98. Malaguarnera R, Belfiore A. The emerging role of insulin and insulin-like growth factor signaling in cancer stem cells. *Front Endocrinol (Lausanne)* (2014) **5**:10. doi:10.3389/fendo.2014.00010
99. Jiang K, Yang Z, Cheng L, Wang S, Ning K, Zhou L, et al. Mediator of ERBB2-driven cell motility (MEMO) promotes extranuclear estrogen receptor signaling involving the growth factor receptors IGF1R and ERBB2. *J Biol Chem* (2013) **288**:24590–9. doi:10.1074/jbc.M113.467837

Conflict of Interest Statement: The authors declare that the research was conducted in the absence of any commercial or financial relationships that could be construed as a potential conflict of interest.

Received: 16 May 2014; accepted: 11 July 2014; published online: 25 July 2014.
*Citation: Zane M, Catalano V, Scavo E, Bonanno M, Pelizzo MR, Todaro M and Stassi G (2014) Estrogens and stem cells in thyroid cancer. Front. Endocrinol. **5**:124. doi: 10.3389/fendo.2014.00124*
This article was submitted to Thyroid Endocrinology, a section of the journal Frontiers in Endocrinology.

Chapter 4

Breast cancer stem cells rely on fermentative glycolysis and are sensitive to 2-deoxyglucose treatment

D. Ciavardelli, C. Rossi, D. Barcaroli, S. Volpe, A. Consalvo, M. Zucchelli, A. De Cola, **E. Scavo**, R. Carollo, D. D'Agostino, F. Forlì, S. D'Aguanno , M. Todaro, G. Stassi, C. Di Ilio, V. De Laurenzi and A. Urbani

Published in *Cell Death and Disease*, 2014.

OPEN

Citation: Cell Death and Disease (2014) 5, e1336; doi:10.1038/cddis.2014.285

www.nature.com/cddis

Breast cancer stem cells rely on fermentative glycolysis and are sensitive to 2-deoxyglucose treatment

D Ciavardelli*[,1,2], C Rossi[2,3], D Barcaroli[2,3], S Volpe[4], A Consalvo[2,3], M Zucchelli[2,3], A De Cola[2,3], E Scavo[4], R Carollo[4], D D'Agostino[2,3], F Forlì[2,3], S D'Aguanno[5], M Todaro[4], G Stassi[4], C Di Ilio[3], V De Laurenzi*[,2,3,7] and A Urbani[5,6,7]

A number of studies suggest that cancer stem cells are essential for tumour growth, and failure to target these cells can result in tumour relapse. As this population of cells has been shown to be resistant to radiation and chemotherapy, it is essential to understand their biology and identify new therapeutic approaches. Targeting cancer metabolism is a potential alternative strategy to counteract tumour growth and recurrence. Here we applied a proteomic and targeted metabolomic analysis in order to point out the main metabolic differences between breast cancer cells grown as spheres and thus enriched in cancer stem cells were compared with the same cells grown in adherent differentiating conditions. This integrated approach allowed us to identify a metabolic phenotype associated with the stem-like condition and shows that breast cancer stem cells (BCSCs) shift from mitochondrial oxidative phosphorylation towards fermentative glycolysis. Functional validation of proteomic and metabolic data provide evidences for increased activities of key enzymes of anaerobic glucose fate such as pyruvate kinase M2 isoform, lactate dehydrogenase and glucose 6-phopshate dehydrogenase in cancer stem cells as well as different redox status. Moreover, we show that treatment with 2-deoxyglucose, a well known inhibitor of glycolysis, inhibits BCSC proliferation when used alone and shows a synergic effect when used in combination with doxorubicin. In conclusion, we suggest that inhibition of glycolysis may be a potentially effective strategy to target BCSCs.
Cell Death and Disease (2014) **5,** e1336; doi:10.1038/cddis.2014.285; published online 17 July 2014

One of the main problems in the therapy of breast tumour is long-term relapse. This can in part be explained by failure to eradicate a subset of cells within the tumour that are then capable of sustaining tumour growth. These cells share a number of features with stem cells and have therefore been called cancer stem cells (CSCs). CSCs have been isolated from a variety of solid tumours, including breast cancer[1] and appear to have role in resistance to treatment as well as in metastasis formation.[2] Indeed, CSCs present several intrinsic mechanisms of resistance to conventional antitumour drugs and radiation therapy such the overexpression of adenosine triphosphate (ATP)-binding cassette (ABC) drug transporters, activation of survival pathways, increased production of anti-apoptotic factors, higher defences against oxidative stress, and efficient repair of DNA damage.[3] Therefore the development and validation of new therapeutic strategies targeting CSCs is urgently needed to improve clinical outcome.

Recently, the interest on studying cancer metabolism and the so called Warburg effect has grown as targeting specific metabolic pathways might be a promising approach to cancer therapy.[4,5] Warburg effect defines cancer dependence on fermentative glycolysis allowing for the diversion of key metabolites into cellular biosynthetic pathways in proliferating cancer cells,[6] including CSC, and it has been suggested that it can be exploited to develop new pharmacological treatments that can counteract the chemo-resistance of these cells.[7,8]

It has also been suggested that metabolic changes may have a causal role in inducing different phenotypic states of cancer cells. As an example, Dong *et al.*[9] have shown that

[1]School of Human and Social Science, 'Kore' University of Enna, Enna, Italy; [2]Center of Excellence on Aging (Ce.S.I.), 'G. d'Annunzio' Foundation, Chieti, Italy; [3]Department of Experimental and Clinical Sciences, 'G. d'Annunzio' University of Chieti-Pescara, Chieti, Italy; [4]Department of Surgical and Oncological Sciences, Laboratory of Cellular and Molecular Pathophysiology, University of Palermo, Palermo, Italy; [5]IRCCS S. Lucia, Rome, Italy and [6]Department of Internal Medicine, University of Rome 'Tor Vergata', Rome, Italy

*Corresponding authors: D Ciavardelli, School of Human and Social Science, 'Kore' University of Enna, Via della Cooperazione, Enna 94100, Italy. Tel: +39 0935 536364; Fax: +39 0935 536943; E-mail: domenico.ciavardelli@unikore.it or d.ciavardelli@unich.it

or V De Laurenzi, Department of Experimental and Clinical Sciences, 'G. d'Annunzio' University of Chieti-Pescara, Via dei Vestini 31, Chieti 66100, Italy. Tel: +39 0871 541587; Fax: +39 0871 541542; E-mail: delaurenzi@unich.it

[7]Both authors have been acting as senior investigators and should be considered as equal last authors.

Abbreviations: 2-DG, 2-deoxy-D-glucose; AA, amino acid; ABC, ATP-binding cassette; AcCs, acylcarnitines; ADP, adenosine diphosphate; ATP, adenosine triphosphate; anti-CD24-PE-Cy7, antibody-CD24-R-phycoerythrin-cyanine dye7; anti-CD44-APC, antibody-CD44-allophycocyanin; Arg, Arginine; BCSC, breast cancer stem cell; bFGF, basic fibroblast growth factor; CD24, cluster of differentiation 24; CD44, cluster of differentiation 44; CSC, cancer stem cell; DMEM, Dulbecco's Modified Eagle Medium; Doxo, doxorubicin; DTT, dithiothreitol; EGF, epidermal growth factor; EMRT, exact mass retention time cluster; ETC, electron transport chain; FA, fatty acid; G6PDH, glucose 6-phosphate dehydrogenase; GC–MS, gas-chromatography mass spectrometry; Gly, glycine; HIF-1α, hypoxia-inducible factor 1α; His, histidine; IPA, Ingenuity Pathway Analysis; LC-MS/MS, liquid chromatography tandem mass spectrometry; LDH, lactate dehydrogenase; LDH-A, lactate dehydrogenase A; NAD, nicotinamide adenine dinucleotide; NADP, nicotinamide adenine dinucleotide phosphate; PK, pyruvate kinase; PKM2, pyruvate kinase M2; PMSF, phenylmethylsulfonyl fluoride; RLU, relative light units; ROS, reactive oxygen species; SDAC, spheroid-derived adherent cell; TCA, tricarboxylic acids cycle; Val, valine; WB, western blotting

Received 03.3.14; revised 21.5.14; accepted 27.5.14; Edited by M Agostini

silencing of the gluconeogenic enzyme fructose-1,6-biphosphatase that activates fermentative glycolysis results in a stem-like phenotype. Despite their importance, the metabolic features of CSCs still remains largely unknown. Recently, it has been shown that CSCs isolated from several solid tumours display significant alteration of energy metabolism and are more glycolytic compared with more differentiated tumour cells[10–13]or normal stem cells.[14] However, this is still a controversial issue as previous studies have shown that CSCs are less glycolytic than the differentiated ones.[15]

Here, using an integrated proteomic and targeted metabolomic approach, we show that the metabolism of breast cancer stem cells (BCSCs) grown as spheres is strongly linked to fermentative glycolysis compared with the same cells grown in adherent differentiating conditions (spheroid-derived adherent cells (SDACs)). On the basis of these evidences, we sought to test the effect of a well-characterized glycolytic inhibitor, 2-deoxy-D-glucose (2-DG),[16,17] alone or in combination with the widely used chemotherapeutic doxorubicin (Doxo) on BCSCs' growth and proliferation. Our results indicate that BCSCs are highly sensitive to 2-DG that also shows a synergic effect with Doxo treatment.

Results

Differential proteomics analysis indicates a shift toward fermentative glucose metabolism in BCSC spheres. In this study, we have analysed differential protein expression profiles of BCSCs and SDACs. As previously reported,[18] the *in vitro* model adopted for differentiated cells, conventionally reported as SDACs, relies on sphere cells cultured in Dulbecco's modified Eagle medium (DMEM) supplemented with 10% fetal bovine serum (FBS) in adherent conditions. These cells express higher levels of cluster of differentiation 24 (CD24) as expected for SDACs (Supplementary Figure S1).[19,20]

Compared with the gel electrophoresis-mass spectrometry (GC–MS) proteomics approach, label-free liquid chromatography tandem mass spectrometry (LC-MS/MS) provides a high throughput and low expensive analytical method for characterization of complex protein mixtures with suitable sensitivity and repeatability. Protein identification, quantification, and data quality of exact mass retention time clusters (EMRTs), which are the recorded mass species associated to their exact masses and retention times, were evaluated. A total of 39 379 and 39 379 EMRTs were determined for the comparison of BCSCs grown as spheres *versus* SDACs for 3.5 and 7 days, respectively. For each replicate conditions, the distribution of mass error was under 15 p.p.m. (Figures 1a, d and g for BCSCs and SDAC collected after 3.5 days and 7 days, respectively), the intensity coefficient of variation expressed as percentage (% CV intensity) had a Gaussian distribution with all values $<4.5\%$ (Figures 1b, e and h for BCSCs and SDAC collected after 3.5 days and 7 days, respectively) and the retention time coefficient of variation expressed as percentage (% CV RT) was $<10\%$ (Figures 1c, f and i for BCSCs, SDAC collected after 3.5 days and 7 days, respectively) with most of the species $<5\%$. Applying the stringent criteria of protein identification and quantification described in the Materials and Methods, we identified 54 and 28 proteins differentially expressed in BCSCs compared with SDACs collected after 3.5 and 7 days in differentiating conditions. The lists of differential proteins are shown in Supplementary Tables S1 and S2, while the details of peptide identifications are reported in Supplementary Tables S3 and S4.

Venn analysis (Figure 1j) shows that 19 proteins were upregulated in spheres as compared with both time points of differentiation, whereas 5 were downregulated in the same experimental conditions. Interestingly, the expression levels of these proteins did not change between 3.5 and 7 days in adherent conditions (Figure 1k), thus suggesting that the differences were strictly related to the stem-like condition. We therefore decided to use SDACs collected after 3.5 days in adherent conditions for all the subsequent studies, thereby focusing on early changes between the BCSC and SDAC condition.

Bioinformatic analysis of these differentially expressed proteins identified two significant overlapping protein networks related to the haematological, immunological, and inflammatory diseases (score $=62$) and the free radical scavenging and cancer pathway (score $=3$) (Figures 2a and b). Functional analysis based on GO terms indicated that several of the differentially expressed proteins are strictly related to glycolysis ($P=3\times10^{-13}$) and gluconeogenesis ($P=2\times10^{-8}$) (Figure 2c). In particular, the increased expression levels of key enzymes of fermentative glycolysis such as pyruvate kinase M2 (PKM2) and lactate dehydrogenase A (LDH-A) in spheres compared with SDACs might indicate that spheres essentially metabolize glucose through a non-oxidative pathway even under normoxic conditions. This hypothesis is in line with the reported upregulation of hypoxia-inducible factor 1α (HIF-1α) in CSC[12,21] and with the predicted activation of HIF-1α-dependent pathway as suggested (z-score $=2.791$) by the higher expression in BCSC as compared with SDACs of several proteins involved in this pathway such as triosephosphate isomerase 1, phosphoglycerate kinase 1, galectin 1, LDH-A, heat-shock 70-kDa protein, glyceraldheyde 3-phosphate dehydrogenase, enolase 1, and aldolase A. Indeed,

Figure 1 Data quality evaluation, Venn analysis, and expression ratios for significantly regulated proteins in BCSCs compared with SDACs. Analytical reproducibility of mass spectra was assessed in BCSCs, and cells were allowed to differentiate as SDACs for 3.5 and 7 days. Bar charts show the mass relative standard deviation (RSD) and the intensity and retention time coefficients of variation (% CV) of exact mass retention time clusters detected in BCSCs (**a**, **b**, **c**), and SDACs collected at 3.5 days (**d**, **e**, **f**) and 7 days (**g**, **h**, **i**) post-differentiation (pd). (**j**) Four-way Venn diagram analysis of differentially expressed proteins identify 15 loci. Numbers in parentheses represent the total number of identified proteins clustered in each locus. BCSCs compared to SDACs 3.5 days pd show 25 and 5 proteins specifically up-regulated and down-regulated, respectively; BCSCs show 4 proteins up-regulated compared to SDACs 7 days pd; BCSCs show 19 and 5 proteins up-regulated and down-regulated, respectively compared to SDACs regardless of differentiation time. The Swiss-Prot accession numbers are listed in table (see the Supplementary Tables S1 and S2 for a detailed description). Analysis was performed using the four-way Venn Diagram Generator freely available at http://www.pangloss.com/seidel/Protocols/venn4.cgi. (**k**) Bar chart displays the mean protein expression level ratios ($n=3$) of 19 and 5 proteins up- and down-regulated, respectively in BCSCs compared to SDACs regardless of differentiation time . The red line indicates the expression ratio $=1$

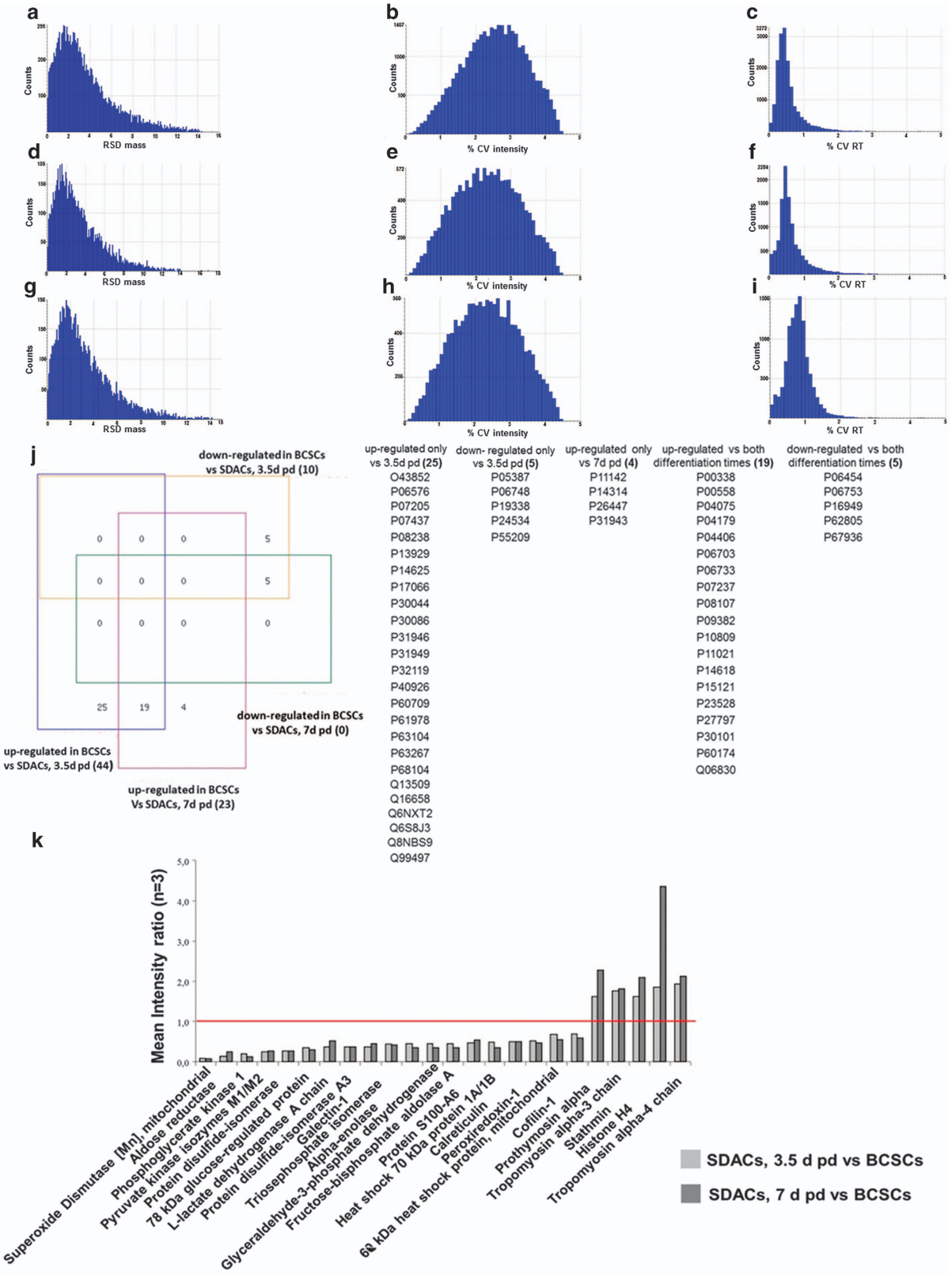
a
b
c
d
e
f
g
h
i
Counts
RSD mass
% CV intensity
% CV RT
j
down-regulated in BCSCs vs SDACs, 3.5d pd (10)
down-regulated in BCSCs vs SDACs, 7d pd (0)
up-regulated in BCSCs vs SDACs, 3.5d pd (44)
up-regulated in BCSCs Vs SDACs, 7d pd (23)
0 0 0 5
0 0 0 5
0 0 0 0
25 19 4
up-regulated only vs 3.5d pd (25)
O43852
P06576
P07205
P07437
P08238
P13929
P14625
P17066
P30044
P30086
P31946
P31949
P32119
P40926
P60709
P61978
P63104
P63267
P68104
Q13509
Q16658
Q6NXT2
Q6S8J3
Q8NBS9
Q99497
down- regulated only vs 3.5d pd (5)
P05387
P06748
P19338
P24534
P55209
up-regulated only vs 7d pd (4)
P11142
P14314
P26447
P31943
up-regulated vs both differentiation times (19)
P00338
P00558
P04075
P04179
P04406
P06703
P06733
P07237
P08107
P09382
P10809
P11021
P14618
P15121
P23528
P27797
P30101
P60174
Q06830
down-regulated vs both differentiation times (5)
P06454
P06753
P16949
P62805
P67936
k
Mean Intensity ratio (n=3)
5,0
4,0
3,0
2,0
1,0
0,0
Superoxide Dismutase [Mn], mitochondrial
Aldose reductase
Phosphoglycerate kinase 1
Pyruvate kinase isozymes M1/M2
Protein disulfide-isomerase
78 kDa glucose-regulated protein
L-lactate dehydrogenase A chain
Protein disulfide-isomerase A3
Galectin-1
Triosephosphate isomerase
Alpha-enolase
Glyceraldehyde-3-phosphate dehydrogenase
Fructose-bisphosphate aldolase A
Protein S100-A6
Heat shock 70 kDa protein 1A/1B
Calreticulin
Peroxiredoxin-1
60 kDa heat shock protein, mitochondrial
Cofilin-1
Prothymosin alpha
Tropomyosin alpha-3 chain
Stathmin
Histone H4
Tropomyosin alpha-4 chain
SDACs, 3.5 d pd vs BCSCs
SDACs, 7 d pd vs BCSCs

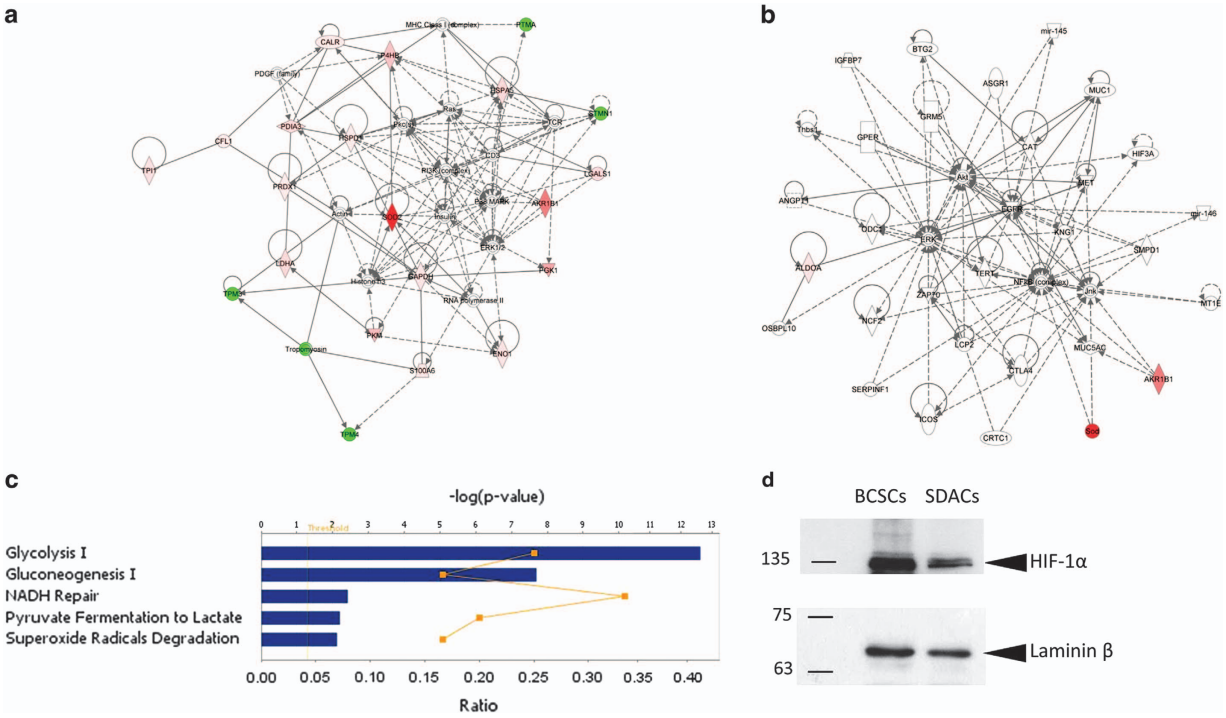

Figure 2 Functional and protein network analysis indicates increased glycolytic activity and activation of HIF-1α pathway in BCSCs. Ingenuity Pathway Analysis of differentially expressed proteins in BCSCs compared with SDACs result in two interaction network related to (**a**) the haematological, immunological, and inflammatory diseases and (**b**) the free radical scavenging and cancer pathway. Diagrams show focus genes (the differentially expressed proteins) that are depicted in green (downregulated) or red (upregulated). Solid and dashed lines indicate the direct and indirect interactions, respectively, and the arrows indicate the modulatory role of proteins or endogenous chemicals. (**c**) The canonical pathways associated with BCSCs are glycolysis, gluconeogenesis, and superoxide radical degradation. Functional pathway analysis was performed using the Ingenuity Pathway Analysis tool for the significantly regulated proteins in BCSCs compared with SDACs. The bar graph shows the scores ($-\log_{10}P$) associated to the pathways enriched with regulated proteins as determined using right-tailed Fisher's exact test with threshold <0.050. The yellow line indicates the ratio calculated as the number of proteins in a given pathway that meet the cutoff criteria ($P=0.050$) divided by the total number of molecules that make up that pathway. (**d**) BCSCs upregulate normoxic HIF-1α. Nuclear extracts were assessed for HIF-1α and laminin β by WB. WB shows that the HIF-1α expression level significantly decreases in cells allowed to differentiate as SDACs for 3.5 days

a western blotting (WB) analysis confirms that BCSCs express higher levels of HIF-1α as compared with SDACs (Figure 2d).

Targeted metabolomics shows increased lactic fermentation rate and inhibition of fatty acid (FA) beta-oxidation in BCSCs. In order to verify whether BCSCs were more glycolytic when grown as spheroids than when grown as SDACs, we performed targeted metabolomic analysis of glycolysis intermediates. We found that levels of fructose 1,6-diphospate, pyruvate, lactic acid, and ribose 5-phosphate were significantly higher in BCSCs (Figure 3a, Supplementary Table S5). In addition, we did not find significant differences in concentrations of Krebs cycle intermediates with exception of succinic acid, which was significantly higher in BCSCs (Figure 3a, Supplementary Table S5), and fumaric acid, which was higher in BCSCs, but the difference with SDACs was not statistically significant (mean ± S.D. = 1995 ± 257 and 1233 ± 638 ng/mg^{-1} in BCSCs and differentiated cells, respectively; $P=0.204$).

Our data also indicate relevant alterations of acylcarnitines (AcCs) and amino acids (AA) profiles in BCSCs. The concentrations of valine (Val), ornitine, phenylalanine, arginine (Arg), tyrosine, serine, histidine (His), proline, glycine (Gly), and lysine/glutamine increased in BCSCs as compared with SDACs (Figure 3b; Supplementary Table S5). Both Lys and Gln are undistinguishable by LC-MS/MS, and we have been able to assess their overall concentration. In contrast, alanine (Ala) significantly decreased in BCSCs compared with SDACs (Figure 3b; Supplementary Table S5).

Of note, we found a significant lower levels of free carnitine in spheres as compared with SDACs (Figure 3b, Supplementary Table S5), suggesting the inhibition of AcCs synthesis and finally of FA beta-oxidation. Consistently with this hypothesis, short, medium, and long-chain AcCs were undetectable in BCSCs. In contrast, AcCs were all quantifiable in SDACs (Supplementary Table S5).

BCSCs show higher activity of key enzymes of anaerobic glucose metabolism. We further validated the expression level of PKM2 and LDH-A, key enzyme of aerobic glycolysis, by WB analysis of protein extracts collected from BCSCs and SDACs. We confirmed that PKM2 and LDH-A were significantly upregulated in BCSCs compared with SDACs (Figure 4a, $P=0.008$ and 0.034, respectively; $n=3$). Furthermore, BCSCs displayed increased PK (mean ± S.D. = 2.5 ± 0.7 and 1.0 ± 0.2 μmol/mg$_{Protein}$/min in BCSCs and SDACs, respectively; $P=0.0001$; $n=6$) and LDH-A (mean ± S.D. = 2.0 ± 0.8 and 1.3 ± 0.1 μmol/mg$_{Protein}$/min in

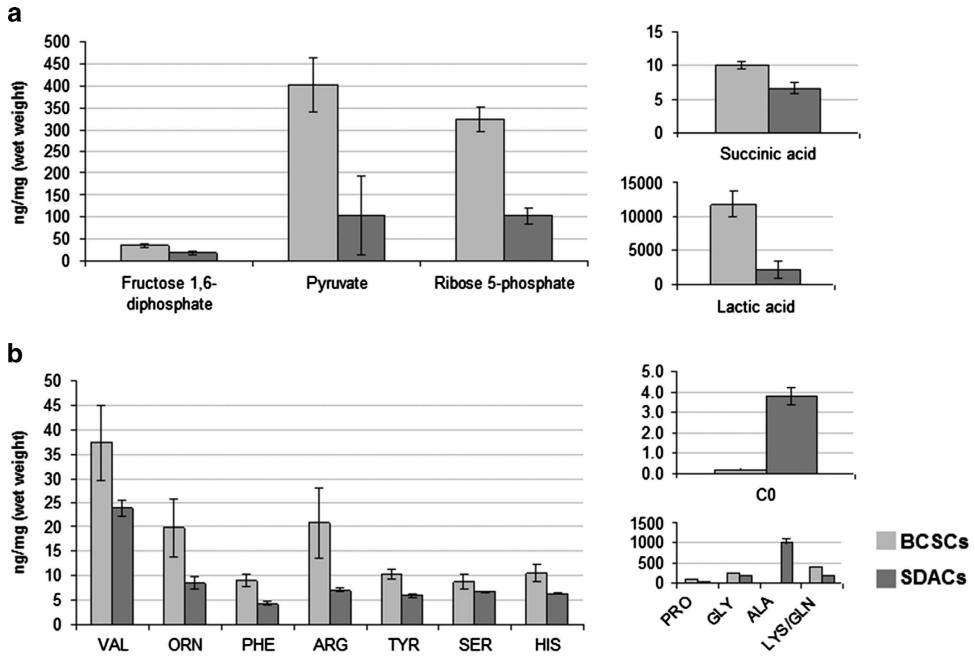

Figure 3 Targeted metabolomics reveals significant alterations of glycolytic intermediates, glucose-derived non-essential amino acids, free carnitine, and AcCs, suggesting increased lactic fermentation and inhibition of FAoxidation in BCSCs. Bar graphs show the mean concentrations of (**a**) glycolytic and Krebs cycle intermediates and (**b**) amino acids and free carnitine in BCSCs and SDACs. Results of targeted metabolomic analysis are available in the Supplementary Table S5. The differences shown in the bar graphs are all significant (two-tailed *t*-test, $P<0.050$). Concentrations are expressed as ng/mg (wet weight). Bars show the mean value ± S.D. ($n=6$)

BCSCs and SDACs, respectively; $P=0.044$; $n=6$) activity (Figures 4b and c).

In order to confirm that the metabolic differences observed are indeed due to differences between CSCs and more differentiated cancer cells, we sorted $CD24^{-/low}$ cells within the sphere culture, supposed to be the less differentiated more stem-like cells, and compared them with a more differentiated population expressing higher CD24 levels. We assessed the expression levels and enzymatic activities of LDH and PK in $CD24^{-/low}$ and $CD24^{+}$ BCSCs. In accordance with a more glicolitic phenotype, $CD24^{-/low}$ cells show higher levels (Figure 4d) and activities of PK (mean ± S.D. = 19.2 ± 0.3 and 2.0 ± 0.4 μmol/$mg_{Protein}$/min in $CD24^{-/low}$ and $CD24^{+}$ cells, respectively; $P=6\times10^{-13}$; $n=6$) and LDH (mean ± S.D. = 3.6 ± 0.3 and 2.5 ± 0.5 μmol/$mg_{Protein}$/min in $CD24^{-/low}$ and $CD24^{+}$ cells, respectively; $P=0.002$; $n=6$) (Figures 4e and f) as compared with $CD24^{+}$ cells.

Glucose 6-phosphate dehydrogenase (G6PDH) is the key enzyme of pentose phosphate pathway, the metabolic process providing NADPH to the cells that is required for anabolic pathways. Our proteomic data also show that G6PDH is more expressed in BCSCs although the difference with SDACs is not statistically significant (data not shown). Indeed by WB analysis, we show that G6PDH is upregulated in spheres compared with SDACs ($P=0.036$; $n=3$; Figure 4a), and its activity is significantly increased (mean ± S.D. = 2.3 ± 0.8 and 1.2 ± 0.3 μmol/$mg_{Protein}$/min in BCSCs and differentiated cells, respectively; $P=0.004$; $n=6$; Figure 4g). According to the increase of G6PDH expression and activity, we found a decreased $NADP^{+}$/NADPH ratio in spheres (mean ± S.D. = 0.94 ± 0.05 and 1.063 ± 0.004 in BCSCs and SDACs, respectively; $P=0.013$, Figure 4h). These results suggest increased biosynthesis of NADPH through the pentose phosphate pathway in BCSCs compared with SDACs.

BCSCs show increased reduced nicotinamide adenine dinucleotide (NADH) consumption and cytosolic ATP production. Adenosine diphosphate (ADP)/ATP and NAD^{+}/NADH ratios are indices of aerobic or anaerobic energy metabolism, cellular energy turnover, and redox cellular state. We found that NAD^{+}/NADH ratios are significantly higher in BCSCs compared with SDACs (mean ± S.D. = 11.9 ± 0.6 and 6.7 ± 0.3 in BCSCs and differentiated cells, respectively; $P=2\times10^{-4}$, Figure 4i). This is associated with the increase of NADH consumption and decreased NAD^{+} production in BCSCs. In fact, NADH concentrations (mean ± S.D. = 0.06 ± 0.04 and 0.13 ± 0.02 μmol/l in BCSCs and SDACs, respectively; $P=0.050$) as well as NAD^{+} levels (mean ± S.D. = 0.73 ± 0.04 and 0.88 ± 0.07 μmol/l in BCSCs and SDACs, respectively; $P=0.045$) significantly decrease in BCSCs compared with SDACs.

BCSCs also show an increased ADP/ATP ratio (mean ± S.D. = 0.23 ± 0.03 and 0.15 ± 0.06 in BCSCs and differentiated cells, respectively; $P=0.016$, Figure 4j).

Of note, we found that treatment with rotenone, an uncoupling agent of the electron transport chain (ETC), increases the ADP/ATP ratio in SDACs (mean ± S.D. = 0.13 ± 0.02 and 0.247 ± 0.006 for control and SDACs treated with rotenone, respectively; $P=0.001$), while it has no effect on the ATP production in BCSCs (mean ± S.D. = 0.21 ± 0.02 and 0.20 ± 0.01 for control and BCSCs treated with rotenone, respectively; $P=0.732$). These findings suggest that uncoupling of ETC markedly inhibits ATP

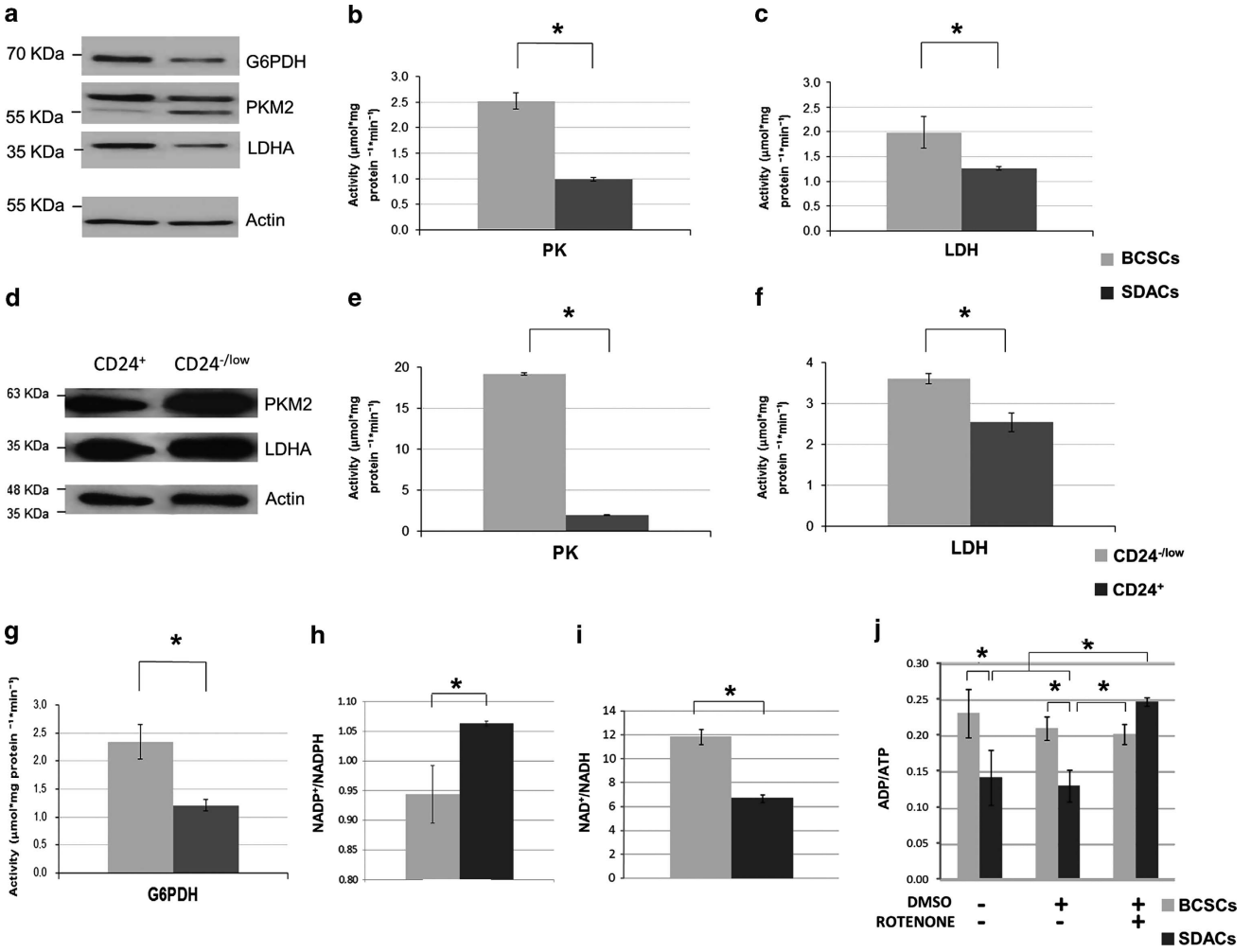

Figure 4 The expression levels and activities of glycolytic enzymes are increased in BCSCs and correlate with altered energy and redox status of BCSCs. (**a**) WB showing PKM2, LDH-A, and G6PDH expression in BCSCs compared with SDACs. β-Actin is used as a protein-loading control. A representative WB of three independent experiments is shown. (**b**) PK and (**c**) LDH, and enzyme activities evaluated in spheres (BCSCs) as compared with differentiated cells (SDACs). Bar graphs show the mean activity ($n=6$) expressed as μmol/mg$_{Protein}$/min, and bars represent the S.E.M. (**d**) WB showing the expression of PKM2 and LDH-A in cells sorted for CD24 expression. β-Actin is used as a loading control. (**e**) PK and (**f**) LDH activity in CD24$^{-/low}$ cells compared with CD24^{+} BCSCs. Bar graphs show the mean activity ($n=6$) expressed as μmol/mg$_{Protein}$/min, and bars represent the S.E.M. (**g**) G6PDH enzyme activity evaluated in spheres (BCSCs) as compared with differentiated cells (SDACs). Bar graphs show the mean activity ($n=6$) expressed as μmol/mg$_{Protein}$/min, and bars represent the S.E.M. (**h**) NADP^{+}/NADPH, (**i**) NAD^{+}/NADH, and (**j**) ADP/ATP ratios in BCSCs compared with SDACs. Treatment with rotenone does not affect ATP production in BCSCs, whereas strongly increases the ADP/ATP ratio and inhibits mitochondrial ATP production in SDACs. No changes in the ADP/ATP ratio are observed in BCSCs and SDACs after addition of dimethylsulphoxide (DMSO) alone used as a vehicle control. Bars show the mean value ± S.D. ($n=3$). *$P<0.050$ (unpaired two-tailed *t*-test or two-factor ANOVA)

production in SDACs but not in BCSCs that rely on lactic fermentation (Figure 4j).

2-deoxyglucose (2-DG) inhibits BCSCs' growth and survival. Overall, our data indicate that BCSCs display an anaerobic metabolic phenotype compared with SDACs. Therefore, we tested the effect, on BCSCs' growth and survival, of 2-DG, a compound known to inhibit the first phase of glycolysis, alone or in combination with Doxo, a chemotherapeutic agent used for the treatment of breast cancer.

Our results show that Doxo exerts a cytostatic effect on BCSCs but a very modest, if any, toxic effect (Figures 5a and b). Notably, BCSCs were substantially blocked in the G2 phase of cell cycle (data not shown). In contrast, 2-DG provides a significant time-dependent cytotoxic effect inducing up to 44% apoptosis after 48 h of treatment (Figure 5b).

Interestingly, the combination of 2-DG with Doxo results in a higher cytotoxic effect compared with the treatment with Doxo alone or 2-DG alone after 2 days reaching 80% apoptosis after 48 h (Figure 5b). As expected, more differentiated cells are more responsive to Doxo; however they appear less sensitive to 2-DG than BCSCs (Figure 5c). This is in line with a less glycolityc metabolism. Again, the combined treatment results in a much higher response also in SDACs (Figure 5c).

Discussion

Growing evidence show that a subset of cancer cells, known as CSCs, are key drivers of tumour progression, being the clonogenic population that supports tumour growth. According to the CSC model, failure to eradicate these cells with current therapies can result in tumour recurrence. As these

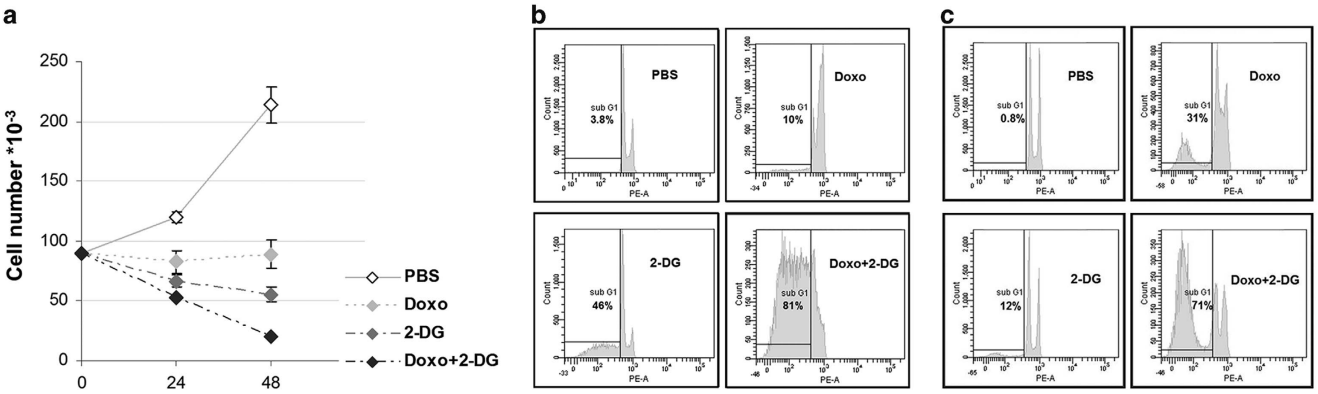

Figure 5 2-DG induces apoptosis of BCSCs, and its effect is increased by the combination with doxorubicin. (**a**) BCSCs are treated with doxorubicin (Doxo) and 2-deoxyglycose (2-DG) alone or the combination of Doxo and 2-DG (Doxo + 2-DG). Doxo treatment provides cytostatic effect, but cell counts does not significantly differ 24 and 48 h after Doxo administration (Fischer's LSD *post-hoc* test, $P = 0.768$). In contrast, treatment with 2-DG alone decreases BCSCs counts compared with control, 24 h (Fischer's *post-hoc* test, $P = 0.055$) and 48 h ($P = 8 \times 10^{-4}$) Doxo treatment. The treatment with Doxo + 2-DG significantly decreases cell counts compared with 24 h ($P = 0.0009$) and 48 h ($P = 1 \times 10^{-6}$) Doxo treatment and 48 h treatment with 2-DG alone (Fischer *post-hoc* test, $P = 0.002$). Evaluation of apoptosis in (**b**) BCSCs and (**c**) SDACs treated for 48 h with 2-DG, Doxo, or a combination of the two. The percentage of hypo-diploid events evaluated by Flow Cytometry after propidium iodide staining is shown

cells are in general highly chemo- and radio-resistant, there is an urgent need for therapeutic agents to selectively target this population.[2,3] Several signal transduction pathways have been shown to contribute to the stem-like phenotype and have been proposed as potential therapeutic targets; moreover, recent studies indicate that targeting CSC metabolism in combination with classical chemotherapeutic agents may provide valuable strategy to eradicate CSCs. Our integrated proteomic and targeted metabolomic analysis suggest that BCSCs are more dependent on anaerobic glucose metabolism than more differentiated tumour cells.

Increased glycolytic flux and lactate production even in the presence of oxygen suggest a switch of BCSC metabolism from oxidative phosphorylation to aerobic glycolysis, a phenomenon well known as Warburg effect. Furthermore, upregulation of aerobic glycolysis has been shown to correlate with increased tumour aggressiveness and the development of multi-drug resistance.[22,23]

Warburg effect has been considered a cellular response to hypoxic conditions in the tumour microenvironment and the adaptive overexpression of the transcription factor HIF-1α that can promote the survival of cancer cells. The higher levels of HIF-1α in spheres, predicted *in silico* and effectively observed in BCSCs even upon normoxic conditions, results in the increased expression levels of proteins involved in glucose transport and metabolism as well as lactate production through the induction of LDH-A, the key enzyme of glucose fermentation.[24] It has been shown that lactate and pyruvate, found significantly increased in BCSCs, upregulate hypoxia-inducible genes independently of hypoxia by stimulating the accumulation of HIF-1α.[25] Interestingly, we also found that BCSCs are enriched in the Krebs cycle intermediate succinate and show a trend toward increased fumarate concentration. Succinate and fumarate promote HIF-1α accumulation through the inhibition of the oxygen-dependent prolyl hydroxylase domain enzymes that catalyze HIF-1α degradation, thus providing supporting evidences for increased HIF-1α in BCSCs upon normoxic conditions.

LDH-A is thought to be a major molecular mediator of the Warburg effect. LDH-A and LDH-B genes encode for two protein, namely M and H, respectively, that combine to give five isoenzymes, which differ in electrophoretic mobility and Michaelis–Menten constants for lactate and pyruvate. LDH-A, overexpressed in BCSCs, is associated with the conversion of pyruvate to lactate, suggesting increased lactic fermentation in these cells. This hypothesis was supported by the increase of $LDH_{Pyr \rightarrow Lac}$ activity and lactic acid found in spheres. Increased local concentration of the toxic lactic acid and decreased extracellular pH have been recently associated to the Warburg effect and appear to be advantageous for invasion and tumourigenesis.[26–28]

PKM2 is a low activity isoform of PK that promotes the aerobic glycolysis and contributes to anabolic metabolism.[17,29] It is known that PKM2 replaces the normal PK enzyme in proliferating and tumour cells,[30] and a PKM1 (a highly active PK isoform) to PKM2 isoform switch has been associated with increased fermentative metabolism, increased pyruvate and lactate production, and lower oxygen consumption.[17] Notably, PKM2 activity relies on allosteric activation by fructose 1,6-diphosphate[31] and serine.[32] The increased PK activity in the BCSCs is consistent with our data showing a significant increase of these two allosteric effectors in BCSCs as compared with SDACs. Furthermore, PK has a global regulatory role in biosynthetic AA metabolism and affects the concentration of free AAs.[33] In particular, PKM2 upregulation has been shown to stimulate *de novo* serine biosynthesis,[34] which in turn can allosterically activate PKM2, consistently with the higher serine levels that we found in BCSCs. The upregulation of PKM2 and the increase of PK activity may also correlate with the increase of Arg, Val, and His that have been previously reported.[33] The higher biosynthesis rate of glucose-derived non-essential AAs linked to the increase of PK activity suggests that BCSCs divert glucose-derived carbon into non-ATP-producing pathways supporting cellular biomass increase.

The increased expression levels and activity of G6PDH and the increase of ribose 5-phosphate in BCSCs clearly indicates the activation of the pentose phosphate pathway. These findings support the idea that BCSCs shift from catabolic metabolism aimed at energy production toward an anabolic

state aimed at supplying biosynthesis precursors, such as NADPH. According with this hypothesis, the NADP/NADPH ratio is significantly decreased in spheres, indicating increased intracellular NADPH levels.

BCSCs also show a high ADP/ATP ratio that may indicate decreased production of oxidatively derived mitochondrial ATP, and thus alternative ATP-generating pathways in BCSCs as well as increased levels of cytosolic ADP, required to maintain the high rate of glycolysis. Of note, the treatment with rotenone, a mitochondrial complex I inhibitor, significantly impairs ATP production of cells upon differentiation without significant effects on BCSCs. Therefore, BCSCs are less dependent on the mitochondrial activity than normal cancer cells and rely on aerobic glycolysis for ATP production.

It has been reported that glycolytic cells show low cytosolic and mitochondrial NAD^+/NADH ratios that inhibits the tricarboxylic acids cycle (TCA) favouring anaerobic glycolysis.[35] Furthermore, enhancement of NAD^+/NADH levels inhibits tumourigenesis and metastasis in breast cancer.[36] Unexpectedly, BCSCs are characterized by higher NAD^+/NADH level compared with SDACs. This seems to be in contrast with the aggressive phenotype of this cells and their tumour-forming ability. However, our data are consistent with the hypothesis that BCSCs can consume NADH without producing ATP from mitochondrial electron transport. The decrease of NADH levels and the corresponding increase of NAD^+/NADH ratio in BCSCs could be related to the increase of homolactic fermentation rate to regenerate a sufficient NAD^+ pool and maintain the high rates of glycolysis, increasing NADH consumption or to the inhibition of the TCA cycle. In fact, it is known that increased concentration of TCA cycle intermediates inhibits the cycle. The increase of succinate concentration and the trend toward significant increase of fumarate in BCSCs may partly explain the increased NAD^+/NADH ratio through the inhibition of the TCA cycle. The strong inhibition of FA beta-oxidation that we observed in BCSCs provides further evidences of silencing of mitochondrial activity. Although the exact role of inhibition of FA oxidative catabolism inhibition is currently unclear, these preliminary results warrant further investigations.

It is worthy of note that the Warburg effect has been linked to mitochondrial stability and the cellular redox balance in cancer cells.[37] Promoting glycolysis and limiting mitochondrial activity may inhibit mitochondrial reactive oxygen species (ROS) production. It has been recently demonstrated that low levels of ROS generation through the glycolytic shift contributes to maintaining a CSC phenotype.[9] We found that BCSCs not only rely on aerobic glycolysis but also strongly overexpress several antioxidant enzymes such as mitochondrial superoxide dismutase and synthesize more NADPH than differentiated cells. Increased NADPH biosynthesis may indicate increased source of reducing equivalents and an improvement of the anti-oxidant defence through the proxiredoxin, thioredoxin, and glutathione systems. Of note, it has been recently shown that the key regulator of aerobic glycolysis PKM2 has a relevant role in maintaining cellular redox homeostasis allowing greater diversion of glycolytic intermediates into pentose phosphate pathway and NADPH biosynthesis in response to oxidative stress.[38] Therefore it is possible that BCSCs set in motion such mechanisms to counteract ROS.

Pharmacological targeting of aerobic glycolysis overcomes the drug resistance of CSCs isolated from several solid tumours. In particular, it has been shown that inhibition of glycolysis restores drug sensitivity in high malignant tumour cells through the inactivation of ABC transporters that provide the efflux mechanism for chemotherapeutic drugs in CSCs.[39] The synthetic glucose analogue, 2-DG is one of the glycolysis inhibitors that has been shown to inhibit solid tumour growth and is currently under Phase I/II clinical trials.[40,41] Of note, it has been recently suggested that combination of 2-DG with widely used chemotherapeutics such as trastuzumab may be a valuable strategy to overcome drug-resistant BCSCs.[42] Here we show that acute treatment with 2-DG has a significant cytotoxic effect and induces apoptosis of BCSCs. These findings are consistent with data showing that 2-DG significantly affects the ability of CSCs to form spheroids.[14] The cytotoxic effect of 2-DG have been previously explained not only by inhibition of glycolysis and the following metabolic stress but also by indirect effects on several signalling pathways such as inhibition of mammalian target of rapamycin signalling[43] or direct effects on pro-apoptotic proteins, such as Bcl-2 homologous antagonist/killer.[44]

In contrast, the widely used chemotherapeutic drug Doxo provides only a cytostatic effect on CSCs and has been shown to lead to enrichment of cells with CSC characteristics within the population, thus potentially increasing resistance and risk of recurrence.[45] Interestingly, we found that the combination of Doxo with 2-DG shows a synergic effect, significantly enhancing BCSCs' death in a time-dependent manner. Moreover, the combined treatment has an important effect also on more differentiated cancer cells, suggesting that this combination may target different cancer cell populations. Doxo is known to increase ROS production, which can mediate mitochondrial damage and apoptosis in a p53-independent manner.[46,47] It is also known that 2DG treatment results in increased ROS.[48,49] This may provide a rationale for the enhancement of the effect of Doxo by 2-DG. On the other hand, combining 2-DG with other drugs may enhance the low *in vivo* cytotoxicity of 2-DG[40] and overcome the cytostatic effect of classical chemotherapeutic agents as well. In fact, targeting aerobic glycolysis with 2-DG markedly overcomes Doxo resistance of BCSCs, thus providing promising pharmacological application against BCSCs.

Materials and Methods

Chemicals. All chemicals were supplied by Sigma-Aldrich (Shnelldorf, Germany) and Fluka (Shnelldorf, Germany) unless otherwise stated.

Tissue collection, isolation, and culture of cancer cells. Human breast cancer tissues were obtained from patients undergoing surgery in accordance with the ethical standards of the institutional Committee on Human Experimentation (authorization no. CE-ISS 09/282). Tumour tissues were mechanically and enzymatically digested with collagenase (1.5 mg/ml; Gibco Life Technologies, Grand Island, NY, USA) and hyaluronidase (20 mg/ml) in DMEM (Gibco), shaking for 1 h at 37 °C. The resulting cell suspension was plated in ultra-low attachment flasks (Corning Incorporated, Corning, NY, USA) in serum-free medium supplemented with basic fibroblast growth factor (10 ng/ml) and epidermal growth factor (20 ng/ml) as previously described.[50] This procedure yielded BCSC lines that were subjected to genotyping to validate each cell line's individuality and were further tested for their ability to generate tumour xenografts that replicated the histology of the parental tumour. To achieve the *in vitro* differentiation of BCSCs, dissociated sphere cells were cultured in DMEM for the

indicated times (3.5 or 7 days) supplemented with 10% fetal bovine serum (FBS) in adherent conditions. These cells were conventionally indicated as SDACs.[18]

Cell proliferation assay. Cell viability was determined at 24 and 48 h by trypan blue dye exclusion assay following the treatment of BCSCs with 35 mmol/l 2-DG as previously reported,[14] doxorubicin hydrochloride (1 μmol/l), and a combination of the two drugs at the same concentrations. Control samples were performed in phosphate-buffered solution (PBS).

Cytofluorimetric analysis. Flow cytometric cellular DNA content evaluation was performed according to Nicoletti *et al.*[51] Briefly, cells were collected by trypsinization, pelleted at 800 $\times$ *g* for 10 min and fixed in 70% ethanol overnight at $-20\,^{\circ}$C. Samples were then washed in PBS and incubated at 37 °C, for 15 min with a 13 Kunitz units RNAse A solution and for 20 min with 50 μg/ml propidium iodide. Twenty thousand events were acquired (FACSCanto II Instrument, BD Biosciences, San Jose, CA, USA) and analysed by using the BD FACSDIVA software (BD Biosciences).

Flow cytometric analysis of surface markers CD24 and cluster of differentiation 44 (CD44) was performed on 2×10^5 cells per sample. Cells were washed in PBS, resuspended in 100 μl of specific antibody (antibody-CD24-R-phycoerythrin-cyanine dye7 (anti-CD24-PE-Cy7), 561646, BD Pharmingen (Franklin Lakes, NJ, USA); antibody-CD44-allophycocyanin (anti-CD44-APC), 559942, BD Pharmingen) diluted in 0.5% bovine serum albumin, and incubated for 20 min at room temperature in the dark. Cell viability solution (555815, BD Biosciences) was used for detection of non-viable cells according to manufacturer's protocol. Samples were then washed and stored at 4 °C in the dark until acquisition. A FACSCantoII flow cytometer, running with FACSDiVa software (BD Biosciences), was used for sample acquisition and analysis.

Cell sorting of $CD44^+/CD24^+$ and $CD44^+/CD24^{-/low}$ sub-populations was performed on single cell suspension from BCSC double stained with anti-CD24-PE-Cy7 antibody and anti-CD44-APC antibody. Cells were sorted with fluorescence-activated cell sorting Aria III cell sorter (BD Biosciences). Sub-populations of cells co-expressing CD44 and CD24 at higher levels or CD24 weak/absent were collected, and a small amount of cells were re-analysed to check for purity.

Immunoblotting. Cells grown as BCSCs and SDACs were collected by centrifugation at 1200 revolutions/min. Cell pellets were washed twice with ice-cold PBS, resuspended in a 50 mmol/l tris(hydroxymethyl)aminomethane (Tris)/HCl (pH 7.5), 150 mmol/l NaCl, 1 mmol/l EDTA, 1 mmol/l NaF, 10% Glycerol (V/V), 1 mmol/l MgCl, 1% Triton X-100 (V/V) ice-cold buffer containing proteinase inhibitor cocktail and incubated for 30 min on ice. Sample lysates were centrifugated at 10 000 $\times$ *g* for 10 min, and supernatants were collected. Equal amounts of whole proteins extracts and nuclear extract (B-625 Sigma N-XTRACT, Shnelldorf, Germany) for HIF-1α immunodetection were resolved on 10% sodium dodecyl sulphate–polyacrylamide gel electrophoresis gel using a mini-gel apparatus (GmbH Bio-Rad Laboratories, Hercules CA, USA), transferred onto polyvinylidene fluoride membranes and subsequently blocked with 5% non-fat dry milk in PBS/0.1% (V/V) Tween 20. Immunodetection was performed by incubating the membranes with the different primary antibodies diluted in blocking buffer for 2 h at room temperature or overnight at 4 °C. The following antibodies were used: anti-LDH (PA5-27406, Thermo Scientific, Rockford, IL, USA), anti-PKM2 (PA-23034, Thermo Scientific), anti-G6PD (PA5-27359, Thermo Scientific), anti-HIF-1α (NB100-449, Novus Biologicals, Cambridge, UK), anti-Actin (clone AC-15, A5441 Sigma-Aldrich), and anti-Laminin β (M-20) (sc-6217, Santa Cruz Biotechnology, Inc., Santa Cruz, CA, USA). Immunoreactive bands were visualized with SuperSignal West Dura Substrate (Pierce Biotechnology, Rockford, IL, USA).

Differential proteomic analysis. Sample preparation, data acquisition and data processing were performed as previously described.[52–54] A total of 100 μg of protein extracts from the different conditions in separate experiments were precipitated with a mix of ethanol, methanol, and acetone (ratio 2 : 1 : 1, V/V) and then dissolved in 100 mmol/l Tris/HCl pH 7.9 containing 6 M urea and 0.1% 3-[(3-cholamidopropyl)dimethylammonio]-1-propanesulfonate and sonicated. The reduction of proteins was performed by adding 100 mmol/l dithiothreitol (DTT) (1 h at 36 °C) and 200 mmol/l iodoacetamide (1 h at room temperature). Protein samples at a final concentration of 2 μg/μl were digested with 1 : 20 (w/w) sequence-grade trypsin (Promega, Madison, WI, USA) at 36 °C overnight. The reactions were stopped by adding 1 μl of 10% (V/V) trifluoroacetic acid. A total of 0.25 μg of the protein digestion was loaded onto the nanoACQUITY UPLC System (Waters Corporation, Milford, MA, USA) coupled to a quadrupole-time of flight (Q-Tof) Premier mass spectrometer (Waters Corporation). Before loading, a digested enolase from *Saccharomyces cerevisiae* (Waters Corporation) was added to the sample as internal standard at a final concentration of 200 fmol/l. Samples were injected onto a Symmetry C18 5 μm, 180 μm $\times$ 20 mm precolumn (Waters Corporation) for preconcetration and desalting and were subsequently separated using a NanoEase BEH C18 1.7 μm, 75 μm $\times$ 25 cm nanoscale LC column (Waters Corporation) maintained at 35 °C. Mobile phase A was water with 0.1% formic acid, and mobile phase B was 0.1% formic acid in acetonitrile. Peptides were eluted by a gradient of 3–40% mobile phase B over 150 min at a flow rate of 250 nl/min followed by a gradient of 40–90% mobile phase B over 5-min and a 15-min rinse with 90% mobile phase B. The Q-Tof Premier mass spectrometer (Waters Corporation) was programmed to step between low (4 eV) and high (15–40 eV) collision energies using a scan time of 1.5 s over 50–1990 *m/z*. Samples from each condition were run at least in triplicate. The best replica for each condition was used for the subsequent analysis. The Continuum LC-MS data were processed and searched using ProteinLynx GlobalServer v2.3 (PLGS) (Waters Corporation). Protein identification was performed using the embedded ion accounting algorithm of the software and by searching a Uniprot/SWISSProt human database release 2011_02 (20253 entries), to which the sequence from the enolase of *S. cerevisiae* was appended. The parameters for the database search were as follows: automatic tolerance for precursor ions, automatic tolerance for product ions, minimum of three fragment ions matched per peptide, minimum of seven fragment ions matched per protein, minimum of two peptides matched per protein, one missed cleavage, and carbamidomethylation and oxidation of methionine as modifications. The false positive rate of the identification algorithm is typically 3–4% with a randomized database appended to the original one, which is five times the size of the original utilized database.[55,56] The identified proteins displayed in the protein table were normalized against the P00924 entry (Enolase *S. cerevisiae*), and peptides from Enolase *S. cerevisiae* digestion that were the most reproducible for retention time and intensity deriving (*m/z* 807.42, *m/z* 814.49, *m/z* 1286.71, *m/z* 1288.70, *m/z* 1755.94, *m/z* 1789.83, *m/z* 1840.89) were used to normalize the EMRT table, the list of paired peptide exact masses and retention time. The list of normalized proteins was screened according to the following criteria: proteins that were identified in at least two out of the three injections of the same conditions; proteins with $0 < P < 0.05$ or $0.95 < P < 1$, and proteins with an expression level ratio between the conditions > 1.3 on decimal scale. If $0 < P < 0.05$, the likelihood of downregulation is $> 95\%$, and if $0.95 < P < 1$ the likelihood of upregulation is $> 95\%$. Setting the threshold of ratio at 1.3 on a decimal scale allowed us to consider the average relative fold change ± 0.30 on a natural log scale. This setting is typically 2–3 times higher than the estimated error of the intensity measurements.[56]

Targeted metabolomic analysis by GC–MS. GC–MS analysis of cell lysates was performed as previously described.[57] Briefly, cell samples (approximately 1.5×10^6 cells) were extracted with a solution of ethanol/water (50 μl, 80 : 20, V:V), and cell homogenate (50 μl) were precipitated with 100 μl of cold 0.1% (V/V) methanolic trichloroacetic acid immediately after homogenization. Internal standards ($^{13}C_4$ malic acid, $^{13}C_4$ succinic acid, $^{13}C_6$ glucose; IS) were then added to give a final concentration of 10 μg/ml. Samples were centrifuged at 10 000 $\times$ *g* for 30 min, and supernatants were collected and dried in a SpeedVac system (ThermoSavant, Waltham, MA, USA). The dried extracts were derivatized with 20 μl of 20 mg/ml of methoxyamine hydrochloride solution in pyridine for 60 min at 70 °C followed by reaction with 20 μl of N,O-bis(trimethylsilyl)trifluoroacetamide with 1% of trimethylchlorosilane for 60 min at 70 °C. GC–MS analysis was performed using a 6890N gas-chromatograph equipped with a 7863 Series auto-sampler and coupled with a 5973N mass spectrometer (Agilent Technologies, Palo Alto, CA, USA) operating in electron impact ionization mode. Three microlitres were injected in pulsed-splitless mode by applying a pressure of 80 psi. The injector temperature was kept at 250 °C. Chromatographic separations were obtained using a fused silica capillary column HP-5MS (30 m x 0.25 mm, Agilent Technologies). Helium was used as carrier gas at a constant flow rate of 1 ml/min. The GC oven was programmed as follows: start at 70 °C (hold time 1 min), which was raised at 4 °C/min to 300 °C (hold time 5 min). The mass spectrometer was automatically calibrated using per-fluoro tributylamine as calibration standard. For quantification, the mass spectrometer was used in the selective ion monitoring mode, and mass spectra were recorded in positive modes by monitoring the following ions: *m/z* 174 (pyruvic acid; IS: $^{13}C_3$ pyruvic acid, *m/z* 177), *m/z* 147 (lactic acid; IS: $^{13}C_4$ succinic acid, *m/z* 251), *m/z* 247 (succinic acid; IS: $^{13}C_4$

succinate, *m/z* 251), *m/z* 245 (fumaric acid; IS: $^{13}C_4$ malic acid, *m/z* 236), *m/z* 233 (malic acid; IS: $^{13}C_4$ malic acid, *m/z* 236); *m/z* 328 (glyceraldheyde 3-phosphate; IS: $^{13}C_4$ malic acid, *m/z* 236), *m/z* 357 (3-phosphoglyceric acid; IS: $^{13}C_4$ malic acid, *m/z* 236), *m/z* 375 (citric acid; IS: $^{13}C_4$ malic acid, *m/z* 236), *m/z* 319 (glucose; IS: $^{13}C_6$ glucose, *m/z* 323), *m/z* 387 (glucose 6-phosphate; IS: $^{13}C_6$ glucose, m/z 323), and *m/z* 459 (fructose 1,6-diphosphate; IS: $^{13}C_6$ fructose 1,6-diphosphate, *m/z* 462). Mass spectrometer operating parameters were: interface temperature 300 °C, ion source 250 °C, and quadrupole 150 °C. The external standard method and internal standard correction were applied for quantification of target metabolites. Data acquisition was performed using the G1701CA ChemStation software (Agilent Technologies).

Determination AAs and AcCs. AA and AcCs analysis was performed by LC-MS/MS as previously described.[58,59] Cell samples (approximately 1.5×10^6 cells) were extracted with a solution of Ethanol/Water (50 μl, 80 : 20, V:V). The samples were then sonicated and centrifuged (15 600 r.p.m. at 4 °C for 20 min), and the supernatant was recovered. The lysate (7 μl) were added to 100 μl of the stable isotope-labeled IS obtained from the NeoBase Non-derivatized MSMS Kit (Perkin Elmer Life and Analytical Sciences, Turku, Finland). The sample were analysed by direct infusion mass spectrometry using a LC-MS/MS system consisting of an Alliance HT 2795 HPLC Separation Module coupled to a Quattro Ultima Pt ESI tandem quadrupole mass spectrometer (Waters Corporation). The instrument was operated in positive electrospray ionization mode using MassLynx V4.0 Software (Waters Corporation). A detailed description of electrospray ionization mass spectrometry acquisition parameters are available in Supplementary Table S6. Auto data processing was performed using the NeoLynx (Waters Corporation) software.

Pyruvate kinase activity. PK activity was measured by converting the product pyruvate into lactate using LDH, with a concomitant conversion of NADH to NAD^+, resulting in a decrease in absorbance at 340 nm.[60] In all, 7×10^6 cells were lysed in 200 μl of buffer containing 10 mmol/l Tris–HCl (pH 7.5), 1.5 mmol/l $MgCl_2$, 20 mmol/l NaCl, 1 mmol/l DTT, 1 mmol/l phenylmethylsulfonyl fluoride, and protease inhibitor cocktail. After two centrifugations at 17 000 $\times$ *g* for 30 min each, PK activity was measured in the supernatant by a LDH-coupled assay. The 200-μl reaction mixture was prepared on ice containing 100 mmol/l Tris–HCl (pH 8.0), 100 mmol/l KCl, 10 mmol/l MgCl2, 0.5 mmol/l EDTA, 0.2 mmol/l NADH, 1.5 mmol/l ADP, 5 mm phosphoenolpyruvate, and 200 units/ml LDH. The reaction was initiated by the addition of 0.7 μg of total cell extract. PK activity was calculated at 37 °C by monitoring the absorbance at 340 nm every 30 s for 5 min in an microplate reader (Spectra max 190, Molecular Devices, Sunnyvale, CA, USA). A unit of PK activity is defined here as the amount of enzyme required to oxidize 1 μmol of NADH per minute under these experimental conditions.

LDH activity. Direct LDH activity ($LDH_{Pyr \rightarrow Lac}$) was spectrometrically assayed as previously described[61,62] using a tunable microplate reader (Spectra max 190, Molecular Devices). Briefly, cell pellets were lysed in 0.010 mol/l PBS (20 ml/g of pellet, wet weight; pH = 7.4). Cell lysates were centrifuged at 2000 $\times$ *g* for 3 min at 4 °C to remove cell debris. Supernatants were further centrifuged 8000 $\times$ *g* for 10 min at 4 °C in order to obtain cytosolic fractions. Protein concentration was determined according to the Bradford assay.[63] Therefore, pyruvate (25 μl, 2.50 g/l) and NADH (100 μl, 0.3 g/l) were added to the samples (10 μl corresponding to 0.5 μg of total proteins) and the decrease of absorbance at 340 nm was measured at 37 °C every 30 s for 5 min. $LDH_{Pyr \rightarrow Lac}$ activity is expressed as μmol/$mg_{protein}$/min.

G6PDH activity. G6PDH was assayed using a tunable microplate reader (Spectra max 190, Molecular Devices), according to the spectrophotometric methods previously described[64] with minor modifications. Cell pellets were homogenized, and protein quantification were performed as described for LDH activity assay. To measure G6PDH activity, the sample (10 μl corresponding to 0.5 μg of total proteins) was added to a solution containing glucose 6-phosphate (0.2 mmol/l), $NADP^+$ (0.1 mmol/l), Tris/HCl buffer (50 mmol/l, pH = 8.1), and $MgCl_2$ (1 mmol/l). The final volume was 150 μl. The increase of absorbance at 340 nm was measured every 30 s for 5 min at 37 °C. G6PDH activity was expressed as μmol/mg protein/min.

NAD^+/NADH and $NADP^+$/NADPH determination. NAD^+/NADH ratio were measured by a ultrasensitive colorimetric assay (EnzyChrom NAD^+/NADH Assay Kit (E2ND-100), BioAssay Systems, Hayword, CA, USA) according to the manufacturer's instructions. This assay is based on a LDH cycling reaction.[65] Briefly, cells were lysed with either 100 μl NAD^+ extraction buffer for NAD^+ determination or 100 μl NADH extraction buffer for NADH determination. After heating at 60 °C for 5 min, 20 μl of assay buffer and 100 μl of the opposite extraction buffers (NADH extraction buffer or NAD^+ extraction buffer, respectively) were added. The samples were then centrifuged at 14 000 r.p.m. for 5 min, and the supernatants (40 μl) were used for NAD^+/NADH assays. The optical density (OD) was read at 565 nm in a tunable microplate reader (Spectra max 190, Molecular Devices) for time 0 and after 15 min. NAD^+ and NADH concentrations were measured as: (ΔOD-*b*0)/*b*1, where *b*0 and *b*1 are the intercept and slope of the external calibration curve.

$NADP^+$/NADPH ratio were measured by a ultrasensitive colorimetric assay (EnzyChrom $NADP^+$/NADPH Assay Kit (ECNP-100), BioAssay Sistems) following the manufacturer's instructions. This assay is based on a glucose dehydrogenase cycling reaction.[65] The absorbance was measured at 565 nm using a tunable microplate reader (Spectra max 190, Molecular Devices), and the same procedure applied for NAD^+/NADH determination was performed. All analysis were performed in triplicate.

ADP/ATP ratio determination. ADP/ATP ratio was measured based on luciferin–luciferase reaction using Enzylight ADP/ATP ratio assay kit (ELDY-100) (BioAssay Systems) following the manufacturer's instructions. Briefly, BCSCs cells were seeded in a 96-well flat-bottom plate and incubated for 3 days to allow for cell differentiation and recovery (1×10^4 cells at 100 μl per well). BCSCs (1×10^4 cells) were treated with the assay buffer (90 μl) containing luciferin–luciferase. After 1 min, luminescence (relative light units (RLU) A) was recorded by Lumat LB 9507 Ultra Sensitive Tube Luminometer (Berthold Technologies, Oak Ridge, TN, USA). The luminescence was read also after 10 min (RLU B). This measurement provided background before measuring ADP. Therefore, 5 ml ADP reagent was added to each well, and after 1 min, luminescence (RLU C) was obtained. ADP/ATP ratio was measured as: (RLU C − RLU B)/RLU A. All analysis were performed in triplicate. The same procedure was applied for the measurement of ADP/ATP ratio in BCSCs and SDACs following treatment with rotenone (50 μmol/l) for 60 min.

Statistical and bioinformatic analysis. Differences between the protein expression levels, enzymatic activities, and metabolite concentrations in BCSCs and SDACs were assessed by unpaired two-tailed *t*-test. Two-factor ANOVA followed by Fisher's least significant difference (LSD) *post-hoc* test was performed in order to assess the significance of the treatment effects. Data were ranked and aligned where Levene test failed to show homoscedasticity. Aligned rank transformation (ART) of data was performed using the ART web software available at http://faculty.washington.edu/aimgroup/proj/art/artweb/.[66] Treatment (PBS, Doxo, 2-DG, and Doxo + 2-DG) and the treatment time (24 or 48 h) were the independent factors. *P*-values < 0.050 were considered statistically significant. Statistical analysis was performed using the Statistica 6.0 (StatSoft Inc., Tulsa, OK), XLStat2007.1 (Microsoft, Redmond, WA, USA) and Microsoft Excel software.

Protein network analysis was performed using the Ingenuity Pathway Analysis (IPA) application (Ingenuity System, http://www.ingenuity.com). IPA constructs hypothetical protein interaction clusters on the basis of the Ingenuity Pathways Knowledge Base. Direct and indirect relationships between the identified proteins were shown as networks on the base of all genes, and endogenous chemicals present in the Ingenuity Knowledge Network scores are calculated as $-\log$ (*P*-value) and indicate the likelihood that focus genes (i.e., the identified proteins within a specific network) are clustered together. Biological functions and canonical pathways over-represented among the identified proteins were also assigned to networks stored in the Ingenuity Pathways Knowledge Base. Biological functions and canonical pathways were ranked in accordance to their significance. Significance was evaluated by exact Fisher's test. A *P*-value of 0.01 corresponding to a score of 2 was considered the cutoff for the analysis.

Conflict of Interest

The authors declare no conflict of interest.

Acknowledgements. This work has been supported by grants from AIRC (2011-IG11450) and Italian Ministry of Health (Ricerca Finalizzata 2009, RF-2009-1491608) to VDL and from MIUR (RBAP11WCRZ_003) to AU.

1. Al-Hajj M, Wicha MS, Benito-Hernandez A, Morrison SJ, Clarke MF. Prospective identification of tumorigenic breast cancer cells. *Proc Natl Acad Sci USA* 2003; **100**: 3983–3988.
2. Liu S, Wicha MS. Targeting breast cancer stem cells. *J Clin Oncol* 2010; **28**: 4006–4012.
3. Vidal SJ, Rodriguez-Bravo V, Galsky M, Cordon-Cardo C, Domingo-Domenech J. Targeting cancer stem cells to suppress acquired chemotherapy resistance. *Oncogene* 2013; e-pub ahead of print 7 October 2013; doi:10.1038/onc.2013.411.
4. Zhao Y, Butler EB, Tan M. Targeting cellular metabolism to improve cancer therapeutics. *Cell Death Dis* 2013; **4**: e532.
5. Galluzzi L, Kepp O, Vander Heiden MG, Kroemer G. Metabolic targets for cancer therapy. *Nat Rev Drug Discov* 2013; **12**: 829–846.
6. Vander Heiden MG, Cantley LC, Thompson CB. Understanding the Warburg effect: the metabolic requirements of cell proliferation. *Science* 2009; **324**: 1029–1033.
7. Menendez JA, Joven J, Cufi S, Corominas-Faja B, Oliveras-Ferraros C, Cuyas E *et al.* The Warburg effect version 2.0: metabolic reprogramming of cancer stem cells. *Cell Cycle* 2013; **12**: 1166–1179.
8. Pecqueur C, Oliver L, Oizel K, Lalier L, Vallette FM. Targeting metabolism to induce cell death in cancer cells and cancer stem cells. *Int J Cell Biol* 2013; **2013**: 805975.
9. Dong C, Yuan T, Wu Y, Wang Y, Fan TW, Miriyala S *et al.* Loss of FBP1 by Snail-mediated repression provides metabolic advantages in basal-like breast cancer. *Cancer Cell* 2013; **23**: 316–331.
10. Yuan S, Wang F, Chen G, Zhang H, Feng L, Wang L *et al.* Effective elimination of cancer stem cells by a novel drug combination strategy. *Stem Cells* 2013; **31**: 23–34.
11. Palorini R, Votta G, Balestrieri C, Monestiroli A, Olivieri S, Vento R *et al.* Energy metabolism characterization of a novel cancer stem cell-like line 3AB-OS. *J Cell Biochem* 2014; **115**: 368–379.
12. Gammon L, Biddle A, Heywood HK, Johannessen AC, Mackenzie IC. Sub-sets of cancer stem cells differ intrinsically in their patterns of oxygen metabolism. *PLoS One* 2013; **8**: e62493.
13. Zhou Y, Zhou Y, Shingu T, Feng L, Chen Z, Ogasawara M *et al.* Metabolic alterations in highly tumorigenic glioblastoma cells: preference for hypoxia and high dependency on glycolysis. *J Biol Chem* 2011; **286**: 32843–32853.
14. Morfouace M, Lalier L, Bahut M, Bonnamain V, Naveilhan P, Guette C *et al.* Comparison of spheroids formed by rat glioma stem cells and neural stem cells reveals differences in glucose metabolism and promising therapeutic applications. *J Biol Chem* 2012; **287**: 33664–33674.
15. Vlashi E, Lagadec C, Vergnes L, Matsutani T, Masui K, Poulou M *et al.* Metabolic state of glioma stem cells and nontumorigenic cells. *Proc Natl Acad Sci USA* 2011; **108**: 16062–16067.
16. Fantin VR, St-Pierre J, Leder P. Attenuation of LDH-A expression uncovers a link between glycolysis, mitochondrial physiology, and tumor maintenance. *Cancer Cell* 2006; **9**: 425–434.
17. Christofk HR, Vander Heiden MG, Harris MH, Ramanathan A, Gerszten RE, Wei R *et al.* The M2 splice isoform of pyruvate kinase is important for cancer metabolism and tumour growth. *Nature* 2008; **452**: 230–233.
18. Lombardo Y, Scopelliti A, Cammareri P, Todaro M, Iovino F, Ricci-Vitiani L *et al.* Bone morphogenetic protein 4 induces differentiation of colorectal cancer stem cells and increases their response to chemotherapy in mice. *Gastroenterology* 2011; **140**: 297–309.
19. Bartucci M, Dattilo R, Moriconi C, Pagliuca A, Mottolese M, Federici G *et al.* TAZ is required for metastatic activity and chemoresistance of breast cancer stem cells. *Oncogene* 2014; e-pub ahead of print 17 February 2014; doi:10.1038/onc.2014.5.
20. Todaro M, Turdo A, Bartucci M, Iovino F, Dattilo R, Biffoni M *et al.* Erythropoietin activates cell survival pathways in breast cancer stem-like cells to protect them from chemotherapy. *Cancer Res* 2013; **73**: 6393–6400.
21. Keith B, Simon MC. Hypoxia-inducible factors, stem cells, and cancer. *Cell* 2007; **129**: 465–472.
22. Milane L, Duan Z, Amiji M. Role of hypoxia and glycolysis in the development of multi-drug resistance in human tumor cells and the establishment of an orthotopic multi-drug resistant tumor model in nude mice using hypoxic pre-conditioning. *Cancer Cell Int* 2011; **11**: 3.
23. Harris AL. Hypoxia–a key regulatory factor in tumour growth. *Nat Rev Cancer* 2002; **2**: 38–47.
24. Koukourakis MI, Pitiakoudis M, Giatromanolaki A, Tsarouha A, Polychronidis A, Sivridis E *et al.* Oxygen and glucose consumption in gastrointestinal adenocarcinomas: correlation with markers of hypoxia, acidity and anaerobic glycolysis. *Cancer Sci* 2006; **97**: 1056–1060.
25. Lu H, Shah P, Ennis D, Shinder G, Sap J, Le-Tien H *et al.* The differentiation of skeletal muscle cells involves a protein-tyrosine phosphatase-alpha-mediated C-Src signaling pathway. *J Biol Chem* 2002; **277**: 46687–46695.
26. Anderson KM, Tsui P, Guinan P, Rubenstein M. The proliferative response of hela cells to 2-deoxy-D-glucose under hypoxic or anoxic conditions: an analogue for studying some properties of *in vivo* solid cancers. *Anticancer Res* 2006; **26**: 4155–4162.
27. Brown JM. The hypoxic cell: a target for selective cancer therapy–eighteenth Bruce F. Cain Memorial Award lecture. *Cancer Res* 1999; **59**: 5863–5870.
28. Gillies RJ, Gatenby RA. Adaptive landscapes and emergent phenotypes: why do cancers have high glycolysis? *J Bioenerg Biomembr* 2007; **39**: 251–257.
29. Vander Heiden MG, Locasale JW, Swanson KD, Sharfi H, Heffron GJ, Amador-Noguez D *et al.* Evidence for an alternative glycolytic pathway in rapidly proliferating cells. *Science* 2010; **329**: 1492–1499.
30. Mazurek S, Boschek CB, Hugo F, Eigenbrodt E. Pyruvate kinase type M2 and its role in tumor growth and spreading. *Semin Cancer Biol* 2005; **15**: 300–308.
31. Dombrauckas JD, Santarsiero BD, Mesecar AD. Structural basis for tumor pyruvate kinase M2 allosteric regulation and catalysis. *Biochemistry* 2005; **44**: 9417–9429.
32. Chaneton B, Hillmann P, Zheng L, Martin AC, Maddocks OD, Chokkathukalam A *et al.* Serine is a natural ligand and allosteric activator of pyruvate kinase M2. *Nature* 2012; **491**: 458–462.
33. Bluemlein K, Gluckmann M, Gruning NM, Feichtinger R, Kruger A, Wamelink M *et al.* Pyruvate kinase is a dosage-dependent regulator of cellular amino acid homeostasis. *Oncotarget* 2012; **3**: 1356–1369.
34. Ye J, Mancuso A, Tong X, Ward PS, Fan J, Rabinowitz JD *et al.* Pyruvate kinase M2 promotes *de novo* serine synthesis to sustain mTORC1 activity and cell proliferation. *Proc Natl Acad Sci USA* 2012; **109**: 6904–6909.
35. Bauer DE, Harris MH, Plas DR, Lum JJ, Hammerman PS, Rathmell JC *et al.* Cytokine stimulation of aerobic glycolysis in hematopoietic cells exceeds proliferative demand. *FASEB J* 2004; **18**: 1303–1305.
36. Santidrian AF, Matsuno-Yagi A, Ritland M, Seo BB, LeBoeuf SE, Gay LJ *et al.* Mitochondrial complex I activity and NAD+/NADH balance regulate breast cancer progression. *J Clin Invest* 2013; **123**: 1068–1081.
37. Gogvadze V, Norberg E, Orrenius S, Zhivotovsky B. Involvement of Ca2+ and ROS in alpha-tocopheryl succinate-induced mitochondrial permeabilization. *Int J Cancer* 2010; **127**: 1823–1832.
38. Anastasiou D, Poulogiannis G, Asara JM, Boxer MB, Jiang JK, Shen M *et al.* Inhibition of pyruvate kinase M2 by reactive oxygen species contributes to cellular antioxidant responses. *Science* 2011; **334**: 1278–1283.
39. Nakano A, Tsuji D, Miki H, Cui Q, El Sayed SM, Ikegame A *et al.* Glycolysis inhibition inactivates ABC transporters to restore drug sensitivity in malignant cells. *PLoS One* 2011; **6**: e27222.
40. Maschek G, Savaraj N, Priebe W, Braunschweiger P, Hamilton K, Tidmarsh GF *et al.* 2-deoxy-D-glucose increases the efficacy of adriamycin and paclitaxel in human osteosarcoma and non-small cell lung cancers *in vivo*. *Cancer Res* 2004; **64**: 31–34.
41. Zhang XD, Deslandes E, Villedieu M, Poulain L, Duval M, Gauduchon P *et al.* Effect of 2-deoxy-D-glucose on various malignant cell lines *in vitro*. *Anticancer Res* 2006; **26**: 3561–3566.
42. Zhao Y, Liu H, Liu Z, Ding Y, Ledoux SP, Wilson GL *et al.* Overcoming trastuzumab resistance in breast cancer by targeting dysregulated glucose metabolism. *Cancer Res* 2011; **71**: 4585–4597.
43. Dennis PB, Jaeschke A, Saitoh M, Fowler B, Kozma SC, Thomas G. Mammalian TOR: a homeostatic ATP sensor. *Science* 2001; **294**: 1102–1105.
44. Yamaguchi R, Perkins G. Finding a panacea among combination cancer therapies. *Cancer Res* 2012; **72**: 18–23.
45. Calcagno AM, Salcido CD, Gillet JP, Wu CP, Fostel JM, Mumau MD *et al.* Prolonged drug selection of breast cancer cells and enrichment of cancer stem cell characteristics. *J Natl Cancer Inst* 2010; **102**: 1637–1652.
46. Kotamraju S, Konorev EA, Joseph J, Kalyanaraman B. Doxorubicin-induced apoptosis in endothelial cells and cardiomyocytes is ameliorated by nitrone spin traps and ebselen. Role of reactive oxygen and nitrogen species. *J Biol Chem* 2000; **275**: 33585–33592.
47. Wang S, Konorev EA, Kotamraju S, Joseph J, Kalivendi S, Kalyanaraman B. Doxorubicin induces apoptosis in normal and tumor cells *via* distinctly different mechanisms. intermediacy of H(2)O(2)- and p53-dependent pathways. *J Biol Chem* 2004; **279**: 25535–25543.
48. Coleman MC, Asbury CR, Daniels D, Du J, Aykin-Burns N, Smith BJ *et al.* 2-deoxy-D-glucose causes cytotoxicity, oxidative stress, and radiosensitization in pancreatic cancer. *Free Radic Biol Med* 2008; **44**: 322–331.
49. Shutt DC, O'Dorisio MS, Aykin-Burns N, Spitz DR. 2-deoxy-D-glucose induces oxidative stress and cell killing in human neuroblastoma cells. *Cancer Biol Ther* 2010; **9**: 853–861.
50. Todaro M, Alea MP, Di Stefano AB, Cammareri P, Vermeulen L, Iovino F *et al.* Colon cancer stem cells dictate tumor growth and resist cell death by production of interleukin-4. *Cell Stem Cell* 2007; **1**: 389–402.
51. Nicoletti I, Migliorati G, Pagliacci MC, Grignani F, Riccardi C. A rapid and simple method for measuring thymocyte apoptosis by propidium iodide staining and flow cytometry. *J Immunol Methods* 1991; **139**: 271–279.
52. Ciavardelli D, D'Orazio M, Pieroni L, Consalvo A, Rossi C, Sacchetta P *et al.* Proteomic and ionomic profiling reveals significant alterations of protein expression and calcium homeostasis in cystic fibrosis cells. *Mol Biosyst* 2013; **9**: 1117–1126.
53. Ciavardelli D, Ammendola S, Ronci M, Consalvo A, Marzano V, Lipoma M *et al.* Phenotypic profile linked to inhibition of the major Zn influx system in Salmonella enterica: proteomics and ionomics investigations. *Mol Biosyst* 2011; **7**: 608–619.
54. D'Aguanno S, D'Agnano I, De Canio M, Rossi C, Bernardini S, Federici G *et al.* Shotgun proteomics and network analysis of neuroblastoma cell lines treated with curcumin. *Mol Biosyst* 2012; **8**: 1068–1077.

55. D'Aguanno S, D'Alessandro A, Pieroni L, Roveri A, Zaccarin M, Marzano V *et al.* New insights into neuroblastoma cisplatin resistance: a comparative proteomic and meta-mining investigation. *J Proteome Res* 2011; **10**: 416–428.
56. Vissers JP, Langridge JI, Aerts JM. Analysis and quantification of diagnostic serum markers and protein signatures for Gaucher disease. *Mol Cell Proteomics* 2007; **6**: 755–766.
57. Kanani H, Chrysanthopoulos PK, Klapa MI. Standardizing GC–MS metabolomics. *J Chromatogr B Analyt Technol Biomed Life Sci* 2008; **871**: 191–201.
58. Sirolli V, Rossi C, Di Castelnuovo A, Felaco P, Amoroso L, Zucchelli M *et al.* Toward personalized hemodialysis by low molecular weight amino-containing compounds: future perspective of patient metabolic fingerprint. *Blood Transfus* 2012; **10**(Suppl 2): s78–s88.
59. Rizza S, Copetti M, Rossi C, Cianfarani MA, Zucchelli M, Luzi A *et al.* Metabolomics signature improves the prediction of cardiovascular events in elderly subjects. *Atherosclerosis* 2014; **232**: 260–264.
60. Shimada N, Shinagawa T, Ishii S. Modulation of M2-type pyruvate kinase activity by the cytoplasmic PML tumor suppressor protein. *Genes Cells* 2008; **13**: 245–254.
61. Krieg AF, Rosenblum LJ, Henry JB. Lactate dehydrogenase isoenzymes a comparison of pyruvate-to-lactate and lactate-to-pyruvate assays. *Clin Chem* 1967; **13**: 196–203.
62. Bomba M, Ciavardelli D, Silvestri E, Canzoniero LM, Lattanzio R, Chiappini P *et al.* Exenatide promotes cognitive enhancement and positive brain metabolic changes in PS1-KI mice but has no effects in 3xTg-AD animals. *Cell Death Dis* 2013; **4**: e612.
63. Bradford MM. A rapid and sensitive method for the quantitation of microgram quantities of protein utilizing the principle of protein-dye binding. *Analyt Biochem* 1976; **72**: 248–254.
64. Lohr GW, Waller HD. Glucose-6-phosphate dehydrogenase. Bergmeyer HU (ed). *Methods of Ezymatic Analysis.* Academic Press: New York, 1974, p 636.
65. Matsumura H, Miyachi S. Cycling assay for nicotinamide adenine dinucleotides. *Methods Enzymol* 1980; **69**: 465–470.
66. Wobbrock JO, Findlater L, Gergle D, Higgins JJ. The aligned rank transform fornonparametric factorial analyses using only ANOVA procedures. *Proceedings of the ACM Conference on Human Factors in computing systems (CH'11);* 7–12 May, 2011. Vancouver, British Columbia, Canada. ACM Press: New York, NY, USA, 2011, pp 143–146.

Supplementary Information accompanies this paper on Cell Death and Disease website (http://www.nature.com/cddis)

Acknowledgments

One night I dreamed a dream.
I was walking along the beach with my Lord. Across the dark sky flashed scenes from my life. For each scene, I noticed two sets of footprints in the sand, one belonging to me and one to my Lord.
When the last scene of my life shot before me I looked back at the footprints in the sand. There was only one set of footprints. I realized that this was at the lowest and saddest times of my life. This always bothered me and I questioned the Lord about my dilemma.
"Lord, You told me when I decided to follow You, You would walk and talk with me all the way. But I'm aware that during the most troublesome times of my life there is only one set of footprints. I just don't understand why, when I need You most, You leave me."
He whispered, "My precious child, I love you and will never leave you, never, ever, during your trials and testings. When you saw only one set of footprints, It was then that I carried you."

Margaret Fishback Powers, Footprints in the Sand.

These words, a source of strength and inspiration, have been with me in every moment of my life and probably they will accompany me forever. Three years ago, at the beginning of my adventure in the field of Cancer Research, I was not certain if it was the right path to be taken but I undertook this new challenge with enthusiasm and commitment. Despite many difficulties, I am now glad that I kept walking this path and I think I would have never done better. I am really thankful to the Stassi's Lab that has made possible this thesis: Alice, Tiziana, Annalisa, Miriam, Virginia, Tony, Mary, Alessandro, Gimmy, Marco, Rosachiara, Laura, Tatiana, Simone, Ciccio, Aurora, Debora and Giovanni. I am grateful to the Lab Heads Matilde Todaro and Giorgio Stassi for welcoming me in their Lab. Every day, they give me an example of sacrifice and dedication to Research. A huge thanks goes out to my Tutor Matilde for sticking by me in this adventure lasted three years.

An immense thanks goes out to Tiziana and Annalisa, my days in Stassi's Lab not have been the same without their, two colleagues but also two friends with whom I spent unforgettable moments.

I thank the Prof. Dieli, coordinator of the International PhD program in Immunopharmacology.

I deeply thank my family for their unconditional love and patience.

Thank you to my friends " the two Annas", Alessandra and Giovanni for having grown up together and for putting up with me over the years.

Thank you to Alessandra and Massimiliano, my second family, for your fondness.

Thanks to Riccardo and Marco for making me laugh even in the worst moments.

Thanks to people who are no longer part of my life… c'est la vie.

Curriculum Vitae (last three years of PhD)

Personal information

Name: **EMANUELA SCAVO**
Date of birth: 14/11/1982
Nationality: Italian

Education and training

01/01/2013 to 31/12/15
International PhD Program in Immunopharmacology
University of Palermo, Italy

2013/2015
PhD Student at University of Palermo, Italy
Laboratory of Cellular and Molecular Pathophysiology
University Hospital "Paolo Giaccone", Italy
Lab Head: Prof. Giorgio Stassi

2012/2015
II level University Master Degree in Applied Biotechnology and Bioinformatics in the study and diagnosis of genetic diseases
University of Palermo, Italy

Awards

2014-2015
Temporary Research Fellow in Innovative technology platforms for tissue engineering
Laboratory of Cellular and Molecular Pathophysiology – Department of Surgical and Oncological Sciences
University Hospital "Paolo Giaccone", Italy
PON01_00829. Supervisor Giuseppe Lembo MD
University of Palermo

2013 – 2014
Fellowship in Training of young researchers in Immunopharmacology, Genomics and Proteomics and Cell Biology of Neoplasms – Biology of Tumor Processes
PON01_01059. Supervisor Giorgio Stassi MD
University of Palermo

Scientific papers and participation to international meetings

- Normal vs cancer thyroid stem cells: the road to transformation.M Zane, **E Scavo**, V Catalano, M Bonanno, M Todaro, R De Maria and G Stassi. Oncogene, 2015.

- Estrogens and stem cells in thyroid cancer. M Zane,V Catalano, **E Scavo**, M Bonanno, MR Pelizzo, M Todaro and G Stassi. Frontiers in Endocrinology, 2014

- Breast cancer stem cells rely on fermentative glycolysis and are sensitive to 2-deoxyglucose treatment. D Ciavardelli, C Rossi, D Barcaroli, S Volpe, A Consalvo, M Zucchelli, A De Cola, **E Scavo**, R Carollo, D D'Agostino, F Forlı', S D'Aguanno, M Todaro, G Stassi, C Di Ilio, V De Laurenzi, and A Urbani. Cell Death and Disease, 2014.

- Thyroid stem cell trasformation: the way to thyroid carcinomas. **E Scavo**, M Bonanno, S Di Franco, L Mangiapane, A Giammona, T Apuzzo, A Benfante, M Todaro, G Stassi . Poster presentation. ABCD Congress, Bologna 2015.